DEVELOPMENT OF VASCULARIZED ADIPOSE TISSUE CONSTRUCT BASED ON ADIPOSE TISSUE EXTRACELLULAR MATRIX AND SILK FIBROIN

A THESIS SUBMITTED TO
THE GRADUATE SCHOOL OF NATURAL AND APPLIED SCIENCES
OF
MIDDLE EAST TECHNICAL UNIVERSITY

BY

ALİŞAN KAYABÖLEN

IN PARTIAL FULFILLMENT OF THE REQUIREMENTS
FOR
THE DEGREE OF MASTER OF SCIENCE
IN
BIOMEDICAL ENGINEERING

JULY 2015

Approval of the thesis:

DEVELOPMENT OF VASCULARIZED ADIPOSE TISSUE CONSTRUCT BASED ON ADIPOSE TISSUE EXTRACELLULAR MATRIX AND SILK FIBROIN

Submitted by **ALİŞAN KAYABÖLEN** in partial fulfillment of the requirements for the degree of **Master of Science in Biomedical Engineering, Middle East Technical University** by,

Prof. Dr. Gülbin Dural Ünver
Dean, Graduate School of **Natural and Applied Sciences** _____

Prof. Dr. Işık Hakan Tarman
Head of Department, **Biomedical Engineering** _____

Assoc. Prof. Dr. Ayşen Tezcaner
Supervisor, **Engineering Sciences Dept., METU** _____

Assoc. Prof. Dr. Fatih Zor
Co-Supervisor, **Plastic and Reconstructive Surgery, GATA**_____

Examining Committee Members:

Assoc. Prof. Dr. Sreeparna Banerjee
Biology Dept., METU _____

Assoc. Prof. Dr. Ayşen Tezcaner
Engineering Sciences Dept., METU _____

Assoc. Prof. Dr. Dilek Keskin
Engineering Sciences Dept., METU _____

Assoc. Prof. Dr. Senih Gürses
Engineering Sciences Dept., METU _____

Assist. Prof. Dr. Pınar Yılgör Huri
Biomedical Engineering Dept., Ankara University _____

Date: _____

I hereby declare that all information in this document has been obtained and presented in accordance with academic rules and ethical conduct. I also declare that, as required by these rules and conduct, I have fully cited and referenced all material and results that are not original to this work.

Name, Last name : Alişan Kayabölen

Signature :

ABSTRACT

DEVELOPMENT OF VASCULARIZED ADIPOSE TISSUE CONSTRUCT BASED ON ADIPOSE TISSUE EXTRACELLULAR MATRIX AND SILK FIBROIN

Kayabölen, Alişan

M.S., Biomedical Engineering

Supervisor: Assoc. Prof. Dr. Ayşen Tezcaner

Co-Supervisor: Assoc. Prof. Dr. Fatih Zor

June 2015, 108 Pages

Adipose tissue engineering is a promising field for regeneration of soft tissue defects. However, vascularization is needed since cells in the middle layer of thick implants cannot reach to nutrient and oxygen by diffusion. Finding a biocompatible scaffold with good mechanical properties is another problem in this field. In this study, we aimed to develop a thick functional vascularized adipose tissue which supports cell viability and functionality with similar mechanical properties with the adipose tissue. For this purpose, hydrogels were prepared by mixing human decellularized adipose tissue (DAT) and silk fibroin at different ratios. Then, both preadipocytes and endothelial-like cells pre-differentiated from rat adipose derived stem cells (ASCs) were encapsulated in hydrogels. *In vitro* analyses showed that hydrogels with 1:3 (v/v) DAT:Fibroin ratio support cell viability. ASCs pre-differentiated into adipogenic lineage for 1 week started to accumulate lipid vesicles, and ones pre-differentiated into endothelial lineage formed capillary-like structures inside hydrogel only after 3 days of encapsulation. This mixture

was shown to be gelated *in vivo* too, and implanted subcutaneously. No severe immunological response or significant degradation of the hydrogels was observed in histopathological analysis 3 days postimplantation. Histology results for 3 weeks showed that hydrogel was degraded from outside, and capillaries reached to the center of hydrogel. *In vivo* analysis of cell encapsulated hydrogels are under study. Based on *in vitro* and *in vivo* results 1:3 - DAT:Fib hydrogels hold promise for adipose tissue engineering applications.

Keywords: Adipose tissue engineering, decellularization, cell encapsulation, hydrogel, vascularization

ÖZ

YAĞ DOKUSU HÜCREDIŞI MATRİKSİ VE İPEK FİBROİNİNDEN DAMARLI ADİPOZ DOKU KONSTRÜKTÜ GELİŞTİRİLMESİ

Kayabölen, Alişan

Yüksek Lisans, Biyomedikal Mühendisliği

Tez Yöneticisi: Doç. Dr. Ayşen Tezcaner

Ortak Tez Yöneticisi: Doç. Dr. Fatih Zor

Haziran 2015, 108 Sayfa

Yağ doku mühendisliği, yumuşak doku hasarlarının rejenerasyonu için umut verici bir alandır. Kalın implantların iç katmanlarındaki hücreler besin ve oksijene ulaşamadığı için damarlaşma sağlanması ihtiyaç vardır. Diğer bir problem de biyouyumlu ve iyi mekanik özelliklere sahip hücre taşıyıcılar bulabilmektir. Bu çalışmada, doğal dokuyla mekanik olarak uyumlu, hücre canlılığını ve farklılaşmasını destekleyen, kalın ve fonksiyonel bir damarlaşma sağlanmış yağ doku üretmeyi amaçladık. Bu amaçla, deselülerize edilmiş yağ doku (DAT) ve ipek fibroini farklı oranlarda karıştırılarak hidrojeller elde edilmiştir. Daha sonra, yağ doku kökenli kök hücrelerden farklılaştırılan öncül yağ doku hücreleri ve endotel-benzeri hücreler bu hidrojeller içine hapsedilmiştir. *In vitro* çalışmalar, 1:3 (v/v) DAT:Fibroin oranlı hidrojellerin hücre canlılığını desteklediğini göstermiştir. Aynı zamanda, hidrojel içine hapsedildikten yalnızca 3 gün sonra adipojenik yönde 1 hafta farklılaştırılan ASC'ler yağ damlacıkları toplamaya, endotel yönde 1 hafta farklılaştırılan ASC'ler ise kılcal damar-benzeri yapılar

oluşturmaya başlamıştır. Bu karışım *in vivo* uygulamada da jelleştirilebilmiş ve deri altına yerleştirilmiştir. Erken analizlerde (1 haftalık) şiddetli bir immün reaksiyon veya parçalanma gözlemlenmemiştir. Geç analizlerde (3 haftalık) ise hidrojelin dıştan başlayarak parçalandığı ve kılcal damarların hidrojelin merkezine kadar ulaştığı gözlemlenmiştir. Hücre enkapsüle edilmiş hidrojellerin *in vivo* analizleri devam etmektedir. Mekanik testler, *in vitro* hücre kültür çalışmaları ve *in vivo* uygulamaların ön analiz sonuçlarına dayanarak, 1:3 DAT:Fib hidrojelleri yağ doku mühendisliği için uygun taşıyıcılar olarak önerilmiştir.

Anahtar kelimeler: Yağ doku mühendisliği, deselülerizasyon, hücre hapsetme, hidrojel, damarlaşma

to the dreams giving motivation to do anything and making life livable…

ACKNOWLEDGEMENTS

Foremost, I would like to express my sincere gratitude to my thesis advisor Assoc. Prof. Dr. Ayşen Tezcaner. I am grateful to her for her continuous support, motivation and immense patience. She always believed in me, even when I had very bad or unexpected results and lost my all motivation. Her continuous guidance have the biggest role in my research, experiments and writing of this thesis.

I am also very thankful to Assoc. Prof. Dr. Dilek Keskin as my secret co-supervisor. I found the opportunity to study with her from my undergraduate special project until the end of my thesis. She was always helpful, and encourage my studies with brillant advices.

I would also like to thank my co-supervisor Assoc. Prof. Dr. Fatih Zor for the management of the animal studies part of my thesis. His great knowledge on his field gave me high confidence about these experiments. Also, Op. Dr. Andaç Aykan who is the leading actor of animal experiments deserves a big thank. His magical hands and practical solutions under problematic circumstances saved us too many times. I am also thankful to Assoc. Prof. Dr. Yıldırım Karslıoğlı for his great helps in histological analyses and evaluations, to senior biologists Pınar Elçi and Meral Sarper for their assistance in cell culture experiments.

I would like to thank my thesis committee members Assoc. Prof. Dr. Sreeperna Banerjee, Assist. Prof. Dr. Pınar Yılgör Huri and Assoc. Prof. Dr. Senih Gürses for their interests in my study and participation and valuable comments in my thesis jury.

I would also like to thank Scientific and Technological Research Council of Turkey (TÜBİTAK) for its master thesis grant under BİDEB 2210 program, and Gülhane Military Medical Academy (GATA) for providing financial support to this project.

I am thankful to all my lab friends; Ali Deniz Dalgıç who is also my great housemate for his originalities in all topics and cooperations for the wild life plans; Aydin Tahmasebifar for his helps in mechanical tests and nice passes in football matches; Ayşegül Kavas for encouraging me in all studies and friendship at night watch; Bengi Yılmaz for her logical advices in experiments and being my first cell culture teacher; Deniz Atila for creative discussions on many topics and sharing nice songs in lab; Engin Pazarçeviren for making us feel like Roman Empire citizens and inoculating love for ISIS and governors; Hazal Aydoğdu for having a huge role in my graduation by her academical reminders, and accommpanying in marathons; Merve Güldiken for converting boring times to fun (sometimes to fear!) by amazing (!) songs, lovely (!) poems, and nice chats; Ömer Aktürk for promoting me with his entrepreneurial spirit and pioneering in many topics; Özge Erdemli for her helps especially in my first days in lab, and great knowledge about any kind of lab works; Sibel Ataol, my cheerful office mate, for her sincere friendship, motivations and helps in the experiments and research that we did together, and our regular scientific conversations when Merve is not around; Reza Moonesirad for the great managing of lab works as the chief and not leaving me alone in unusual working hours; Yağmur Çalışkan for make me feel in my hometown and her helps in moving our new house; Zeynep Barçın for being the lovely mother of lab and feeding us with delicious foods even if she is far now.

I would also like to thank all members of METU Orienteering and Navigation Team for making my university life “special”. I tasted team work, success, enthusiasm, fun, organisation, beauty of nature, ambition and many special things with them while subjecting to stressful realities of life.

I am also thankful to my all friends who encourages me during this period especially to; Kübra Narcı for being a real friend and standing by me for years; Berke Gürkan for being my soul twin, Eda Koyuncu for her sincere friendship even after any kind of jokes; Elif Yurdanur Taşel and Erdinç Taşel for being my family in Ankara and

contributing many valuable things to my life; Bilal Kabaklı and Emre Akşit for being my brothers who are normally pose danger for my academic career, but I find myself by them; Duygu Tolunay, Mehmet Ünal and Mehmet Ali Erol for their great contributions and motivations in my life as the other members of family; and Havva Çalılı for being motivation of my life by sharing it.

This study would not be possible without supports of my family. Therefore, the biggest thank is to my family, to my father Naci Kayabölen, my mother Semra Kayabölen, and my brother Özgür Kayabölen who are always trust, believe in and encourage me whatever I did throughout my life.

TABLE OF CONTENTS

LIST OF TABLES

TABLES

LIST OF FIGURES

FIGURES

LIST OF ABBREVIATIONS

SVF; Stromal-Vascular Fraction,
WAT; White Adipose Tissue,
PPAR; Peroxisome Proliferator-Activated Receptor,
STAT; Signal Transducer and Activator of Transcription,
CHOP; C/EBP Homologous Protein,
KLF; Kruppel-Like Factors,
PREF1; Preadipocyte Factor 1,
SHH; Sonic Hedgehog,
BMP; Bone Morphogenic Protein,
IGF; Insulin-Like Growth Factor,
bFGF; Basic Fibroblast Growth Factor,
TGF; Transforming Growth Factor,
ECM; Extracellular Matrix,
MMP; Matrix Metalloproteinase,
PLA; Poly Lactic Acid,
DAT; Decellularized Adipose Tissue,
VEGF; Vascular Endothelial Growth Factor,
PDGF; Platelet Derived Growth Factor,
SDF-1; Stromal Cell-Derived Factor 1,
EPC; Endothelial Progenitor Cells,
EC; Endothelial Cells,
DNase; Deoxyribonuclease,
RNase; Ribonuclease,
sGAG; Sulfated Glycosaminoglycan,
EtO; Ethylene Oxide,
BCA; Bicinchoninic Acid,
BSA; Bovine Serum Abumin,
ELISA; Enzyme-Linked Immuno Sorbent Assay,
DMMB; Dimethyl Methylene Blue,
PBE; Phosphate Buffer EDTA,
ChS; Chondroitin Sulfate,
TNE; Tris Sodium EDTA,
RFU; Relative Fluorescence Unit,
PAGE; Polyacrylamide Gel Electrophoresis,
TEMED; Tetramethylethylenediamine,
APS; Ammonium Persulfate,
Fib; Fibroin,
ASC; Adipose Derived Stem Cell,
FBS; Fetal Bovine Serum,
IBMX; 3-Isobutyl-1-Methylxanthine,
EGM; Endothelial Growth Medium,
EGF; Epidermal Growth Factor,
FITC; Fluorescein Isothiocyanate,
vWF; Von Willebrand Factor,
TCP; Tissue Culture Plate.

CHAPTER 1

INTRODUCTION

1.1. Adipose Tissue

Adipose or fat tissue is a loose connective tissue specialized for energy storage in the form of fat, especially as triglycerides. It also serves as an insulator and cushion to body (Rosen and Spiegelman, 2000). It mainly consists of adipocytes, and there are also fibroblasts, endothelial cells, preadipocytes, stem cells and immune cells in adipose tissue (Lanza et al., 2007). Since adipocytes have high lipid content, they can be easily separated from other cells by centrifugation. Therefore, all other cells form a cell fraction, which is called as stromal-vascular fraction (SVF) (Meissburger, 2010). Adipose tissue is also accepted as a major endocrine organ, which produces leptin, adiponectin, estrogen and resistin (Kershaw and Flier, 2004). In mammals, there are two types of adipose tissue: brown adipose tissue and white adipose tissue (Figure 1).

1.1.1. White Adipose Tissue

White adipose tissue (WAT) is the most common type of fat in human and it has important roles such as energy storage, insulation and mechanical cushion. It stores energy in the form of fat and provides to other cells in the energy deprivation times of body (Symonds, 2012). It has the ability of accumulation and mobilization of fat. Hormones such as leptin, adiponectin, etc. are produced mainly by white adipose tissue (Symonds, 2012). WAT is found in two main depots in mammals, subcutaneously and intra-abdominally. Adipocytes in white adipose tissue have a big, single lipid droplet,

which is enclosed with a membrane. Nearly 90% of the cell volume is occupied by this droplet, so nucleus and other organelles are found in a very narrow cytoplasm. Mitochondria number is too low compared to brown adipose tissue, and there are few blood vessels in white adipose tissue, so blood supply is also poor.

1.1.2. Brown Adipose Tissue

Brown adipose tissue is found mainly in small-sized mammals such as mice and newborn human baby, and also in hibernating mammals (Gesta et al., 2007). It has a big role in non-shivering thermogenesis; its function is heat generation by metabolizing lipids. So, it needs more mitochondrial activity, nutrient and oxygen. Its brown color comes from highly rich blood vasculature and high number of mitochondria in adipocytes (Enerbäck, 2009). Normally, proton motive force across the inner membrane of mitochondria is converted to ATP, however, in brown adipose tissue mitochondria; it is dissipated as heat (Symonds, 2012). Thus, it helps to maintain constant body temperature. Inside adipocytes, lipids are found as small droplets in high number rather than single, big droplet found in adipocytes in white adipose tissue. When animals grow and get bigger, their surface to volume ratio decreases and they shiver. As a result of this shivering their body temperature is maintained easier. Brown adipose tissue becomes metabolically inactive as animals get older, however, cold exposure can activate it again.

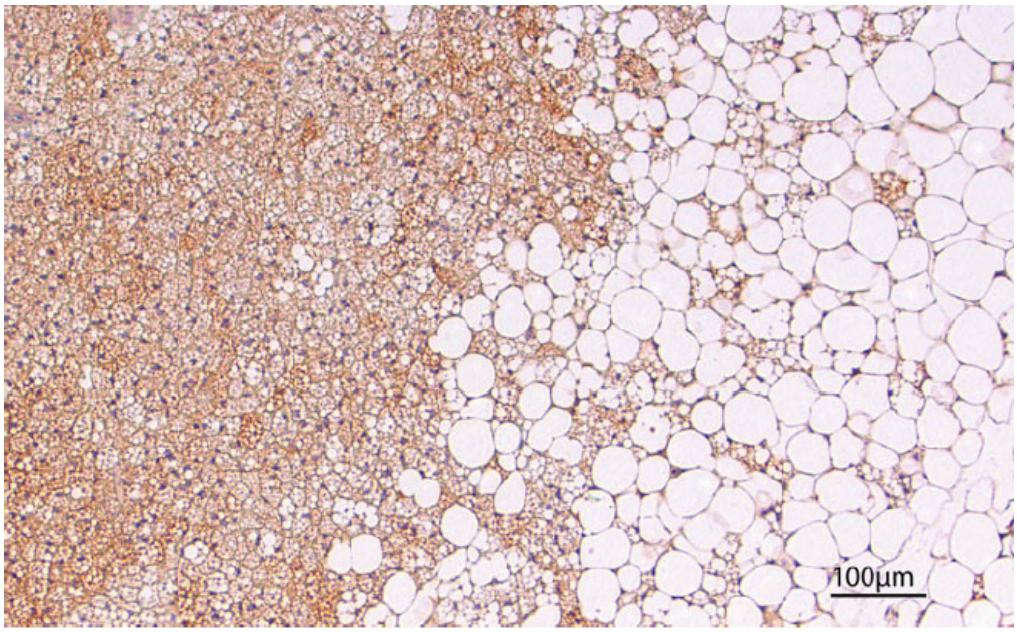

Figure 1. Direct comparison of brown and white adipocytes in histological section of interscapular adipose tissue (Symonds, 2012).

1.2. Adipogenic Differentiation

Adipose tissue contains mesenchymal stem cells, which have multilineage differentiation capacity (Niemela et al., 2008). Differentiation of these stem cells into mature adipocytes is a highly complicated process, which involves many cellular and molecular events (Figure 2). During these processes, fibroblast-like stem cells acquire morphological changes and turn into lipid droplet accumulated adipocytes. Also, the composition and type of the cytoskeletal and extracellular components change during differentiation (Tong and Hotamisligil, 2001).

In vitro differentiation studies by using either immortalized cell lines such as 3T3-L1 and 3T3-F442A or primary cell pool in the stromal vascular fraction (SVF) of the adipose tissue have revealed significant results about differentiation pathways and molecular mechanisms. These cell lines or primary preadipocytes can be successfully

differentiated into mature adipocytes *in vitro*. Therefore, differences of these cells in gene expression levels with similar cell types, which cannot be differentiated into adipocytes such as 3T3-C2 cells, give valuable information about responsible factors for differentiation.

1.2.1. Molecular Mechanisms

Adipogenic differentiation is a highly complicated process, which has many cascade mechanisms. Primarily for differentiation of preadipocytes, growth arrest is required, and this situation is regulated mostly at transcriptional level. The two major regulators are CCAAT/enhancer-binding proteins (C/EBPβ and C/EBPδ) and peroxisome proliferator activated receptor- γ (PPAR-γ) (Tontonoz et al., 1994). PPAR-γ activates many adipogenic genes and induces cell to get out of the cell cycle and remain in growth arrest. C/ EBPβ and C/EBPδ are generally needed in early stages of differentiation and induce PPAR-γ expression by binding promoter region of PPAR-γ and C/EBPα (Mandrup and Lane, 1997). C/EBPα and PPAR-γ also activates expression of each other creating a positive feedback loop. They work together and trigger gene expressions needed for appearance and maintenance of adipogenic phenotype such as lipogenesis, insulin sensitivity, glucose transportation, fatty acid binding, leptin and adiponectin secretion etc. (Lowe et al., 2011). STAT5, CHOP10 and KLFs are the other major transcription factors that have important effects on adipogenic differentiation (Rosen and MacDougald, 2006). Also, expression of some factors is inhibited during adipocyte differentiation such as PREF1 (Lee et al., 2003) and GATA family (Tong et al., 2000).

On the other hand, regulation at transcriptional level is not the only way for regulating adipogenesis. For instance, extracellular signaling pathways such as WNT or sonic hedgehog (SHH) inhibit adipogenesis. However, some extracellular proteins such as members of BMPs, IGFs, FGFs and TGFβ can induce adipogenic differentiation (Lowe et al., 2011).

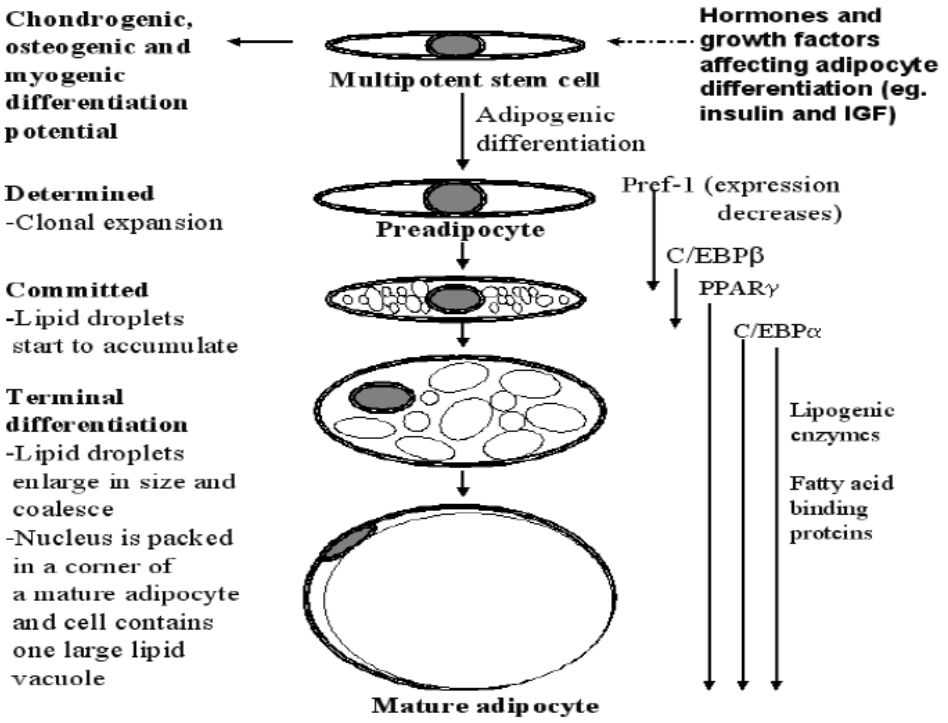

Figure 2. An overview of cellular and molecular events during adipogenesis. Arrows reflect the durations of molecular events (Niemela et al., 2008).

1.2.2. Cytoskeletal and Extracellular Matrix Components

During differentiation process, both cytoskeletal and ECM components change in terms of type and composition. In early stages, ECM, rich in fibronectin and collagen type I and III, is converted to a basement membrane which is rich in laminin, entactin, collagen type IV and VI and glycosaminoglycans (Selvarajan et al., 2001). In addition, a morphological change from fibroblastic preadipocytes into spherical adipocytes occurs during adipogenesis. This situation is the result of decreasing in actin and tubulin expression (Spiegelman and Farmer, 1982).

1.3. Natural Vascularization Strategies

In human body, there is a highly complicated vascular network. It is distributed to whole body to supply nutrient and oxygen to each part of the body. This network is built by different vascularization processes, which start at embryonic development and these processes continue during adulthood (Kässmeyer et al., 2009). Vasculogenesis is one of these processes that occurs during embryogenesis (Risau and Flamme, 1995). It is the *de novo* process of vascularization in which vessels are formed in a previously non vascular tissue by organization of endothelial progenitor cells into a vascular network.

Neovascularization, (Takahashi et al., 1999) is like vasculogenesis, but it takes place in adulthood. There are endothelial progenitor cells which are responsible for *de novo* blood vessel formation, mainly in bone marrow and also in a small amount in blood vessels. When a vascularization signal is present, these cells differentiate into endothelial cells to form new blood vessels. Corneal neovascularization is an example of such processes.

Another process is angiogenesis in which new vessels are branched from vessels which are already present in tissue. In this process, endothelial cells release an enzyme called matrix metalloproteinase (MMP), which degrades extracellular matrix and allows endothelial cells migrate there to form tubular structures. Stimulations for angiogenesis may be mechanical such as shear stress, or chemical such as growth factors (Prior et al., 1997).

The last way of vascularization is arteriogenesis. During this process, previously existing collateral vessels extend and form bigger arteries. Many steps are observed during arteriogenesis; degradation of basal membrane, proliferation of vascular smooth muscle cells, increase in diameter and wall thickness by both proliferation and apoptosis in all layers (Helisch and Schaper, 2003).

1.4. Adipose Tissue Engineering

Adipose tissue production has a very important role in soft tissue repair. In many cancer cases, adipose tissue is required, especially in breast cancers, for the regeneration of new tissue after tumor resection or the repair of defects in surgical areas. If the tissue required is large, it is difficult to repair by natural mechanisms of the body. Current medical treatments also cannot make natural tissue regeneration possible.

Adipose tissue engineering is a promising field for regeneration of defects in adipose or other soft tissues. In adipose tissue engineering, cells, which are thought to produce new tissue, are seeded on a biocompatible and mostly biodegradable scaffold. Then, this tissue engineered construct is implanted to the defect site to produce new tissue or repair the existing tissue. An enhanced vascularization is also needed inside the scaffold to provide sufficient nutrient and oxygen to cells upon implantation.

1.4.1. Scaffold Materials

One of the important problems in adipose tissue engineering is finding a proper scaffold as cell carrier. Adipose tissue contains collagen type I, III, IV, V, VI, fibronectin, laminin and glycosaminoglycans, as components of extracellular matrix, which have important roles in adipogenesis and other cellular activities (Kubo et al., 2000). There are many natural (Table 1) and synthetic (Table 2) materials used for engineering of the adipose tissue. Scaffolds composed of biopolymers such as collagen or fibrin networks are highly biocompatible, but their *in vivo* degradation rate is very high (Mauney et al., 2007; Cho et al., 2005). Synthetic polymers, on the other hand, can be synthesized with different mechanical properties. One of the main drawbacks in their use can be the byproducts which are harmful for the healthy tissues or the risk of changes in local environment such as pH and inflammation unless they are specifically modified (Liu et al., 2006).

In recent years, silk fibroin has been increasingly used for tissue engineering applications due to its superior properties such as biocompatibility, slow degradation, minimal inflammation and good mechanical properties. Mauney et al. (2007) and Kang et al. (2009) used silk fibroin scaffolds for adipose tissue engineering. In both studies, it was shown that human adipose derived stem cells (hASCs) attached, proliferated and differentiated into adipocytes on these scaffolds. Even though *in vitro* cell attachment and adipogenesis were better on collagen based scaffolds, *in vivo* tissue formation was much better on fibroin scaffolds when compared with collagen and poly lactic acid (PLA) scaffolds (Mauney et al., 2007). Silk fibroin scaffolds remained stable for 4 weeks after implantation supporting new tissue formation while collagen and PLA scaffolds were nearly undetectable because of rapid degradation rates which would have retarded tissue regeneration. Silk fibroin also has a good versatility. For instance, Wang et al. (2008) prepared a sonication-induced hydrogel from aqueous silk fibroin solution, and showed its suitability for encapsulation of human bone marrow derived mesenchymal stem cells (hMSCs). Therefore, silk fibroin is a good candidate for scaffolding in engineering a functional adipose tissue.

An ideal implant should also mimic the three dimensional architecture of natural tissue and have the most similar composition. Thus, decellularized adipose tissue (DAT) was offered as a proper scaffold in its native form or as scaffold component in adipose tissue engineering (Uriel et al., 2009; Young et al., 2011). In these studies, it was shown that hydrogels obtained by decellularization of adipose tissue have good biocompatibility and they support cell attachment and proliferation. However, it is difficult to have good mechanical properties by using DAT only. In another study (Turner et al., 2012), DAT was used to fabricate microcarriers, and it was compared with gelatin microcarriers. Results showed that DAT microcarriers have natural adipo-inductive effect and provide enhanced cellular infiltration and tissue remodeling *in vivo* while gelatin microcarriers did not have such effects. Cheung et al. (2014) also, showed that DAT induces

adipogenic differentiation and adipose tissue formation since it has natural tissue components. In this study, they also used a polymer based hydrogel system to encapsulate DAT powders and adipose derived stem cells (ASCs). By this way, they obtained an injectable gel with adjustable mechanical properties. Recently, Young et al. (2014) injected natural DAT hydrogels, which contain ASCs subcutaneously into mice. ASC contained-hydrogels stimulated neovascularization and did not create a strong immune response. All these studies showed that DAT is a perfect material to regenerate adipose tissue. However, there are no offered vascularization strategies, which are sufficient for these 3D hydrogels. Therefore, producing thick, vascularized and functional tissue is still an important challenge.

Table 1. Natural polymers used for adipose tissue engineering (Choi et al., 2010)

Material	Strength	Weakness
Adipose derived ECM	Native ECM promotes favorable microenvironment for adipogenesis	Has not yet been formulated as a 3D porous scaffold
Collagen	Prevalent in native adipose ECM; promotes favorable adipose outcomes; well characterized	Fast degradation rate in vivo
Decellularized human placenta	Allogeneic approach to generate large adipose substitutes; supports adipose tissue formation	Extensive isolation and decellularization procedure (18 days)
Fibrin	Biocompatible material that can support adipogenesis in vivo	Has not yet been formulated as a 3D porous scaffold
Gelatin	Supports adipogenesis in vivo; retains shape after culture	Primarily used as material for microspheres; 3D construct for adipose tissue engineering not well utilized
Hyaluronan	Favorable mechanical properties; supports adipose tissue formation	3D porous scaffolds have not been widely successful for adipose outcomes
Matrigel	Supports adipogenesis	Cannot be utilized for human in vivo applications
Silk	Supports adipogenesis; favorable mechanical properties; slow degradation rate	Have not been utilized yet for long-term in vivo soft tissue engineering (>6 months)

1.4.2. Cell Sources

Mature adipocytes are not proper cell sources for adipose tissue engineering because of some limitations. First of all, they do not adhere onto culture plate due to their high lipid content. Therefore, they cannot take sufficient nutrient from medium, and making

observations is very difficult. Moreover, they are highly fragile because of their large size, so most of them die within the first 72h of culture (Zhang et al., 2000). Another problem is the lack of proliferation activity in terminally differentiated adipocytes (Prins and O'Rahilly, 1997). For these reasons, mature adipocytes are not suitable candidates for tissue engineering purposes.

Table 2. Synthetic polymers used for adipose tissue engineering (Choi et al., 2010)

Synthetic Polymer	Strength	Weakness
Poly(lactic acid)	Supports adipogenesis *in vitro* and *in vivo*	Degrade *in vivo* after 12 weeks
Poly(glycolic acid)	Supports adipogenesis *in vitro* and *in vivo*	Degrade *in vivo* after 4 weeks
Poly(lactic-co-glycolic acid)	Supports adipogenesis; induces vascularization *in vivo*	Long-term adipose tissue engineering studies have not been performed *in vitro* or *in vivo*
Poly(ethylene glycol)	Supports adipogenesis; maintains shape after *in vivo* culture	*In vivo* degradation rate not well characterized
Fluoropolymers	Maintains shape	Nondegradable; unfavorable surface for cell adhesion
Silicones	Biocompatible	Nondegradable

Preadipocyte cell lines such as 3T3-L1 and 3T3-F442A may be a better alternative than mature adipocytes for in vitro studies since they can easily be cultured *in vitro* and differentiated into adipocytes (Green and Meuth, 1974). However, cell lines may not give same functional responses with the primary cells since they are immortalized by genetic manipulations (Ailhaud, 2001). However, cell lines cannot be used for *in vivo* implantations since they create immunological response in the host. Also, there is a risk of cancer formation when cell lines are used.

Pluripotent mesenchymal stem cells (MSC) are the most common cell sources used for tissue engineering applications due to their proliferation and multilineage differentiation potential. Bone marrow (BM) derived MSC, which can be differentiated to adipocytes were used in many clinical applications for a long time (Barry and Murphy, 2004).

However, harvesting stem cells from bone marrow is a very painful and inefficient procedure considering the isolated stem cell number (De Ugarte et al., 2003).

In recent years, adipose derived stem cells are also being used as adult stem cell source (Zuk et al., 2002). Adipose derived stem cells are thought as ideal cell types for regenerative medicine applications according to the following criteria as reported by Gimble (2003):

- Available in abundant quantities (millions to billions of cells)
- Can be harvested by a minimally invasive procedure
- Can be differentiated along multiple cell lineage pathways in a controllable and reproducible manner
- Can be safely and effectively transplanted in either an autologous or allogeneic manner
- Can be manufactured in accordance with current Good Manufacturing Practice (GMP) guidelines

MSC can easily be harvested from lipoaspirates or small fragments of subcutaneous adipose tissue (Zhu and Nelson, 2013). Up to 100 million stem cells can be isolated from approximately 500 ml of adipose tissue (De Ugarte et al., 2003). Adipose derived MSCs have previously been shown to be able to differentiate into adipocytes, osteocytes, chondrocytes, and myocytes (Zuk et al., 2001). Also, their immune privilege has been shown (Gonzalez-Rey et al., 2010; Yanez et al., 2006) before, so they can be safely used in autologous and allogeneic manner. Production of GMP-compliant adipose tissue derived MSC has also been reported in details in the study of Sensebé et al. (2010). Therefore, adipose tissue can be accepted as one of the most suitable cell source for tissue engineering applications.

1.4.3. Vascularization Strategies

For in vitro studies, many tissue engineered constructs are produced successfully, and they have been generally shown to meet the required properties of the particular tissue. However, only very thin implants or avascular tissue implants can be used in vivo since vascularization is needed for thick implants (Jain et al., 2005). During in vitro studies, cells can be cultured with continuously supply of nutrient and O_2 in bioreactors. Also, waste products are removed by changing culture medium in short intervals. Therefore, they do not need any vascular structures to survive. On the other hand, when they are implanted to body, they need blood vessels to bring them nutrients and O_2, and remove waste products. The diffusion limit of O_2 is around 100-200 μm (Figure 3) (Novosel et al., 2011). Thus, any cell more distant to a capillary will not take enough O_2 and will not survive. This is the main reason of why cells in the middle part of the scaffold die after implantation into body. For this reason, vascularization inside the scaffold is necessary for successful implantation.

When a construct is implanted in vivo, the body naturally forms vessels, which grow into the implant. However, these naturally formed vessels extend only 20-30 micrometers in a day, so for complete vascularization of a millimeter-size implant takes several weeks (Clark and Clark, 1939). During this long process, cells have nutrient and O_2 deficiency and this mostly causes the death of these cells. Even if they don't die, there will be a gradient of nutrition and O_2 between the cells found outside and inside of the implant which creates an irregular cell differentiation (Malda et al., 2004). Thus, there is a need for acceleration of vascularization process for implanted constructs.

In thin tissues such as skin, the natural vascularization process may be enough or in avascular tissues such as cartilage, there is no need for vascularization. Therefore, for these tissues, tissue engineered constructs may be successful and many clinical approaches have been performed in recent years (Wisser and Steffes, 2003; Rodriguez et

al., 1999; Atala et al., 2006). On the other hand, enhanced vascularization should be provided for thicker tissues such as bone, muscle and adipose (Johnson et al., 2007). For instance, adipose tissue has a well-developed capillary network. Because of its energy storage function, blood flow is required to delivery and transfer of energy molecules such as fatty acids and signaling molecules such as hormones. Therefore, to engineer a functional adipose tissue, a well-developed capillary network is needed.

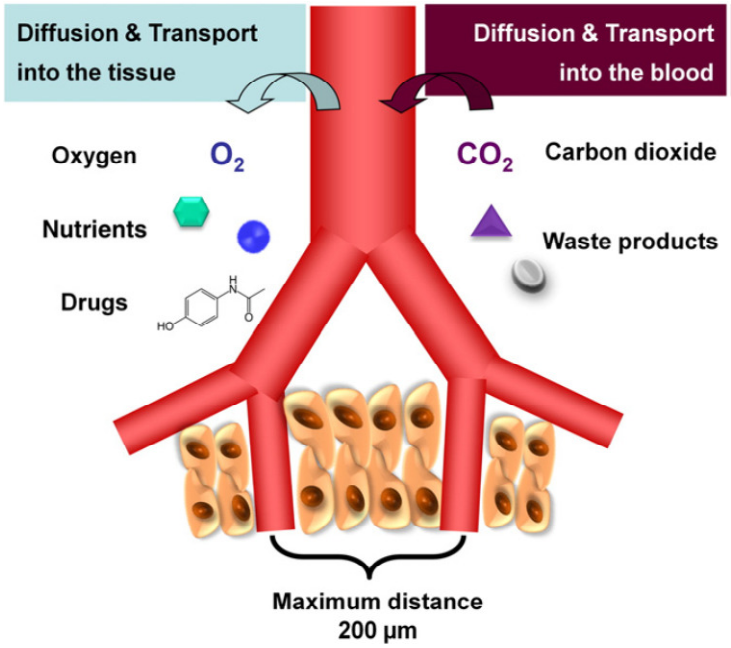

Figure 3. Illustration of nutrient and oxygen supply to tissue, and removal of waste products from the tissue via blood vessels (Novosel et al., 2011).

There are some techniques which are used to accelerate vascularization processes such as scaffold designing, angiogenic factor delivery, immobilization strategy, *in vivo* prevascularization and *in vitro* prevascularization.

1.4.3.1. Scaffold Designing

Some properties of scaffolds are required to enhance vascularization after implantation. Pore size is one of these critical properties. A scaffold with pore sizes larger than 250 μm highly increases vascularization formation (Druecke et al., 2004). Another critical property is pore interconnectivity. Even if there are many pores inside a scaffold, if they are not connected with each other there cannot be a significant increase in vascularization. Interconnectivity is necessary since cells should migrate and form tubular structures inside these connected pores.

Classical techniques for scaffold design such as gas foaming, freeze-drying, phase separation or particulate leaching are used for obtaining such porous scaffolds. However, in these techniques, the porosity and pore interconnectivity are not regular and well-organized (Malda et al., 2004). Generally, pores are formed randomly, so some pores are connected while others are not. These kinds of scaffolds inhibit the vessel formation inside it, so alternative methods should be used to obtain scaffolds, which have more organized pore structures.

Solid free-form fabrication systems such as 3D printing, rapid prototyping, stereolithography; or electrospinning methods; or microfluidic approaches give opportunities to have regular porosity and interconnectivity, as determined inside scaffold (Hutmacher et al., 2004; Kluger et al., 2010; Bettinger et al., 2005). Solid free-form fabrication techniques are computer-based design technique which is used to engineer 3D constructs by adding biomaterial layers to obtain pre-determined morphology, porosity and mechanical properties. In electrospinning, thin fibers of polymers are formed and aligned with an electric field force, so required shapes and interconnectivity can be arranged. Microfluidic systems, on the other hand, are artificial approach for capillary formation. Non-degradable biomaterials or biodegradable elastomers are used to form durable vasculature. Then, endothelial cells are seeded into

these microchannels, and so microvessels are tried to be developed. By all these recent techniques, pre-defined exact shaped-constructs with desired porosity and interconnectivity are built. Therefore, enhanced vascularization can be provided by these kinds of scaffolds.

Proper scaffold designing provides a better environment for vascularization, and it can be arranged and applied according to each engineered tissue. On the other hand, in this method, vascularization should be derived from host body again. Thus, it still requires long time to vascularization reach into the middle part of scaffolds.

1.4.3.2. Angiogenic Factor Delivery

Vessel formation inside implants can be increased by use of some growth factors which called angiogenic factors (Richardson et al., 2001). These factors stimulate endothelial cells and affect them to combine and form new vessels. VEGF (vascular endothelial growth factor) and bFGF (basic fibroblast growth factor) are the most frequently preferred angiogenic factors by the researchers (Hirschi et al., 2002). However, when these angiogenic factors are used alone, new forming vessels become disorganized and leaky (Jain et al., 2005). To prevent that, some strategies can be used. One of them is delivery of stabilization factors together with angiogenic factors. Naturally, vessels are stabilized by smooth muscle cells and pericytes (generally for capillaries) which are called mural cells together (Hirschi et al., 1999). They organize the vessel structure and provide maturation and stabilization of endothelial cells by suppressing their excess growth. Thus, delivery of angiogenic factors such as VEGF, together with stabilization factors such as PDGF (platelet derived growth factor) which enhances the recruitment of mural cells (Carmeliet, 2000) and induces nicely organized vessel formation (Chen et al., 2007). Another way to have an organized vessel formation is through providing a controlled release of angiogenic factors. If the concentration of angiogenic factors is too low, they cannot induce the vessel formation. On the other hand, if their concentration

becomes too high, they lead to vascular leakage (Zisch et al., 2003). Additionally, excess amount of angiogenic factors may cause differentiation of stem cells (whether in defect site or in implant) into undesired tissue forming cells and harm the healing process. Therefore, providing the optimum concentration is very important to have a functional vasculature.

To regulate the delivery of these growth factors and provide the optimum concentrations some indirect delivery methods can be used. For instance, some factors that stimulate cells around the defect site to produce angiogenic factors may be loaded into implants, therefore the local concentrations of angiogenic factors can be regulated by cells. Studies with sonic hedgehog homolog (SHH) (Pola et al., 2001) and BMP (bone morphogenic protein) (Deckers et al., 2002) showed that these indirect approaches gave better results for vessel organization and stabilization. There are also some studies in which chemokines are loaded into scaffold instead of angiogenic factors. For example, Thevenot et al. (2010) showed that SDF1-alpha triggers diffusion of mesenchymal stem cells and endothelial progenitor cells into defect site and help to start angiogenesis.

Another way to regulate the growth factor concentration is controlled release systems. Since growth factors are not stable *in vivo*, they need to be delivered into defect site locally and with a slow rate. To provide this release strategy, these angiogenic factors are loaded in a biodegradable material such as scaffolds, micro or nanospheres, discs, etc. and released into defect site by a time-dependent delivery system (Ko et al., 1995; Karal-Yılmaz et al., 2011). According to degradation rate of biomaterial, releasing rate of growth factors can be determined.

Gene transfer to enhance vascularization is also another strategy. Cells can be transfected with genes, which produce angiogenic factors, and then they are seeded into scaffolds (Yang et al., 2007). By this method, cells produce growth factors continuously and it can highly promote vascularization. However, this process should be performed

carefully since overexpression of multiple angiogenic genes may lead to instable vessel formation.

To conclude, angiogenic factor delivery is an effective way to increase vascularization. With stabilization factors and controlled delivery approaches, vascularization rate can be arranged. However, vessel growth will still be from host, so again it may not be fast enough if used as the single strategy.

1.4.3.3. Immobilization Strategy

During vascularization process, endothelial cells are aligned end to end to form tubular structure; therefore it is evident that cell-to-cell attachment is highly important in this process. New strategies for vascularization of the tissue engineered constructs focus on immobilization of some proteins or peptides, like extracellular matrix proteins or peptides derived from these proteins, which stimulate angiogenesis. Such immobilization helps to induce cell-cell attachment and to form angiogenic tubular structures with such interaction (Conconi et al., 2010) Specific adhesive peptides enhance the attachment of only endothelial cells, while inhibiting the non-specific bindings. . Immobilization of angiogenic factors to scaffolds by a covalent linkage may also be effective to induce vascularization. Since this covalent linkage will be broken by MMPs or plasmins, which are released by surrounding cells, this technique provides a cell-dependent delivery of angiogenic factors. Therefore, like in the indirect angiogenic factor delivery, formation of more organized vessels has been reported (Figure 4) (Ehrbar et al., 2004).

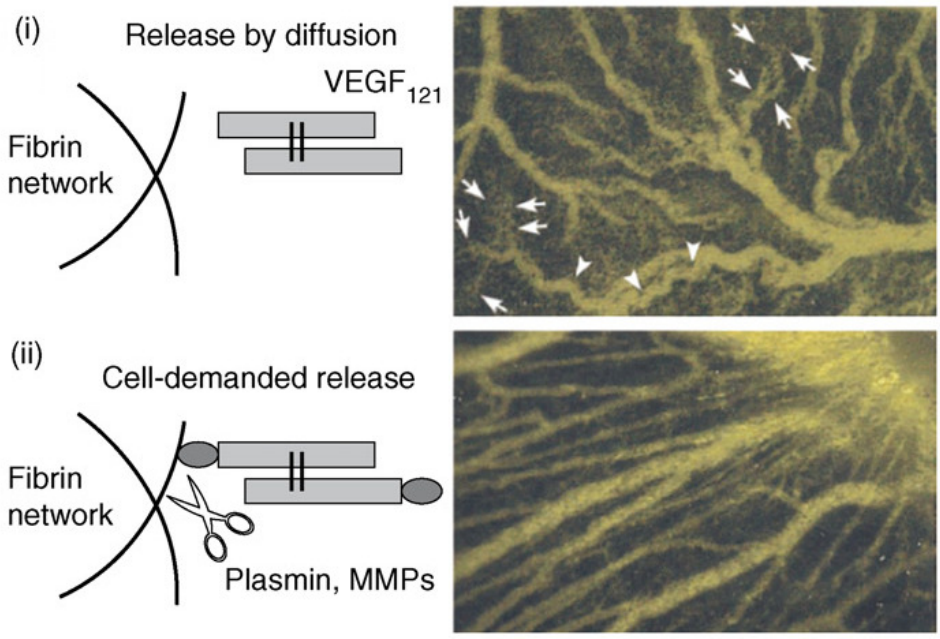

Figure 4. VEGF delivery from fibrin gel scaffold. When VEGF is directly delivered from scaffold by diffusion, newly formed vessels are disorganized, leaky and bad shaped (i). However, if VEGF is released in a cell-dependent way, by plasmin and MMP delivery from cells to digest covalent bond between fibrin and VEGF, vessels are formed as organized and nice shaped structures (ii) (Ehrbar et al., 2004).

1.4.3.4. *In Vivo* Prevascularization

One of the alternative strategies to obtain a functional vasculature in implant is *in vivo* prevascularization (Kneser et al., 2006). In this technique, a scaffold is placed into a healthy region where a transferable vascular axis is present. Since implant will create an inflammation site, host will respond with new vessel formations towards it by angiogenesis from vascular axis. Scaffold is kept here until a complete vascular network is established inside it. Then, it is extracted with surrounding vascular axis. After *in vitro* cell seeding process into scaffold, it is implanted into defect site and both ends of vascular axis are connected to the host vessels microsurgically. Since there is already a vascular network inside the implant, host vessels do not need to reach into the center

part of implant. Thus, vascularization will be rapid and most of cells will stay alive (Figure 5) (Rouwkema et al., 2008).

Although in vivo prevascularization provides very fast anastomose and efficient vascularization, it has some drawbacks too. Firstly, it requires two different surgery operations. Also, finding a proper vascular axis in body is difficult, and some fibrous tissue deposition may occur during prevascularization (Shepherd et al., 2006).

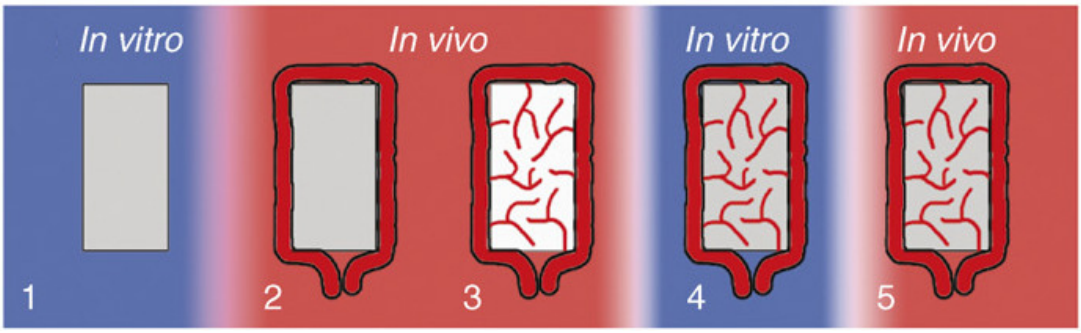

Figure 5. In vivo prevascularization process. 1- Scaffold is prepared in vitro. 2- Scaffold is implanted into a vascular axis. 3- Microcapillaries are extended from vascular axis into the scaffold. 4- Prevascularized scaffolds are explanted with vascular axis 5- Explanted scaffolds are implanted to defect site and anastomosis of vascular axis with host vessels are provided surgically (Rouwkema et al., 2008).

1.4.3.5. *In Vitro* Prevascularization

One of the recent methods used for functional vascularization of implants is *in vitro* prevascularization (Rouwkema et al., 2006; Caspi et al., 2007). In this method, endothelial cells responsible for the formation of capillaries are used. They can create networks when cultured *in vitro,* too. In 3D scaffolds, together with tissue forming cells, they can form tubular structures, which can be thought as capillary network. After capillary network is formed by endothelial cells *in vitro* and tissue forming cells were

seeded, scaffold is implanted into defect site, and host vessels anastomose with capillaries in the scaffold (Figure 6).

Like *in vivo* prevascularization, it is enough for host vessels to reach just outside of scaffold in this method too. Therefore, vascularization process is short since host vessels are not necessary to enter to the middle part of scaffold.

One disadvantage of this method compared with *in vivo* vascularization is the lack of a vascular axis. Since there is no big vessel which surrounds scaffold, there are many capillary ends which should be fused with host vessels. Thus, anastomose in this process is slower than that *in vivo* prevascularization. Another difficult point for this technique is complicated process of vessel formation *in vitro* and finding a proper medium for both endothelial cells and tissue forming cells. On the other hand, since there is no need for extra surgery operation and finding a proper vascular axis, *in vitro* prevascularization is easier and more practical and performable than *in vivo* prevascularization. Also, in many studies, it was shown that extra growth factor addition is not needed for organization of endothelial cells for vessel formation *in vitro* (Shepherd et al., 2006; Rouwkema et al., 2006).

As the cell source, endothelial cells have low proliferation rates, and they are various in genotypic and phenotypic properties. Thus, instead of using endothelial cells directly, endothelial progenitor cells (EPC's) which can be derived from bone marrow, peripheral blood and fat cells can be used for tissue engineering purposes. EPC's can migrate to defect site easier than EC's and they can be differentiated to endothelial cells under proper conditions (Yamahara and Itoh, 2009).

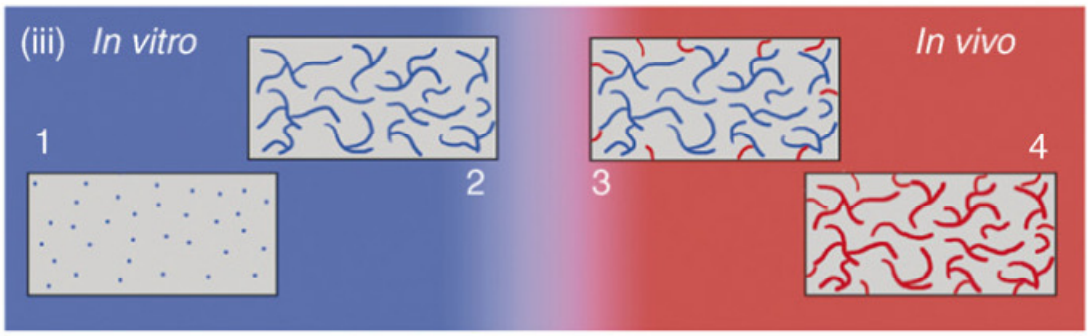

Figure 6. In vitro prevascularization process. 1- Endothelial cells are seeded into scaffold in vitro (together with fibroblasts and required tissue progenitor cells which are not shown here). 2- Microcapillary formation by endothelial cells inside the scaffold. 3- Scaffold is implanted into defect site, and microcapillaries anastomose with host vessels (red ones). 4- Pre-formed vessels are connected with host vasculature entirely and perfusion occurs. (Rouwkema et al., 2008)

Some additional techniques have been used to enhance *in vitro* vascularization. In a study, researchers decellularized a vascular bladder tissue of a porcine (Schultheiss et al., 2005). Then, they seeded urothelial cells and smooth muscle cells together with endothelial progenitor cells on these decellularized constructs. It was shown that such strategy led to *in vitro* vascular network formation inside this structure. These microvessels could be connected to host vessels. Since matrix is natural, adaptation to tissue is easier. Therefore, vascularization and anastomose after implantation were enhanced.

1.5. Decellularization of Tissues

In tissue engineering applications, scaffolds are desired to have similar physical and mechanical properties with natural tissue. Therefore, in many applications, extracellular matrix (ECM) of natural tissues which are obtained by decellularization of required tissue from any other organism, are used as scaffolds. In this process, there are some

important issues which should be cared. These are mainly, preservation of biological composition, mechanical properties and sometimes retention of 3D structure (Badylak et al., 2009; Uygun et al., 2010). Basically, decellularization process consists of lysing cells in the tissue and removing all cell remnants from tissue to prevent any immunological reaction. Physical, chemical and biological methods can be used for decellularization (Table 3).

1.5.1. Physical Decellularization

Physical methods such as freeze-thaw cycles and mechanical forces can be used to decellularize tissues. In these methods, a force that disrupts cell membrane is applied.

Freeze-thaw method is based on rapid changes in temperature of tissue by freezing and thawing cycles. Cell membranes are disrupted during these cycles, and cells are lysed. It causes small disruptions in extracellular matrix and minor loss of ECM proteins (Prasertsung et al., 2008). However, after freeze-thaw process, cell remnants are remained inside tissue. Therefore, it is usually not used alone, instead it accompanies to another decellularization method. Also, hard tissues are more resistant to temperature changes. Thus, it is generally used for soft and thin tissues.

As mechanical force, generally hydrostatic pressure is applied on tissue directly. It is highly effective to disrupt cells, and its process time is shorter when compared with other decellularization methods. However, it is not very effective on tissues, which are densely packed with ECM. This method is also not enough alone for many tissues. It is more effective when combined with enzymatic methods (Hopkinson et al., 2008).

1.5.2. Chemical Decellularization

Another way for decellularization of tissues is using chemicals. Many chemicals give damage to both cell membrane and cellular components. Thus, most decellularization protocols include use of at least one chemical.

Most acids and bases can be used in decellularization since they create damage in cell membrane and solubilize intracellular components including nucleic acids. For example, peracetic acid, acetic acid, hydrochloric acid and sulphuric acid very effective to remove nucleic acid remnants and they give minor damage to ECM (Freytes et al., 2004; Falke et al., 2003; Probst et al., 1997; De Filippo et al., 2002). However, bases such as sodium hydroxide, calcium hydroxide, etc. are more disruptive and give damage to ECM; also they solubilize growth factors in a very efficient way.

Detergents are another group of chemicals that are used to decellularize tissues. There are non-ionic, ionic and zwitterionic detergents. Non-ionic detergents such as Triton X-100 have mild effects compared to others. Their main targets are lipid-lipid and lipid-protein interactions, thus they are more effective in delipidation processes. Since they don't affect protein-protein interactions, extracellular matrix proteins remain functional after decellularization process (Seddon et al., 2004). On the other hand, ionic detergents such as sodium dodecyl sulfate (SDS) and sodium deoxycholate are harsher than non-ionic ones. They are highly effective in removing cell remnants and nuclei from dense tissues. However, detergents also give harm to the ECM proteins; they disrupt the tissue structure of ECM and eliminate growth factors (Reing et al., 2010). Lastly, zwitterionic detergents such as 3-[(3-cholamidopropyl)dimethylammonio]-1-propanesulfonate (CHAPS), have effects in between ionic and non-ionic ones. They are not mild as non-ionic detergents and not harsh as ionic detergents. They are usually used for decellularization of thinner tissues such as lung (Petersen et al., 2010), while they are not so effective for thicker ones (Gui et al., 2010).

Alternatively, hypotonic and hypertonic solutions can be used. Hypotonic solutions such as deionized water or other low ionic strength solutions cause cell lysis (Dahl et al., 2003). Hypertonic solutions prevent nucleic acid binding to proteins (Cox and Emili, 2006). Thus, several cycles of keeping samples in hypotonic and hypertonic solutions are effective for decellularization.

Another group is alcohols, which cause cell lysis by dehydration. They are also highly effective in tissue delipidation, even more effective than lipase (Crapo et al., 2011). Ethanol, methanol and isopropanol are the most common alcohols used for delipidation especially during adipose tissue decellularization (Brown et al., 2011). However, alcohols may lead crosslinking of proteins and so disruption in tissue structure (Gorschewsky et al., 2005).

1.5.3. Biological Decellularization

There are also biological materials, which can be used in decellularization protocols. Both extracellular and intracellular components can be affected by biological agents. Enzymes such as proteases, nucleases and lipase are commonly used for decellularization processes. Proteases such as try sin, collagens and dispose are frequently used since they disrupt ECM and allow cell removal. Trypsin is usually used as an initial digestion process in decellularization of tissue since it is a slow agent for cell removal. However, long exposure can give damage to ECM structure (Yang et al., 2010). Collagenase specifically digests collagen in ECM, so it is used for decellularization when collagen content of final product is not very important (Crapo et al., 2011). Dispase is more effective for decellularization when compared to trypsin; however it gives more damage to ECM hierarchical structure (Prasertsung et al., 2008). On the other hand, nucleases, especially endonucleases such as DNase and RNase are used to remove residual nucleic acids after cell lysis, so they are usually used together

with other agents (Petersen et al., 2010). Lipase is also not used alone usually, since it removes only lipids inside tissue (Brown et al., 2011).

Chelating agents such as EDTA and EGTA are used to facilitate decellularization. These agents bind divalent cations such as Ca^{+2} and Mg^{+2},which are required for attachment of cells to collagen or other ECM molecules (Klebe, 1974).

Protease inhibitors can be used in decellularization protocols to increase efficiency. During decellularization process, proteases, which are normally found inside cells are delivered to ECM since cells are lysed. These proteases digest ECM proteins and disrupt its structure. Thus, protease inhibitors such aprotonin, leupeptin, pepstatin, PMSF and sodium orthovanadate are used to inhibit activities of these proteases and protect ECM structure (Gilbert et al., 2006).

Table 3. Physical, chemical and enzymatic methods and agents for tissue decellularization and their effects (Gilbert et al., 2006).

Method	Mode of action	Effects on ECM
Physical		
Snap freezing	Intracellular ice crystals disrupt cell membrane	ECM can be disrupted or fractured during rapid freezing
Mechanical force	Pressure can burst cells and tissue removal eliminates cells	Mechanical force can cause damage to ECM
Mechanical agitation	Can cause cell lysis, but more commonly used to facilitate chemical exposure and cellular material removal	Aggressive agitation or sonication can disrupt ECM as the cellular material is removed
Chemical		
Alkaline; acid	Solubilizes cytoplasmic components of cells; disrupts nucleic acids	Removes GAGs
Non-ionic detergents; Triton X-100	Disrupts lipid–lipid and lipid–protein interactions, while leaving protein–protein interactions intact	Mixed results; efficiency dependent on tissue, removes GAGs
Ionic detergents; Sodium dodecyl sulfate (SDS)	Solubilize cytoplasmic and nuclear cellular membranes; tend to denature proteins	Removes nuclear remnants and cytoplasmic proteins; tends to disrupt native tissue structure, remove GAGs and damage collagen
Sodium deoxycholate		More disruptive to tissue structure than SDS
Triton X-200		Yielded efficient cell removal when used with zwitterionic detergents
Zwitterionic detergents; CHAPS	Exhibit properties of non-ionic and ionic detergents	Efficient cell removal with ECM disruption similar to that of Triton X-100
Sulfobetaine-10 and -16 (SB-10, SB-16)	Yielded cell removal and mild ECM disruption with Triton X-200	
Tri(n-butyl)phosphate	Organic solvent that disrupts protein–protein interactions	Variable cell removal; loss of collagen content, although effect on mechanical properties was minimal
Hypotonic and hypertonic solutions	Cell lysis by osmotic shock	Efficient for cell lysis, but does not effectively remove the cellular remnants
EDTA, EGTA	Chelating agents that bind divalent metallic ions, thereby disrupting cell adhesion to ECM	No isolated exposure, typically used with
Enzymatic		
Trypsin	Cleaves peptide bonds on the C-side of Arg and Lys	Prolonged exposure can disrupt ECM structure, removes laminin, fibronectin, elastin, and GAGs
Endonucleases	Catalyze the hydrolysis of the interior bonds of ribonucleotide and deoxyribonucleotide chains	Difficult to remove from the tissue and could invoke an immune response
Exonucleases	Catalyze the hydrolysis of the terminal bonds of ribonucleotide and deoxyribonucleotide chains	

1.6. Aim of the Study

In this thesis, the main purpose is to develop a functional vascularized adipose tissue surrounding a blood vessel when there is extensive loss of tissues due to cancer related surgeries, traumatic events, etc. The constructs were silk fibroin and decellularized adipose tissue (DAT) matrix based hydrogels with entrapped endothelial cells and preadipocytes differentiated from adipose derived stem cells.

In the first part of thesis, we aimed to develop a hydrogel composite having optimum properties for use in adipose tissue engineering. For this purpose, ECM matrix was obtained by decellularization of adipose tissue (DAT) extracts. Then, a hydrogel was prepared mixing DAT with different ratios of fibroin. Before gelation, both endothelial cells and preadipocyte cells pre-differentiated from adipose derived stem cells were added to the mixture to achieve a capillary network via endothelial cells, and to obtain adipocytes from adipose derived stem cells for a functional adipose tissue *in vitro*.

In the second part, the aim was to create a vascularized adipose tissue *in vivo*. For this purpose, fibroin and DAT based hydrogels with entrapped endothelial cells and preadipocytes were placed around a blood vessel in rats. It is thought that this vessel will be the main vessel, which feed whole implant, and a capillary network formed by encapsulated endothelial cells will anastomose to the main vessel. Therefore, a highly distributed vascular network will be formed inside the implant, and both nutrients and oxygen will be distributed through the whole implant. By this way, it is expected to have a functional thick adipose tissue and retain its functionality in vivo.

CHAPTER 2

MATERIALS AND METHODS

2.1 Materials

Rat adipose tissue was obtained from Gülhane Military Medical Academy (Ankara, Turkey). Human lipoaspirates were obtanied from Çağ Hastanesi (Ankara, Turkey). Silkworm cocoons were purchased from a local silk factory (Bursa, Turkey). SDS, sodium deoxycholate, lipase, colipase, DNase, RNase, pepsin, BCA, BSA, DMMB, ChS, Bovine collagen type I from bovine achilles tendon, Direct Red 80, Hoechst 33258, calf thymus DNA, Na_2EDTA, Oil Red O, isopropyl alcohol, paraformaldehyde, glycerol, methanol, glacial acetic acid, RPMI, sodium bicarbonate, collagenase type I, IBMX, dexamethasone, insulin, indomethacin, and Matrigel were purchased from Sigma-Aldrich (USA). Tris, 2-mercaptoethanol, bromophenol blue, Acrylamide/Bis solution, TEMED, APS and Coomassie Brilliant Blue R-250 were the products of Bio-Rad (USA). Fermentas SM1811 pre-stained protein ladder was purchased from Thermo Fischer Scientific (USA). DAPI and Presto Blue were purchased from Invitrogen (Germany). DMEM-low glucose, FBS, Pen/Strep and Trypsin/EDTA were purchased from Biochrom (Germany). Na_2HPO_4, Na_2EDTA, Na_2CO_3, NaCl, NaOH, Glycine and LiBr were obtained from Merck Millipore (Germany). 100-µm cell strainers were the products of BD Biosciences (USA). EGM-2 was obtained from Lonza (Switzerland). FITC-conjugated anti-vWF antibody and VEGF was purchased from Abcam (UK). Cell culture plastic-wares were the products of Orange Scientific (Germany).

2.2. Methods

2.2.1. Decellularization and Solubilization of Adipose Tissue

In order to decellularize the adipose tissue, human adipose tissue samples were obtained from patients who had lipoaspiration operations for aesthetic or medical purposes. Samples were obtained with the consent of patients and after getting ethical approval from the Human Ethics Committee of Middle East Technical University (28620816/341-2653). Adipose tissue was decellularized with a modified protocol of Young et al. (2011). Aliquots (50 mL) of lipoaspirates were put into centrifuge tubes and stored at -80^{o}C until decellularization process. Frozen tissue was thawed slowly at room temperature. It was washed by stirring in PBS for 2h. The tissue was strained and decellularized in 1% SDS solution by stirring for 2h. After the decellularization step, tissue was strained again and delipidized enzymatically by keeping in PBS solution which contains 2.5 mM sodium deoxycholate, 100 µg/mL lipase and 50 ng/mL colipase. Tissue matrix was kept in this solution until yellow color was totally removed and white color was observed (12-24h). Then, the decellularized tissue was incubated in solution containing DNase (1 µg/mL) and RNase (50 µg/mL) to remove any remaining DNA fragments. Lastly, it was washed by stirring in dH_2O for 2h and frozen at -80^{o}C. Then, frozen matrix was lyophilized for 6-8h.

After ethylene oxide (EtO) sterilization, obtained decellularized adipose tissue (DAT) powder was dissolved in pepsin/HCl solution. 1 mg pepsin was used for 10 mg of lyophilized matrix (2 mg/mL in 0.1M HCl). DAT matrix was awaited in pepsin/HCl at 37 ^{o}C until it was completely dissolved (2-3h). pH was then raised to 7.4 by 1 M NaOH, and 10X PBS was added until it was diluted to 1X PBS. Final concentration of DAT was set to around 15 mg/mL for minimization of variations due to protein contents in further experiments.

2.2.2. Characterization of Decellularized Adipose Tissue

2.2.2.1. Bicinchoninic Acid (BCA) Total Protein Assay

Protein content of DAT was determined by BCA protein assay. BCA working solution was prepared by mixing BCA with 4% $CuSO_4.5H_2O$ at a volume ratio of 50:1. Calibration curve was constructed in an interval of 0 to 1 mg/mL using Bovine Serum Albumin (BSA) as standard. BSA standards were prepared in Pepsin/HCl buffer in which DAT was solubilized. Standards (20 µL) and diluted samples (20 µL) were mixed with 200 µL of BCA working solution and kept at 60^{o}C for 15 min in dark. The measurements of optical densities were done at 562 nm using ELISA micro-plate reader (mQuant, BioTek Instruments, Winooski, VT).

2.2.2.2. Total Sulfated Glycosaminoglycan (sGAG) Assay

Total sGAG content of DAT samples was determined using dimethyl methylene blue (DMMB) assay (Farndale et al., 1986). Glycine/NaCl solution was prepared by dissolving 3.04 g of glycine, 2.37 g of NaCl and 95 mL of 0.1M HCl in dH_2O with a total volume of 1L and at final pH of 3. DMMB dye solution was prepared by dissolving DMMB in glycine/NaCl solution at a concentration of 16 µg/mL. PBE buffer was prepared by dissolving 7.1 g of Na_2HPO_4 and 1.86 g of Na_2EDTA in 500 mL of dH_2O and final pH was set to 6.5. Then, chondroitin sulfate (ChS) standards were prepared for the calibration curve in a concentration range of 0-100 µg/mL. For preparing standards, 0.0875 g cysteine was firstly dissolved in 50 mL of PBE buffer and filtered. Then, 50 mg of ChS was added in 1 mL of PBE/Cys solution. 0.1 mL of this solution was added to 49.9 mL of PBE buffer to have a stock standard solution (100 µg/mL). The other standard solutions were obtained from stock solution by dilutions. Then, 50 µl of standards and samples were mixed with 1.25 mL of DMMB dye solution, and

absorbance values were obtained immediately at 525 nm in a spectrophotometer (Hitachi U-2800A, Hitachi High-Tech. Corp., Tokyo, Japan).

2.2.2.3. Total Collagen Assay

Collagen content of DAT was determined with Sirius red assay (Tullberg-Reinert and Jundt, 1999). Dye solution was prepared by dissolving Direct Red in dH_2O (100 µg/mL) and adding Picric acid (3 µL/mL) . Then, 0.1N NaOH was added to bring pH to 3.5. Bovine collagen dissolved in 0.5M acetic acid at different concentrations (0-1000 µg/mL) were used to construct the calibration curve. Samples (100 µL) and standards (100 µL) were dried in 96-well plate by keeping at 37°C for 24-48h. Then, 100 µL dye solution was added to wells, and plate was shaken in a shaker for 1h. Afterwards, dye was discarded, and wells were washed with 0.01 M HCl twice. Finally, 100 µL of 0.1N NaOH was added into wells, and optical densities were obtained at 550 nm in micro-plate reader (mQuant, BioTek Instruments, Winooski, VT).

2.2.2.4. DNA Quantitation

DNA content of decellularized adipose tissue was determined using Hoechst. For this assay, stock solutions of Hoechst 33258 and TNE buffer were prepared. 1 mg/mL Hoechst 33258 stock solution was prepared in dH_2O, which can be stored in dark at 4°C for up to 6 months. Then, 10X TNE buffer stock solution which can be stored at 4 °C up to 3 months was prepared by dissolving 1.211 g of Tris base, 0.372 g of Na_2EDTA and 11.67 g of NaCl in 100 mL of dH_2O. pH was adjusted to 7.4 with concentrated HCl. It was filtered before use. 10 mL of 10X TNE buffer was diluted with 90 mL of filtered dH_2O to obtain 1X TNE buffer. Just before the assay, 2X dye solution (200 ng/mL) was prepared by mixing 20 µL Hoechst 33258 stock solution with 100 mL of 1X TNE buffer. 2X DNA standards at different concentrations (20 to 2000 ng/mL) were prepared

via dilutions of calf thymus DNA solution in TNE buffer for constructing the calibration curve. 1X TNE buffer was used as blank solution.

For the assay, DAT solutions were diluted 10 times with TNE buffer. Then, 1 mL of each 2X DNA standard solution, blank and DAT samples were mixed with 1 mL of 2X dye solution in cuvettes, and RFU values were read in fluorometer (Modulus Single Tube Operating Manual, Turner Biosystems, Canada) by using UV channel. The DNA content of decellularized matrix was determined using the calibration curve constructed.

2.2.2.5. Decellularization Confirmation by DAPI Staining

Tissue sections were taken from both unprocessed adipose tissue and decellularized adipose tissue after SDS and Lipase/Colipase treatments via cryomicrotome (METU Central Lab, Turkey). The tissues were firstly fixed in 4% paraformaldehyde solution for 10-15 min. They were then washed with PBS for 3 times. Sections were kept for 3-5 min in the working solution of DAPI (1 µg/mL). After incubation, they were washed with PBS for 3 times again, and images were taken by using a fluorescence microscope (Nikon Eclipse TS100, Japan).

2.2.2.6. Delipidization Confirmation by Oil Red O Staining

Oil Red O staining was performed to analyze the lipid content of the DAT samples. The day before the staining procedure, Oil Red O stock solution was prepared by dissolving 0.62 g of Oil Red O in 125 mL isopropyl alcohol. Solution was stirred on a magnetic stirrer for 2 hours, and it was kept overnight at room temperature. After calculating how much solution will be used for staining procedure, Oil Red O working solution was prepared by mixing stock solution and distilled water in 3:2 ratio (e.g. 12 mL stock solution + 8 mL dH_2O).

Tissue sections were obtained from unprocessed adipose tissue and enzymatically delipidized adipose tissue via cryomicrotome (METU Central Lab, Turkey). They were fixed in 4% paraformaldehyde solution for 10-15 min. Fixed tissue sections were washed first with dH_2O and 60% isopropanol. Then, sections were kept in Oil Red O working solution for 15-20 min, and washed again with dH_2O and 60% isopropanol. Stained tissue sections were mounted with 10% glycerol in PBS, and microscopic analyses were performed.

2.2.2.7. SDS PAGE Analysis of Decellularized Matrix

Molecular weights of peptides present in solubilized DAT samples were analyzed by SDS PAGE method. First, 3X SDS loading buffer was prepared with 1 M Tris/HCl (pH 6.8, 0.18M as final concentration), SDS (6%, w/v), glycerol (30%, v/v), 2-mercaptoethanol (15%, v/v), bromophenol blue (0.01%, w/v) and dH_2O. Samples were boiled in 3X SDS loading buffer at 95^{o}C for 7 min. Then, samples were loaded on 4% stacking gel, and separated on 12% separating gel by running at 200 V for 2h. 4% stacking gel was prepared by diluting 30% Acrylamide/Bis solution (Bio-Rad, USA) with the addition of 0.5 M Tris/HCl (pH 6.8, 0.125 M as final concentration), 0.1% sodium dodecyl sulphate (SDS, w/v%), dH_2O, Tetramethylethylenediamine (TEMED 0.1%, v/v) and Ammonium persulfate (APS 0.05%, w/v). 12% (w/v) separating gel was prepared again by diluting 30% Acrylamide/Bis solution with addition of 1.5 M Tris/HCl (pH 8.8, 0.375 M as final concentration), SDS (0.1%, w/v), dH_2O, TEMED (0.1%, v/v) and APS (0.05%, w/v). Electrophoresis running buffer was prepared with Tris (3%, w/v), glycine (1.44%, w/v) and SDS (0.1%, w/v) in dH_2O (pH 8.3). Fermentas SM1811 pre-stained protein ladder (Thermo Fischer Scientific, USA) was used as ladder and collagen type I from bovine achilles tendon (Sigma, USA) was used to compare peptide bands with DAT samples. Gel was stained with Coomassie Brilliant Blue R-250 (Bio-Rad, USA) for 20 min after microwaving. It was destained in a solution containing

50% dH_2O, 40% methanol, and 10% glacial acetic acid until background color was removed.

2.2.3. Fibroin Extraction from Silkworm Cocoons

Fibroin was extracted from silkworm cocoon by the protocol offered by Rockwood et al (2011). Briefly, silkworm cocoons were cut into small pieces. They were boiled in 0.02 M Na_2CO_3 solution for 30 min. Silk fibers were rinsed with dH_2O three times, each for 20 min. They were squeezed and dried at 37°C for 24 h. Then, 9.3 M LiBr solution was added onto silk fibers and incubated at 60°C for 4h. Silk in LiBr solution was put in a dialysis tube and dialyzed against dH_2O for 48h under continuous stirring with 4-5 times changes of water. Silk solution was removed from dialysis tube and put into a 50 mL-centrifuge tube. It was centrifuged for 20 min twice and supernatant was stored at 4°C. By this method, 7-8% (w/v) fibroin solution was obtained. Fibroin solution was sterilized by autoclaving at 121°C for 20 min.

2.2.4. Preparation of Fibroin and Decellularized Matrix Hydrogels

Solubilized decellularized adipose tissue (DAT) and 8% fibroin solution were mixed in 3:1, 1:1 and 1:3 (v/v) ratios. Then, 10X RPMI solution was added to mixture at a 1:9 ratio to obtain 1X RPMI. pH was adjusted to 7.4 with sodium bicarbonate. 900 μL of the final mixture was taken into a 1.5 mL centrifuge tube and vortexed for 7 minutes at maximum speed. It was let to polymerize for 2 minutes, and then vortexed for 1 more minute. If any white solid particles were formed, they were removed from the mixture and rest of it was let to form gel at 37°C. Gelation was checked by tilting the tube, and time of gelation was noted.

2.2.4.1. Mechanical Tests

Mechanical properties of hydrogels with different DAT to fibroin (Fib) ratios and natural subcutaneous adipose tissue samples were studied by unconfined compression tests. A rectangular mold with 4 mm height was prepared via glass plates and glass slides. DAT:Fib:RPMI mixtures were vortexed and poured into this mold. After gelation, 1 cm-diameter discs were obtained with a punch and put in a small petri dish filled with PBS. Subcutaneous adipose tissue was tried to be cut as discs. Compression test to 30% strain limit was performed via Lloyd LR50K machine (Lloyd Instruments, UK) with a 3 mm/min speed and 0.02 N preload was applied to samples during the test. Initial, transition and final Young's moduli of samples were calculated and compared with those of natural tissue.

2.2.4.2. *In Vitro* Degradation Tests

Degradation profiles of hydrogels with different DAT to fibroin ratios were analyzed by measuring wet weight change in time. 3 copies were prepared from each type of hydrogels which are only fibroin, DAT:Fib - 3:1, DAT:Fib - 1:1 and DAT:Fib - 1:3. To prepare hydrogels, glass molds which are prepared for mechanical tests were used. 1 cm-diameter discs were taken with a punch and placed in wells of 12-well plates. Each well was filled with PBS, and plate was placed into a shaking water bath at 37^{o}C. To measure weight change for 14 days, hydrogels were removed from wells every second days, and weighed after dried only from outside with a filter paper. PBS was changed after each weighing.

2.2.5. Cell Culture Studies

2.2.5.1. Adipose Derived Stem Cell (ASCs) Isolation

Ethical approval for the use of rats for adipose derived stem cell isolation was obtained from GATA Animal Ethical Commitee. Rat adipose tissue was extracted from rat groins at Gülhane Military Medical Academy (GATA, Ankara). It was cut into small pieces and washed in PBS to remove blood and other contaminants. Then, adipose tissue was enzymatically digested for 1h in 0.075% collagenase type I (Sigma, USA) in PBS at 37^{o}C. The volume of collagenase solution was almost equal with the volume of adipose tissue. Digested samples were centrifuged at 1200 g for 5 min, and the supernatant was then removed. Pellets were resuspended in DMEM-low glucose containing 10% FBS and 0.5% Pen/Strep, and strained through 100-µm filter to remove tissue debris. Finally, cells were seeded in a 25 cm^2 plate and kept for 3 days without changing medium. Then, plate was washed with PBS to remove contaminants and non-adherent cells, and medium was replenished once every 2-3 days. Before differentiation, cells at passage 4 were characterized by FACS analyses for their stemness by staining with anti-rat CD11, CD31, CD45 and CD90 antibodies. Staining procedure was explained in the Section 2.2.5.1.1.

2.2.5.1.1. Flow Cytometry Analysis

ASCs were analyzed by FACS analysis to confirm stemness. Anti-CD11, anti-CD31, anti-CD45 and anti CD-90 antibodies were used for analysis. Firstly, cells were trypsinized and centrifuged at 3000 rpm for 5 minutes. Supernatant was discarded and pellet was washed with FACS buffer (PBS with 1% BSA and 0.1% sodium azide), and cells were centrifuged again. Then, 100 µL of fixation solution (4% paraformaldehyde) was put on cells, vortexed and kept for 15 minutes. After fixation, cells were washed with FACS buffer two times by centrifuging, discarding supernatant and resuspending pellet. After last centrifuge, pellet was resuspended in 2 mL of FACS buffer. Then, cells

were aliquoted into 100 µL samples. Primary antibodies were added into aliquots as 1 µg/mL, and kept for 30 minutes at dark. Secondary antibodies were added into aliquots as 1 µg/mL, and kept for 30 minutes at dark. Then, 1 mL of PBS without BSA or sodium azide was added on cells and centrifuged. Pellet was resuspended in 300-400 µL of PBS, and taken for the reading via flow cytometer (BD Accuri C6 Flow Cytometer, BD Biosciences, USA). Gating was done by the reference of unstained ASCs, and mouse isotype IgG was used as control for the experimental antibodies.

2.2.5.2. Adipogenic Differentiation of ASCs

Cells from third passage were seeded on 12-well plates in DMEM-low glucose containing 10% FBS and 0.5% Pen/Strep at a density of 50.000 cells/cm^2. When cells reached almost 90% confluency, they were induced for adipogenic differentiation by changing medium with DMEM-high glucose containing 10% FBS, 0.5% Pen/Strep, 0.5 mM 3-isobutyl-1-methylxanthine (IBMX), 1 µM dexamethasone, 10 µg/mL insulin and 100 µM indomethacin. Medium was replenished once every 2-3 days. Adipogenic differentiation was assessed via Oil Red-O staining after 3 weeks.

2.2.5.3. Endothelial Differentiation

Cells from third passage were seeded at a density of 40.000 cells/cm^2 on gelatin-coated 12-well plates and cultivated in DMEM-low glucose containing 10% FBS and 0.5% Pen/Strep. After 24h, they were induced for endothelial differentiation by changing medium with EGM-2 (Endothelial Growth Medium-2) containing 2% FBS, EGF, bFGF, IGF-1, VEGF, hydrocortisone, ascorbic acid, heparin, gentamicin and amphotericin-B (Lonza, Switzerland). Also, extra VEGF (50 ng/mL) was added to EGM-2 media to enhance differentiation. After 2 weeks in static culture, plates were placed on an orbital shaker and subjected to shear stress at 150 rpm for 2 days at 37^{o}C in a carbon dioxide incubator. During whole process medium was replenished every 2-3 days. Endothelial

differentiation was assessed via three different methods which are cell orientation under shear stress, cord formation on Matrigel, immunofluorescent staining with FITC-conjugated anti-vWF antibodies.

2.2.5.3.1. Cell Orientation Under Shear Stress

Change in cell orientation for cells cultivated under shear stress was studied to characterize endothelial differentiated cells. Both undifferentiated and differentiated cells were seeded on 6-well plates with a density of 50.000 cells/cm^2, and exposed to shear force by growing on an orbital shaker for 2 days. Then, the orientation of cells with respect to any shaking direction axis were checked.

2.2.5.3.2. Cord Formation on Matrigel

Cord formation property of cells was analyzed as another characteristic for endothelial differentiation. Surface of the wells in a 96-well plate were covered with 30 µL of Matrigel, and left for gelation at 37^oC for 30 min. Then, both undifferentiated and differentiated cells were seeded on 96-well plates as 10.000 cells/well. After 16h, cells were checked for cord formations by microscopic examinations.

2.2.5.3.3. Immunofluorescent Staining

Endothelial differentiation was also analyzed by specific immunofluorescent staining. After washing with PBS, cells were fixed with 4% paraformaldehyde for 10-15 min, and washed again with PBS. They were permeabilized with 0.1% Triton X-100 for 3-5 min. Then, cells were blocked with 1% BSA in PBST (0.05% Tween 20 in PBS) with 0.3M Glycine for 30 min. After this step, blocking solution was removed, but cells were not washed. They were incubated with 1:100 diluted FITC-conjugated anti-vWF antibody (Abcam, UK) for 1h in room temperature. After washing with PBS, for nuclei staining, cells were incubated with 0.2 µg/mL of DAPI (Invitrogen, USA) for 2-3 min. Then, they

were washed again, mounted with 70% glycerol in PBS, and analyzed under fluorescence microscope (Nikon Eclipse TS100, Japan).

2.2.5.4. Coculture of Adipogenic and Endothelial Differentiated Cells

Coculture of adipogenic and endothelial differentiated cells was performed to see the effects of each cell type on other's differentiation process. ASCs were kept separately in adipogenic induction medium (AIM) and endothelial induction medium (EIM) for 7 days. Then, both types of cells were trypsinized and seeded on same wells with a 1:2 cell number ratio for adipogenic to endothelial cells. As culture medium AIM and EIM 1:1 mixture was used. On days 7 and 14, cells were stained with Oil Red O and FITC-conjugated anti-vWF antibody for observation of adipogenic and endothelial characteristics, respectively. Also, after 14 days of incubation, cells were subjected to shear force by keeping plate on orbital shaker at 150 rpm for 2 days, and then, they were observed under microscope (Nikon Eclipse TS100, Japan).

2.2.5.5. Cell Attachment and Proliferation Tests on Hydrogels

To study the attachment and proliferation, on DAT:Fib membranes viability measurements were performed. DAT:Fib mixtures were vortexed, poured into wells of a 96-well plate and let to be gelled. After that, adipose derived stem cells (ASCs) were seeded on hydrogels at two different seeding densities: 5.000/well and 50.000/well. Monolayer cultures seeded on tissue culture plate (TCP) with same cell numbers were used as positive control. Cell proliferation on DAT:Fibroin hydrogels was measured with Presto Blue (Invitrogen, USA). Presto Blue was added as 1:9 (v/v) ratio to the culture medium, and kept for minimum of 2h. Then, absorbances were measured at 562 nm using a micro-plate reader (mQuant, BioTek Instruments, Winooski, VT). Empty DMEM was used as negative control for cells seeded on tissue culture plates (TCPS), and cell-free hydrogels were used as negative control for cells seeded on hydrogels.

Therefore, absorbance values of negative controls were substracted from absorbance values of each group to obtain normalized values. Cell viability on TCPS were accepted as 100% viability, and relative viability for each hydrogel group was calculated by comparing normalized absorbance values for growth on hydrogels with those for growth on TCPS.

2.2.5.6 Cell Encapsulation in Hydrogels

ASCs ($1x10^6$ cells/mL) were added to the DAT:Fibroin:RPMI mixtures shortly after vortexing. 50 µL of this mixture was poured in wells of 96-well plate, and kept at 37^oC until gelation. 3:1, 1:1 and 1:3 ratios of DAT:Fibroin were the experimental groups and hydrogels without cells were used as negative controls. At different incubation times cell proliferation was assessed using Presto Blue cell viability assay. Presto Blue dye was added as 1:9 (v/v) ratio to the culture medium, and kept for around 10h. Empty DMEM was used as negative control for cells seeded on TCPS, and cell-free hydrogels were used as negative control for cells encapsulated in hydrogels. The absorbance values of negative controls were substracted from absorbance values of each group to obtain normalized values. Viability on tissue culture plate (TCPS) were accepted as 100% viability, and relative viabilities were calculated by comparing absorbance values for growth in hydrogels with those for growth on TCPS.

Also, to be able to observe cell viablity in hydrogels, Calcein-AM & Propidium Iodide staining was performed. ASCs were encapsulated into 1:3 and 1:1 - DAT:Fib hydrogels at a final cell density of 1 million/mL and 5 million/mL. After 1 and 7 days of incubation, staining was performed. Briefly, media on hydrogels were removed. They were washed with PBS for three times. staining solution (PBS with 10 µM Calcein-AM and 2 µM Propidium Iodide) was added on hydrogels, and kept for 30 minutes. Then, staining solution was removed and hydrogels were washed with PBS for three times. They were analyzed under fluorescent microscope (Nikon Eclipse TS100, Japan).

2.2.5.7. Differentiation Analyses in Hydrogels

To determine the effects of hydrogels on adipogenic differentiation of ASCs, adipogenic differentiation in hydrogels were investigated. Firstly, adipogenic differentiation of monolayer culture of ASCs was induced for 1 week via differentiation medium mentioned above. Then, cells were trypsinized and encapsulated into 1:3 and 1:1 - DAT:Fib hydrogels. After encapsulation, hydrogels were kept in adipogenic maintenance medium (AMM) (DMEM-low glucose with 10% FBS, 0.5% Pen/Strep and 10 µg/mL of insulin).

Similarly, the effect of hydrogel encapsulation on endothelial differentiation of cells, was studied. Firstly, endothelial differentiation was induced by EIM (EGM-2 with extra 50 ng/mL of VEGF) for 1 week. Cells were encapsulated into 1:3 and 1:1 - DAT:Fib hydrogels, and kept in EGM-2. On the days 3 and 7, endothelial characteristics of cells were analyzed via immunofluorescent staining with FITC-conjugated anti-vWF antibody. In addition, to see full endothelial behaviour in hydrogels, ASCs were differentiated in monolayer culture for 2 weeks in EIM, and 2 more days on orbital shaker. Then, these cells were encapsulated into hydrogels, and microscopic images were taken after staining with anti-vWF antibody.

Also, both types of cells (1 week-differentiated endothelial and adipogenic cells) were encapsulated into hydrogels. EGM-2 and AMM were mixed at 1:1 ratio and this medium was used as culture medium. After 3 and 7 days, cryosections were taken from hydrogels and observed under the microscope (Nikon Eclipse TS100, Japan) after hematoxylene and eosin staining.

2.2.6. *In Vivo* Studies

Influence of hydrogels on tissue regeneration and systemic responses such as inflammation or enzymatic degradation were analyzed via *in vivo* studies. DAT:Fib - 1:3 hydrogels were used for *in vivo* studies.

For the pre-analyses of *in vivo* studies, empty hydrogel discs (9 mm in diameter) were implanted subcutaneously into rats to investigate the biocompatibility of discs. After 7 and 21 days, samples were removed after rats were terminated, fixed in 10% formalin and tissue sections were obtained by paraffin embedding after overnight incubation. Tissue sections were analyzed histologically by hematoxylin&eosin (H&E) staining whether any infection or severe acute or chronic inflammation has occured or not.

To show hydrogel formation by surrounding a blood vessel, vortexed DAT:Fibroin mixture was poured in a silicone mold which was placed under the host vessel and monitored for 15 minutes. For the following *in vivo* experiments hydrogel discs (9 mm in diameter) were prepared outside with a vessel rift and placed underneath the blood vessel as enclosing it. This was done for the minimization of sample differences and to be able to compare samples thoroughly.

For *in vivo* studies the experimental groups are as follows:

1- Empty hydrogels implanted around host vessel (n=4),
2- Hydrogels implanted subcutaneously with both pre-differentiated ASCs into adipogenic lineage and endothelial lineage (n=4),
3- Hydrogels implanted around host vessel with pre-differentiated ASCs into adipogenic lineage (n=4),
4- Hydrogels implanted around host vessel with both pre-differentiated ASCs into adipogenic lineage and endothelial lineage (n=4).

For the all *in vivo* experiments with cell encapsulated hydrogels, autologous ASCs were isolated from subcutaneous adipose tissue of each rat.

For the 2nd group, autologous cells were isolated from each rat, adipogenically induced for 1 week *in vitro*, and encapsulated into hydrogels. Rifts were created inside hydrogels by replacing a comb just before gelation. These hydrogels were placed around a host

vessel by placing vessel in rift, to see effects of a main vessel on vascularization of hydrogels. Each hydrogels contained autologous cells of the rat to which they were implanted. After 3, 14 and 28 days, samples were extracted, and analyzed histologically. For the 3rd and 4th groups, autologous ASCs were isolated from adipose tissues of each rat again. These cells were separately induced for adipogenic and endothelial differentiation for 1 week and 2 weeks, respectively. Then, both cell types were encapsulated into hydrogels together with 1:2 adipocyte to endothelial cell ratio, and these hydrogels were placed subcutaneously and around the host vessel, respectively for the 3rd and 4th groups. After 3, 14 and 28 days, samples were extracted, and analyzed by H&E stainings for histological evaluations, Oil Red O staining for adipogenesis, and enothelial specific immunofluorescent stainings for vascularization.

2.2.7. Statistical Analysis

All *in vitro* analyses were performed in triplicates, and all *in vivo* analyses were performed as quadruplicates. One-way analysis of variance (ANOVA) was used to compare groups for significant differences. Pairwise comparisons were performed with Tukey's Comparison Test (SPSS-22 Software, SPPS Inc., USA); $p < 0.05$ was considered for statistically significance.

CHAPTER 3

RESULTS AND DISCUSSION

3.1. Decellularization of Adipose Tissue

During decellularization procedure, cells in human lipoaspirates were removed by SDS treatment for 2h. In the study of Young et al. (2011), tissues were exposed to SDS treatment for 48h. We observed that there was almost no DNA in the fat tissue after 2h treatment by DAPI staining (Figure 8c), and we decided to keep tissues in SDS solution for 2h to minimize the damage in ECM structure. Adipose tissue had a red-orange color with many blood cells and vessels. However, after SDS treatment, free lipids in tissue were washed out and the tissue had a yellow color (Figure 7a and 7b). Then, the whole lipid content was removed by lipase and colipase treatment. After lipid removal with lipase&colipase treatment the color of the tissue turned into white (Figure 7b and 7c). The time required to have a pure white tissue depends mainly on tissue source. However, homogenization of tissue as many times as possible during lipase treatment shortens the process since it helps enzyme to reach lipids. By this way, delipidization could be completed in 12-24h. Alternatively alcohol treatments are also used in decellularization studies to remove lipids from tissue (Brown et al., 2011; Flynn, 2010). However, when we tried to delipidize our tissues by both n-propanol and isopropanol, we obtained hard tissues which are difficult to dissolve at the solubilization step. This could be due to crosslinking of proteins with alcohol treatment. Also, color change from yellow to white occured after 48-72h with alcohol treatment. Therefore, we decided to use lipase and colipase treatment for delipidization of the fat tissue. After delipidization, DNase and RNase endonucleases were used to remove whole nucleic acid remnants. The

next step was lyophilization for obtaining decellularized tissue (DAT) powder that will be used together with isolated silk fibroin for cell encapsulation (Figure 7d). DAT powder was sterilized by ethylene oxide (EtO) treatment before solubilization, and remaining steps were performed under sterile conditions. Then, this DAT powder was cut into small pieces and solubilized in Pepsin/HCl solution (Figure 7e). After solubilization was completed, it was neutralized by 1N NaOH to inactivate pepsin.

During decellularization procedure, the vast majority of the tissue was lost, especially after delipidization step. This is an expected situation since adipose tissue contains high amount of lipids. When we first studied fat tissues extracted from rat groins, we obtained too low amount of final products. Therefore, it was very difficult to perform characterization and optimization experiments. For this reason, we decided to use human lipoaspirates which can be found in high amounts. We obtained around 9-12 mL of solubilized DAT from 100 mL of lipoaspirate. We also tried to use solid subcutaneous fat tissue instead of lipoaspirate. It was more efficient in terms of remaining ECM after delipidization. However, it was hard to find subcutaneous fat and obtain it in big sizes, while high amounts of lipoaspirate can be found easily.

3.2. Characterization of Decellularized Adipose Tissue (DAT)

After DAT was obtained some compositional analysis such as total protein assay, sGAG assay, and total collagen assay were done to determine the protein, proteoglycan and DNA contents of the tissue. SDS PAGE was performed to study the protein composition of the tissue. Also, delipidization was confirmed by Oil Red O stainings.

3.2.1. Total Protein Assay

Total protein amount in DAT solutions was measured by Bicinchoninic Acid (BCA) assay (Smith et al., 1985). The protein content of the DAT was determined using the calibration curve constructed with Bovine Serum Albumin (BSA) standards at different

concentrations (0-1000 µg/mL) in Pepsin/HCl buffer (Figure A1). The protein amounts in DAT samples were around 3-5 mg/mL. Table 4 shows calculated protein contents of different DAT samples. There are some different values reported in literature for final protein concentration in decellularization studies. For instance, Uriel et al. (2008) found total protein amount around 7 mg/mL. In our protocol, we could also obtain a more concentrated form by decreasing the solvent volume in final solubilization part. However, for our further experiments such as gelation, we found that optimum protein concentration range was 3-5 mg/mL. Therefore, we used DAT solutions with 4 mg/mL of protein concentration in the experiments. Turner et al. (2012) also diluted DAT to 2-4 mg/mL range in their study before using in microcarrier prepartion.

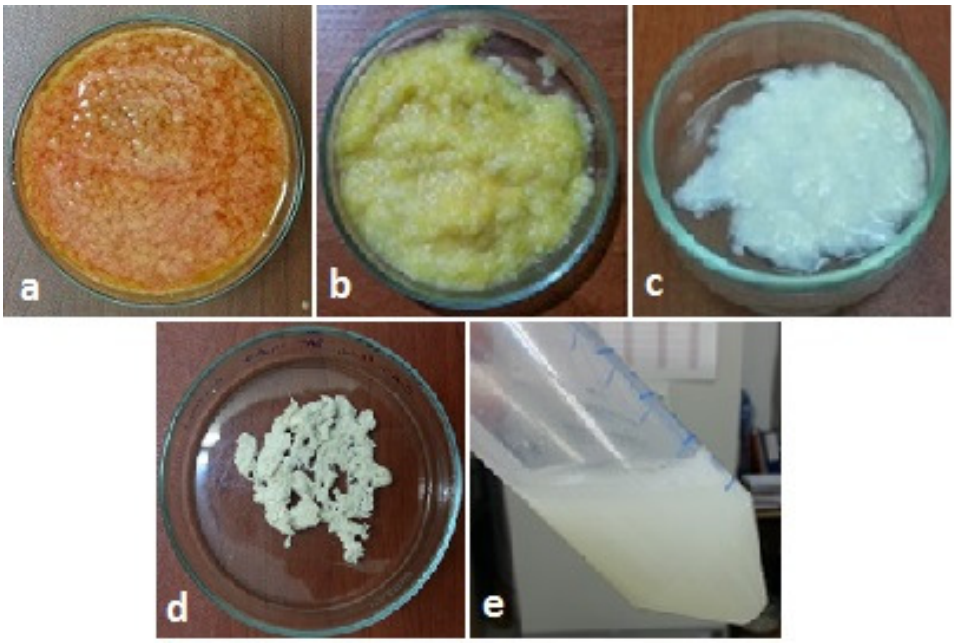

Figure 7. Decellularization steps of human lipoaspirate. a. Untreated human lipoaspirate b. After SDS treatment, blood vessels, free lipids and cells were removed. c. After lipase and DNase & RNase treatment, lipids and nucleic acids were removed. d. After lyophilization a dry, powder-like matrix was obtained. e. After solubilization, DAT solution containing 3-5 mg/mL of protein concentration was obtained.

Table 4. Total protein, sGAG, collagen and DNA contents of DAT samples

	DAT 1	DAT 2	DAT 3	DAT 4	DAT 5	Average
Sample protein concentration (µg/ml)	4861	3388	4059	3253	4831	4078 ± 764
sGAG concentration (µg/mg of dry ECM)	21.54	14.78	17.91	15.42	20.69	18.1 ± 3.03
Collagen concentration (% collagen in protein fraction)	49.8	41.7	46.6	41.3	50.9	46.1 ± 4.45
DNA amount (ng/mg of dry ECM)	301.7	202.4	217.5	188.8	243.1	230.7 ± 44.5

3.2.2. Total Sulfated Glycosaminoglycan (sGAG) Assay

Total sGAG amount in DAT samples was measured by dimethyl methylene blue (DMMB) assay (Farndale et al., 1986). DMMB dye can bind to sGAG and the absorbance measured at 525 nm is directly proportional with the sGAG amount. Calibration curve was prepared by using chondroitin sulfate as standard (0-80 µg/mL) in PBE/Cys solution (Figure A2). sGAG concentrations in DAT samples were calculated as 250-350 µg/mL. To compare these results with the other decellularization studies in literature, these values were recalculated as sGAG amount in dry decellularized ECM. In terms of this notation, average sGAG concentration in DAT samples were found as 18.1 ± 3.03 µg/mg of dry ECM (Table 4). In the decellularization study of Young et al. (2011), average sGAG amount was found as 2.18 ± 0.32 µg/mg of dry ECM. On the other hand, Singelyn et al. found the sGAG amount in decellularized myocardial ECM as 23.2 ± 4.63 µg/mg of dry ECM. Even if there is a wide range for the reported sGAG amount in decellularized ECM samples, it is clear that important amount of sGAG retained in DAT samples in this study.

3.2.3. Total Collagen Assay

Sirius red assay was used to measure the total collagen amount in DAT samples (Tullberg-Reinert and Jundt, 1999). In this method, dye binds to basic groups in collagen fibers via its sulphonic acid groups. Acidic environment increases the binding strength, while basic environment releases dye. Bovine collagen prepared at different

concentrations (0-800 µg/mL) in 0.5 M acetic acid was used for constructing the calibration curve (Figure A3). By using calibration curve, average collagen amounts in DAT samples were calculated as 1850 µg/mL which was almost 46.1 ± 4.45% of the total protein amount (Table 4). Collagen is the main ECM component in adipose tissue. Here, it was shown that most of the collagen molecules retained in DAT samples.

3.2.4. DNA Quantitation

DNA amount in DAT samples was calculated by staining with Hoechst dye. Hoechst is a fluorescent dye that binds to the minor groove of DNA. Therefore, it is commonly used for sensitive imaging of DNA in test samples. Calibration curve was prepared by measuring absorbances of calf thymus DNA (0-1000 ng/mL) in 1X TNE buffer (Figure A4).

Decellularized tissues are commonly used for biomedical purposes. However, it is a potential source for allogeneic or xenogeneic DNA which may cause inflammatory reactions in host (Zheng et al., 2005). In literature, there is no certain limit for DNA amount above which an immune response will be induced. However, even in many commercial biomaterials which are used in clinical treatments, there are some DNA residues (Gilbert et al., 2009). Since most of these DNA residues are very small fragments which are less than 300 bp, they do not create significant immune response in host (Badylak and Gilbert, 2008).

By using calibration curve, average DNA amounts in our DAT samples were calculated as 230.7 ± 44.5 ng/mg of dry ECM (Table 4). It is less than the DNA amount in the study of Young et al. (2011) which was around 0.6 µg/mg of dry ECM, and very close to the value in the study of Young et al. (2014) which was 187 ± 35 ng/mg of dry ECM. In the latter study, the group conducted *in vivo* applications and they observed that there was no significant immune response. Also, because of the harsh effects of the SDS, most of the residual DNA in ECM remains as small fragments which would not cause

immune response. However, the most accurate way to learn whether a material will create an immune response or not is to conduct *in vivo* experiments.

3.2.5. Decellularization Confirmation by DAPI Staining

Cryosections of DAT samples were stained with DAPI to assess complete decellularization. To see the effect of SDS treatment on decellularization, sections from both before and after SDS treatment were stained with DAPI. Images taken on a fluorescent microscope showed that 2h SDS treatment was highly effective to remove cells (Figure 8). Since DAPI is a fluorescent dye which stains nuclei, it also shows nucleic acid residues even if there are no living cells. Therefore, DAPI staining may be thought as visual confirmation of DNA quantitation by Hoechst staining.

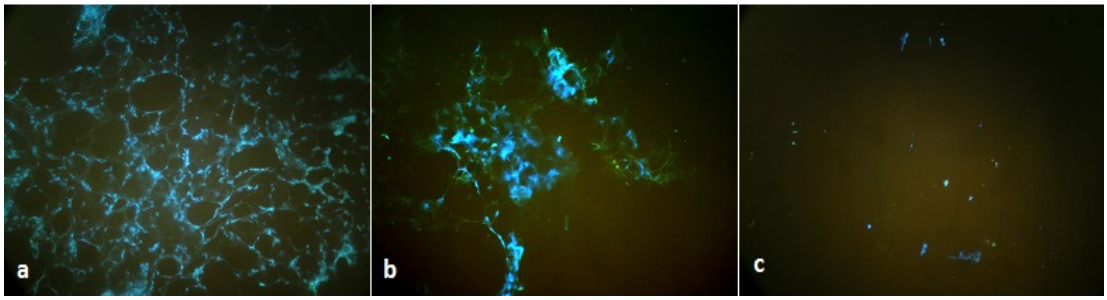

Figure 8. DAPI staining of DAT cryosections (Thickness of the sections is 20 µm). **a.** Before, **b.** after 1h, **c.** after 2h SDS treatment. Nucleic acids were stained with DAPI and seen in blue color. It was observed that SDS treatment for 2h decreased nucleic acid amount dramatically.

3.2.6. Delipidization Confirmation by Oil Red O Staining

Delipidization of adipose tissue can be recognized by naked eye because of the color change (Figure 7b and 7c). Oil Red O staining was performed in cryosections of DAT samples (20 µm in thickness) for confirmation. Oil Red O stains neutral triglycerides and lipids on frozen sections. Lipid removal is highly required for efficiency of further experiments such as lyophilization, solubilization, and gelation. Therefore, lipase and

colipase treatment is necessary in decellularization protocol (Young et al., 2011). Alternatively, alcohols such as isopropanol or n-propanol are used to remove lipids from tissue (Flynn, 2010; Brown et al., 2011). Both lipase treatment and alcohol treatment were performed in our study. However, since alcohols disrupt protein structures and causes crosslinks inside ECM, the final product did not dissolve completely. Also, lipid removal was slower with alcohols, this situation prolongs the procedure, and disturbs protein structure more. Therefore, lipase & colipase solution was chosen as the lipid removal agent. Oil Red O staining showed that there was almost no lipid in DAT samples after lipase & colipase treatment (Figure 9).

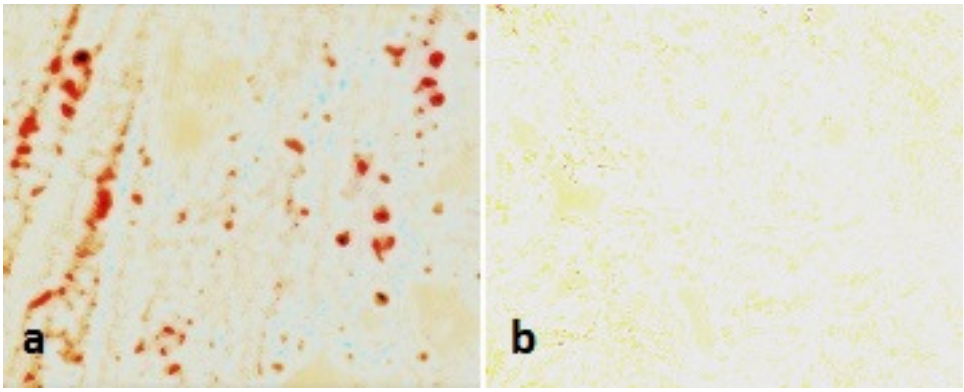

Figure 9. Oil Red O staining of DAT cryosections. **a.** Before lipase & colipase treatment. **b.** After lipase & colipase treatment. Lipase & colipase treatment removed almost all lipids in the matrix of adipose tissue.

3.2.7. SDS PAGE Analysis

SDS PAGE analysis was performed to see and analyze protein fragments in DAT. It was seen that DAT has so many peptide fragments that it is difficult to distinguish bands. This shows that many ECM components remained in DAT even after the harsh decellularization protocol. In addition, some groups of bands in DAT column were also present in the commercial bovine collagen column in gel (Figure 10). Therefore, it is an evidence of presence of collagen in DAT samples. Because of the sample preparation

conditions, ECM proteins might be broken into smaller subunits. Bands around 25, 35 and 40 kDa may be these small subunits. In the study of Young et al. (2011), there were also bands around and below 39 kDa which were assigned to collagen.

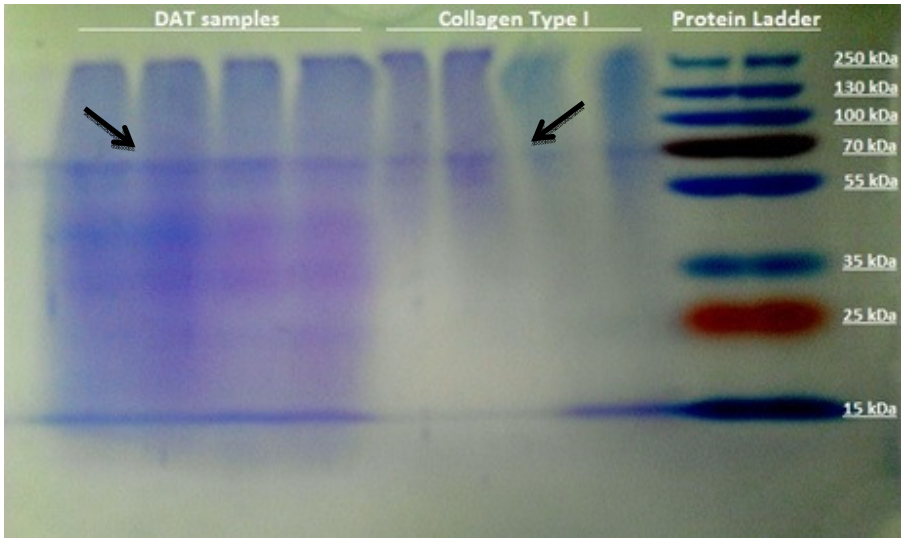

Figure 10. SDS-PAGE gel photo for DAT samples and Collagen type I (12% separating gel). Protein ladder (Fermentas Page Ruler Plus Prestained Protein Ladder, 10 to 250 kDa) was used as a marker. Arrows show the same bands in DAT samples and collagen. It is observed that DAT samples have bands for collagen and many other ECM proteins.

3.3. Fibroin Extraction from Silkworm Cocoon

Silk fibroin was extracted from silkworm cocoons based on the study of Rockwood et al. (2011). Firstly, sericin was removed or degummed by a boiling step. It was shown that sericin proteins did not induce significant inflammation by itself (Panilaitis et al., 2003). There are many studies which reported that native silk proteins create significant immune responses when used without removal of sericin (Soong and Kenyon, 1984; Zaoming et al., 1996; Celedón et al., 2001). Also, removal of sericin will release fibroin fibers and allow dissolution of them in aqueous solution which provides further processing. Therefore, sericin removal (degumming) step is needed for fibroin

extraction. During degumming process, fibroin proteins may also be affected because of long time exposure to high temperature. On the other hand, low temperatures or short time may prevent complete removal of sericin. Teh et al. (2010) showed that boiling silk cocoons for 30 min at 100^{o}C in an alkaline solution is the optimum condition for sericin removal process. These conditions provide complete removal of sericin with negligible effects on structural and mechanical properties of the silk fibroin. At the end of whole extraction process, 8-10% (w/v) aqueous silk fibroin solutions were obtained. To minimize variations, all fibroin solutions were diluted if necessary to a concentration of 8% (w/v) for further experiments. For cell culture studies, sterilization of fibroin solution was needed. Even after 1/10 dilution, it was not possible to filter-sterilize the fibroin solution. Therefore, steam sterilization (autoclaving) was performed. It changed the color of fibroin solution from light yellow to white. Gelation process by vortexing was also affected, but after changing vortexing times it gelled again. For instance, before autoclaving, DAT:Fib mixtures with 1:3 ratio were gelating in 10-15 min by 7 min vortexing. However, after autoclaving, mixtures with same ratio were gelated in 1-1.5h. Therefore vortexing procedure was changed as 7 min vortexing, 1 min waiting and 2 min vortexing (10 min in total). Waiting for 1 min may allow initial crosslinking in mixture, and second vortexing increase this crosslinking more. Mixtures with 1:3 ratio were gelated again in 10-15 min by this vortexing procedure, Therefore, all further experiments were optimized by using autoclaved fibroin solution.

3.4. Preparation of Fibroin and Decellularized Matrix Hydrogels

Hydrogels were formed by vortexing DAT-fibroin mixtures. Yucel et al. (2009) showed that hydrogelation of fibroin solutions can be induced by vortexing. According to them, shear flow created by vortexing increases the formation of macromolecule clusters which have many β-sheet forms in it, and these β-sheet formations lead to permanent gelation. Based on this information, vortexing was used to induce gelation in this study. When fibroin was vortexed alone, especially after autoclaving, it was observed that too

many bubbles and solid particles formed in the solution, and gelation occurred after overnight incubation. On the other hand, vortexing DAT-fibroin mixtures gave much better results such as almost no formation of solid particles and much shorter gelation times (Figure 11). Probably, ECM components present in DAT stabilize fibroin molecules by preventing uneven β-sheet formations and provides better gelation kinetics. Also, there are some studies in which ECM was gelated by itself via its self-assembling components such as laminin, collagen and proteoglycans (Freytes et al., 2008; Uriel et al., 2009). This characteristics of ECM can make DAT a good partner for hydrogel formation. DAT solution (4 mg/mL) was mixed with silk fibroin solution (8%) in three different ratios (3:1, 1:1, 1:3, v/v) to compare gelation kinetics, mechanical properties and so, effects on cell viability and differentiation after encapsulation. In order to minimize the variations in experiments, total protein concentrations in DAT and silk fibroin solutions were fixed as 4 mg/mL and 8%, respectively. In addition, 10X RPMI medium was prepared from powder RPMI, and added to each group with 1:10 ratio after filter-sterilization. Medium was added to the mixture to allow encapsulated cells to reach nutrients easier after gelation. Similarly, Wang et al. (2008) have added medium during cell encapsulation in silk fibroin and observed good cell viability results. Thus, we also decided to use this method. Finally, pH of the mixture was adjusted to 7.4 with sterile $NaHCO_3$ solution addition. This step is also important, because fibroin solution has a slightly acidic pH (around 5.5), and it prevents to have a physiological pH especially when it is in high ratio. $NaHCO_3$ is used for pH regulator in cell culture media, so it was used to adjust pH of the final DAT/fibroin mixture. These extra additions were required to have a proper medium for maintaining cell viability after encapsulation in DAT/fibroin hydrogel. After these additions, optimizations for gelation were done with full mixture. After vortexing for 10 minutes gelation times were 1-2h for 3:1 (DAT:Fib) group, 20-30 min for 1:1 (DAT:Fib) group, and 10-15 min for 1:3 (DAT:Fib) group. As expected, gelation times decreased with increasing fibroin ratio. Optimization of gelation time was very important to put cells into the mixture at the

correct time. If cells were added into the mixture too early, it was observed that they tended to settle down the gel; and if they were put too late, gelation prevented to obtain homogenous distribution throughout the gel.

On the other hand, gelation kinetics were affected negatively if any lipid remnants present in the DAT after delipidization process. It was observed that gelation times increased or even did not occur sometimes if delipidization treatment was inefficient.

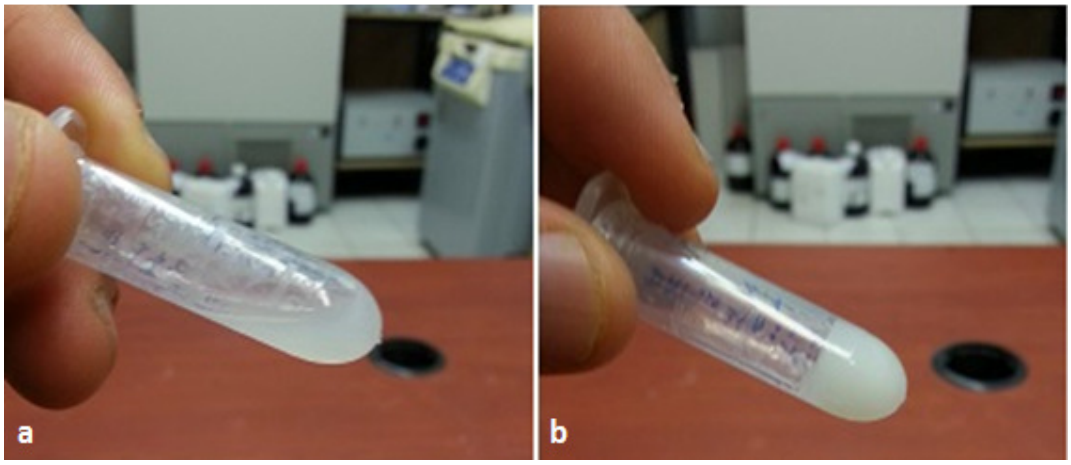

Figure 11. Gelation of DAT:Fib (1:3) mixture by vortexing. a) Before vortexed b) After vortexed for 10 min.

3.4.1. Mechanical Tests

The mechanical properties of the hydrogels with different DAT:Fib ratios were studied with unconfined compression test. To minimize variations, disc samples (1 cm diameter, and 4 mm height) were cut from each hydrogel group after 15 min of gelation, and placed in a petri dish filled with PBS (Figure 12). During the uniaxial compression tests, 10N load cell was used, and a preload of 0.02N was applied to all discs to minimize the effects of initial loading setup. To be able to compare hydrogels with natural adipose tissue, a sample from subcutaneous adipose tissue was obtained. Natural tissue sample was also cut in a disc shape which is similar to hydrogels, and same test was performed.

Figure 12. Sample preparation for mechanical test. **a)** Gelation in glass mold with 4 mm thickness. **b)** Punching disc shaped samples with 1 cm diameter. **c)** 3D structure of disc shaped sample. **d)** Uniaxial unconfined compression test in PBS.

Mechanical properties of each hydrogel group and natural adipose tissue were compared using their stress-strain graphs (Figure 13) and Young's Moduli at different strain levels (Table 5). These results showed that hydrogel group with 3:1- DAT:Fib ratio had poor mechanical properties compared to other groups. Other than initial modulus, all values in Table 5 were significantly different than adipose tissue ($p < 0.05$). It was not stable, and cannot resist to high loads. Its handling was also not easy, since it was easily ruptured during punching or transferring to another place. Therefore, we decided to eliminate this group for the further experiments. The initial strength of the second group with 1:1 - DAT:Fib ratio was better than 3:1 group. It was not significantly different than adipose tissue ($p > 0.05$). However, its Young's modulus did not continuously increase over the test. It started to lose its strength after around 25% strain, especially when compared with natural tissue. Its other values were significantly different than adipose tissue ($p < 0.05$). On the other hand, its handling was easy and it maintained its shape and integrity when there was no load. By looking at Table 5 and Figure 13, it is clear that the 1:3 - DAT:Fib ratio group was the mechanically strongest group. When it is compared with natural tissue, it can be seen that hydrogel have similar mechanical properties with natural tissue. Both in the hydrogel with 1:3 DAT:Fib ratio and natural adipose tissue, Young's Moduli increased continuously. They gained strength via load bearing. Their final stresses were also very close, they were not significantly different ($p > 0.05$), that means they were both resistant to high level of loads. However, the

hydrogel had a higher initial Young's modulus, and it was not as viscoelastic as the natural fat tissue (Figure 13). This is normal, because natural adipose tissue has many lipids which function as a cushion in its structure, and this gives a softness, at first. After some load-bearing, lipids are squeezed and tissue becomes highly resistant to load. On the other hand, hydrogel is free from lipids, so there was no cushioning effect of lipids. Therefore, it should be tough enough to protect its integrity until natural tissue is regenerated by cells inside it. Cheung et al. (2014) prepared and used hydrogels with Young's Moduli of 30.1 ± 4.0 kPa and 37.1 ± 5.0 kPa for adipose tissue engineering. These values are very similar with those for our hydrogel with 1:3 DAT:Fib ratio.

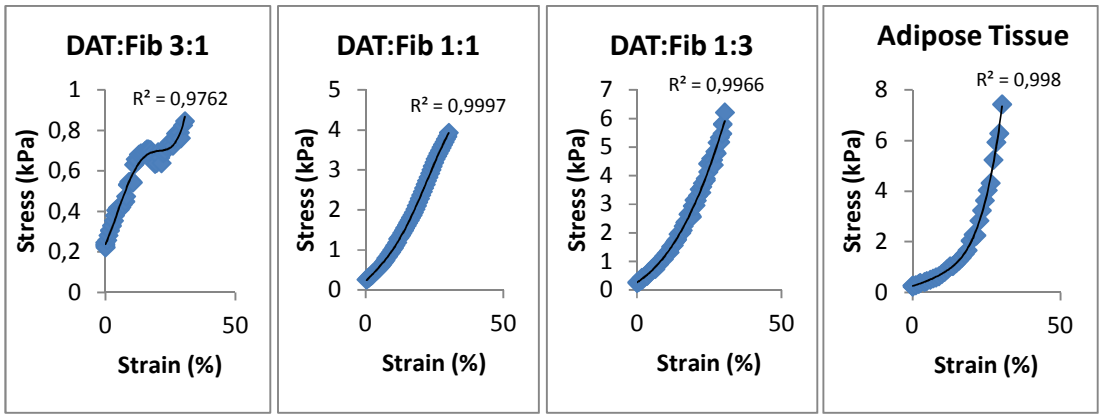

Figure 13. Stress-Strain curves for hydrogel groups and natural adipose tissue. Uniaxial compression tests were performed in PBS, up to 30% strain limit. The strength of the hydrogels increased with increase in fibroin content.

Table 5. Young's moduli values at different strain levels for hydrogel groups and natural adipose tissue. * shows significant difference with adipose tissue as determined by one-way ANOVA with Tukey's comparison test ($p < 0.05$).

DAT:Fib Ratio (v/v)	3:1	1:1	1:3	Adipose Tissue
Initial modulus (10%) (kPa)	2.7 ± 1.2	10.3 ± 1.9	13.4 ± 2.4*	6.6 ± 1.8
Transition modulus (20%) (kPa)	0.17 ± 0.4*	15.9 ± 2.4*	22.4 ± 3.5	24.5 ± 3.6
Final modulus (30%) (kPa)	4.6 ± 1.6*	12.4± 2.1*	33.6 ± 4.8*	87.1 ± 8.7
Final stress (30%) (kPa)	0.9 ± 0.5*	3.9 ± 1.1*	6.2 ± 1.6	7.4 ± 2.9

3.4.2. *In Vitro* Degradation Tests

Hydrogels with 1:1 and 1:3 DAT:Fib ratios were analyzed for *in vitro* degradation properties by incubating in PBS at 37°C in shaking water bath. Hydrogels were expected to degrade in such aqueous environment by hydrolysis reactions and mechanical force created by shaking. Their degradation profiles were evaluated by wet weight change in time. Degradation of DAT:Fib hydrogels were also compared with pure fibroin hydrogels (Figure 14). Fibroin hydrogels were highly resistant to degradation, their wet weight almost did not change in PBS for 2 weeks. This result was very compatible with literature studies. For instance, Wang et al. (2008), prepared sonication induced silk fibroin hydrogels, and measured its degradation by wet weight change. They found that weight of silk fibroin hydrogels remained stable in PBS for 1 week. In parallel with results of compression tests, 1:3 group were much more resistant to degradation than 1:1 group. This is apparently because of the higher fibroin ratio in 1:3 group, and slow degradation rate of fibroin when compared to DAT component.

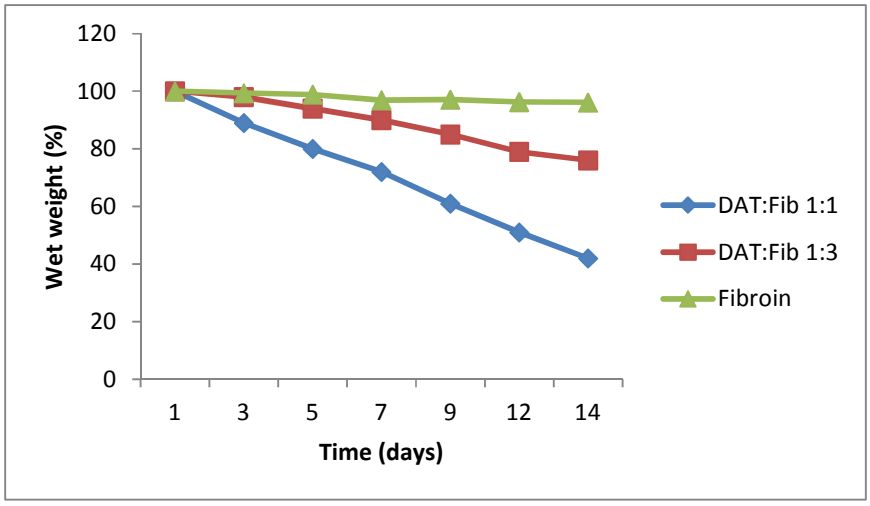

Figure 14. *In vitro* degradation profile of fibroin hydrogel and hydrogels with 1:3 and 1:1 DAT:Fib ratios in PBS. Degradation profiles were determined as percentage of wet weight change in time. Decrease in fibroin concentration accelerated the degradation of the hydrogels.

3.5. Cell Culture Studies

3.5.1 Adipose Derived Stem Cell (ASC) Isolation

ASCs were isolated from rat adipose tissue which was extracted from rat groins (Figure 15a). By flow cytometric analysis at passage 4, isolated ASCs were found as negative for CD11 (99.8%), CD31 (99.0%) and CD45 (99.8%), and positive for CD90 (68.6%) (Figure 16) as expected. These results showed that ASCs protected their stemness over 4 passages. Percentage of positive marker might be higher if cells used for analysis were at earlier passages. Some of the cells had an omellette-like morphology probably due to entering senescence.

In the isolation day, surface of the flask were full with blood cells and small tissue debris. By the second day, blood cells could not survive and began to die. After washing with PBS on 3rd day, both blood cells and tissue debris were removed since they couldn't adhere to the surface. Therefore, adhered ASCs appeared on the surface of the tissue culture flask (Figure 15b). They were spindle shaped and had a morphology similar to fibroblasts as described in literature (Jeong, 2008). There were not too many adhered cells, but they proliferated rapidly and reached confluency on the 7th day (Figure 15c and 15d).

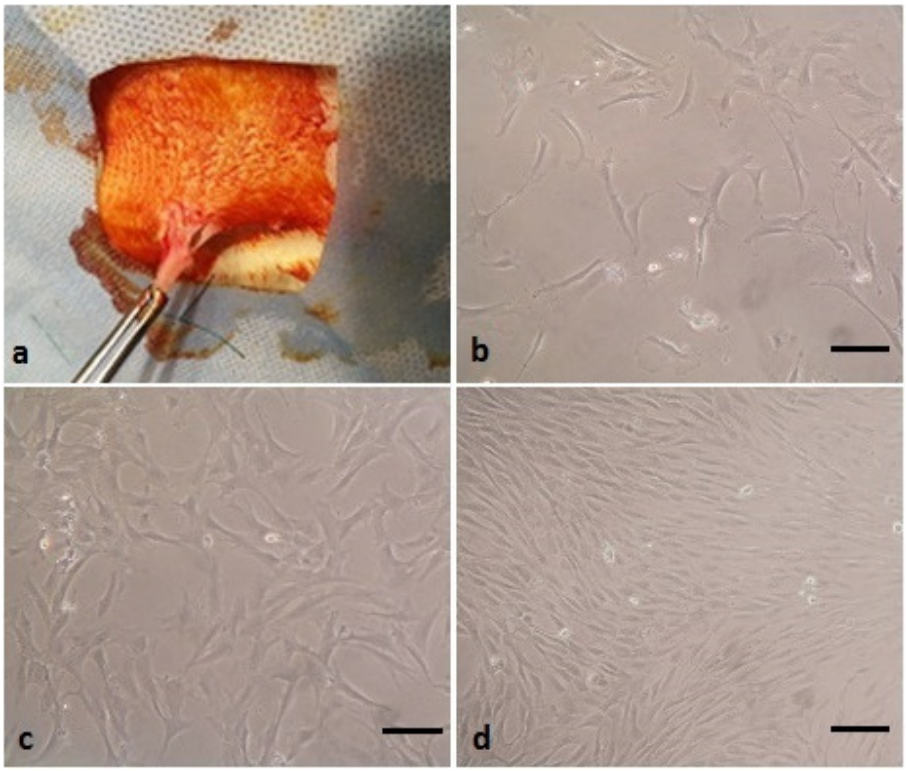

Figure 15. ASCs isolation from rat adipose tissue.**a.** Rat adipose tissue extracted from rat groins **b.** 3rd day after seeding. Fibroblastic cells were observed. **c.** 5th day after the isolation: ASCs were proliferating. **d.** 7th day after the isolation: ASCs reached confluency. Scale bar is 100 µm.

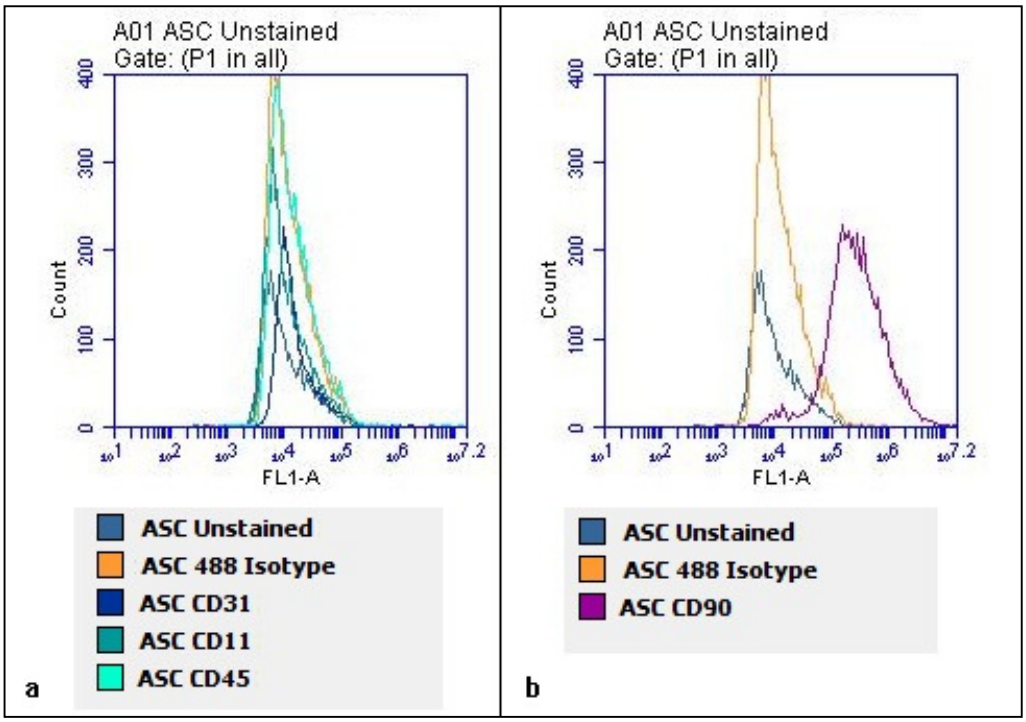

Figure 16. Flow cytometric analysis of ASCs. **a)** Comparison of CD11, CD31 and CD45 analysis with unstained ASCs and mouse isotype IgG control. **b)** Comparison of CD90 with unstained ASCs and mouse isotype IgG control. Flow cytometric analyses showed that ASCs are negative for CD11, CD31 and CD45; but positive for CD90.

3.5.2. Adipogenic Differentiation

ASCs were successfully differentiated into adipogenic lineage. Visible morphological changes occurred during the differentiation process. First, ASCs enlarged and became more round while they had linear and fibroblastic shape before differentiation (Figure 17a and 17b). Then, it was observed that small lipid vesicles were accumulated inside cells (Figure 17b). By time, these small vesicles fused in some cells and formed bigger lipid vesicles like in mature adipocytes. Also, adipogenic differentiation was confirmed by Oil Red O staining after 3 weeks of differentiation (Figure 17c and 17d).

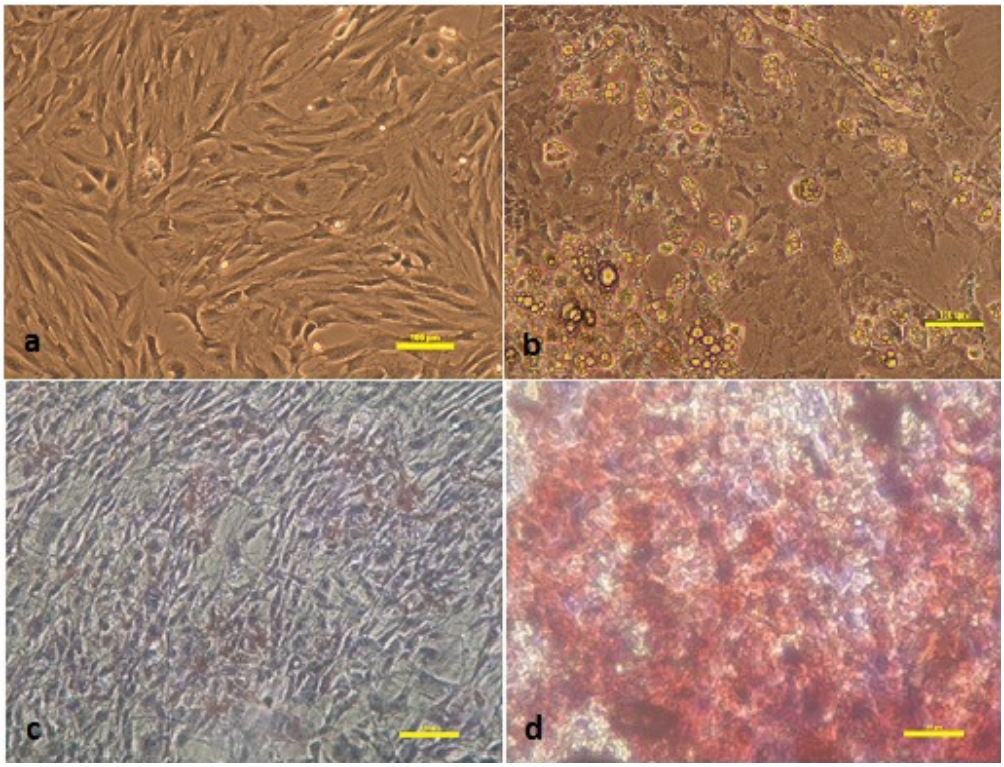

Figure 17. Adipogenic differentiation of ASCs. Phase contrast micrographs of undifferentiated ASCs **(a)**, differentiated ASCs **(b)**, undifferentiated ASCs stained with oil Red O **(c)**, differentiated ASCs stained with oil Red O staining **(d)**. Scale bar is 100 µm.

3.5.3. Endothelial Differentiation

ASCs were successfully differentiated into endothelial lineage. It was confirmed by three different methods (Figure 18).

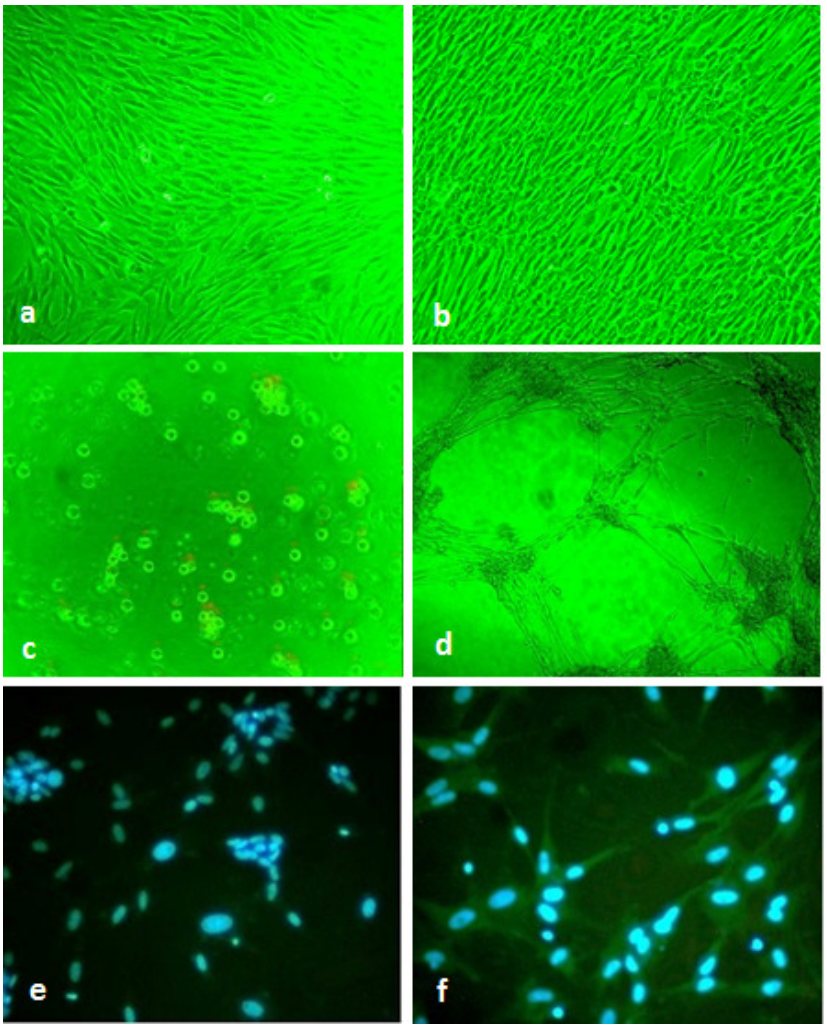

Figure 18. Endothelial differentiation. **a.** Undifferentiated ASCs on TCPS cultured under dynamic conditions (shaken at 150 rpm for 2 days on an orbital shaker) **b.** Differentiated ASCs on TCPS cultured under dynamic conditions (shaken at 150 for 2 days on an orbital shaker). **c.** Undifferentiated ASCs cultured under static conditions on Matrigel. **d.** Differentiated ASCs cultured under static conditions on Matrigel. **e.** Immunofluorescent staining of undifferentiated ASCs with DAPI (light blue) and FITC conjugated Anti-vWF antibody (green). **f.** Immunofluorescent staining of differentiated ASCs with DAPI (light blue) and FITC conjugated anti-vWF antibody (green).

First of all, it was observed that differentiated cells oriented in the shaking direction while undifferentiated cells oriented randomly when cells were cultured under dynamic condition using an orbital shaker (Figure 18a and 18b). This is a characteristic property of endothelial cells. These cells elongate in the direction of the blood flow inside the blood vessels (Dardik et al., 2005). Similarly, Fischer et al. (2009) and Zhang et al. (2009), achieved endothelial differentiation with a similar protocol and they also used cell orientation in flow direction as one of the evidences of endothelial differentiation. Secondly, when these cells were seeded on Matrigel, the differentiated cells formed networks with each other while undifferentiated cells remained round (Figure 18c and 18d). Lastly, immunofluorescent stainings with FITC-conjugated anti-vWF antibody showed that differentiated cells expressed vWF protein, while undifferentiated cells did not express (Figure 18e and 18f). vWF is one of the most important markers of endothelial differentiation. Generally, CD31 is accepted as an early marker and vWF is accepted as late marker of differentiation (Vittet et al., 1996; Fischer et al., 2009; Zhang et al., 2009). It was shown that ASCs can be used to obtain autologous endothelial cells. Especially for the clinical studies, it is important to show that since autologous endothelial cells were normally isolated with a difficult method and in low numbers.

3.5.4. Coculture of Adipogenic and Endothelial Differentiated Cells

ASCs pre-differentiated into adipogenic and endothelial lineages were cocultured with a 1:2 cell number ratio, respectively. Neither adipogenic nor endothelial differentiation of cells was affected negatively from presence of other type of cells. They were differentiated into committed lineage which was induced for 1 week before coculturing. Oil Red O and anti-vWF stainings showed adipogenic and endothelial differentiations, respectively (Figure 19a and 19b). Number of cells with lipid vesicles were low at first week. However, after 2 weeks, the number of these cells increased probably because of late differentiation of some stem cells (Figure 19c and 19d). Even after subjecting to shear force on orbital shaker, cells remained together in their differentiation states

(Figure 20). Zhong et al. (2013), showed that low shear forces (<1 dyne/cm^2) may induce adipogenesis of ASCs, however, as shear force is increased osteogenesis is induced instead of adipogenesis. Interestingly, in our samples adipogenic differentiation of cells were more dense in the periphery of wells where shear stress was more. On the other hand, cells differentiated into endothelial cells were oriented through the flow direction as expected, and adipogenic differentiated cells remained between these oriented cells (Figure 20).

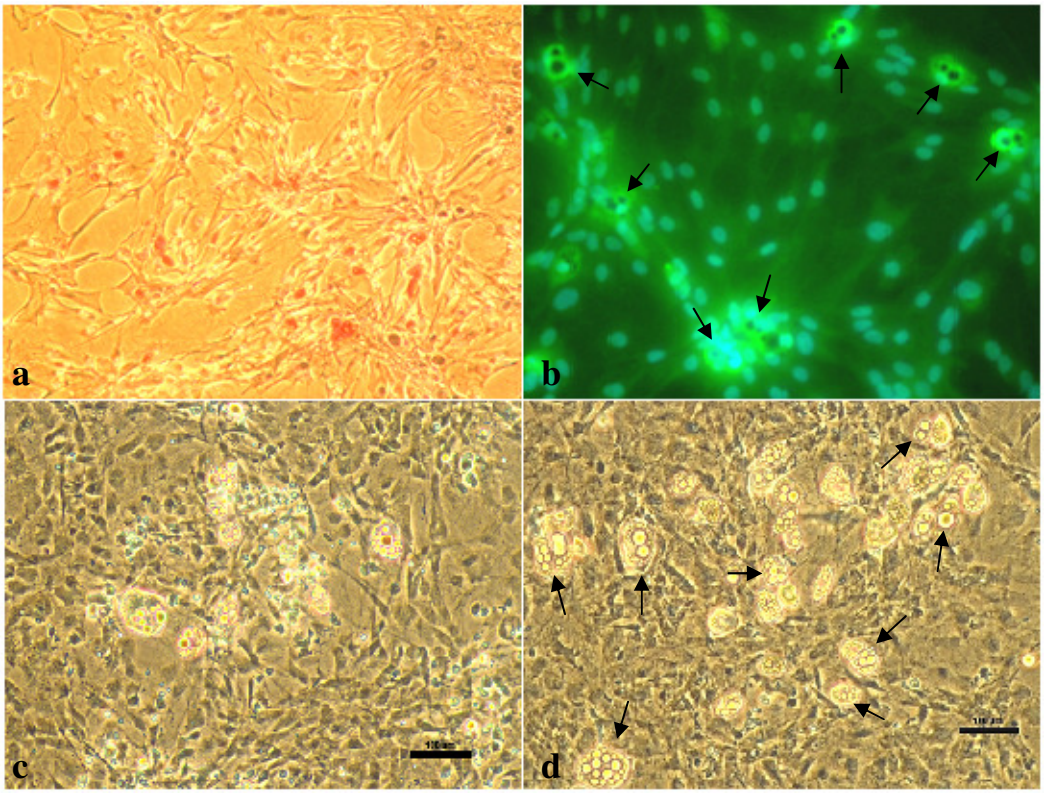

Figure 19. Coculture of adipogenic and endothelial differentiated cells. **a)** Oil Red O staining of cells. **b)** Anti-vWF staining of cells c) Phase contrast micrographs after 1 week, and **d)** 2 weeks of incubation. Arrows show lipid accumulated cells surrounded by endothelial-like cells.

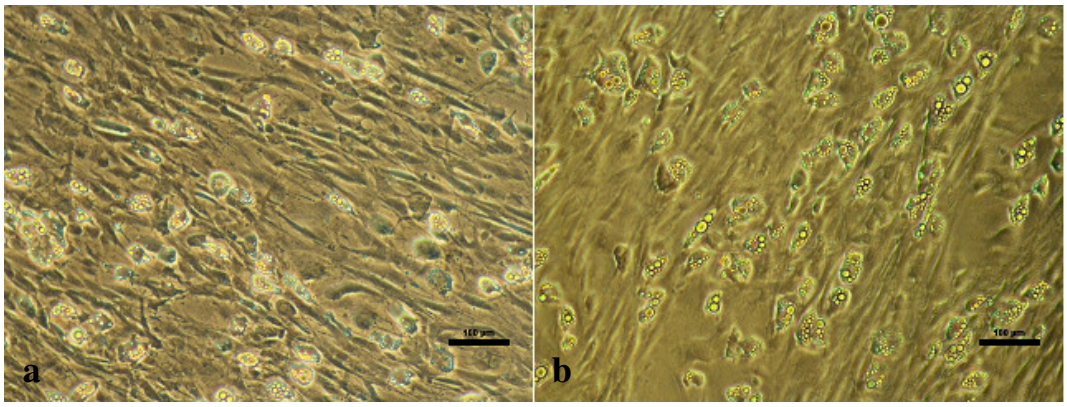

Figure 20. Coculture of endothelial and adipogenic cells on orbital shaker. Cells with lipid vesicles are cells differentiated into adipocytes. Cells elongated in the flow direction are endothelial differentiated cells. Scale bar is 100 µm.

3.5.5. Proliferation of Cells on Hydrogels

The proliferation of ASCs on the hydrogels were analyzed by measuring cell viability after seeding cells on DAT:Fib gels. Figure 21 shows that hydrogels with 1:3 - DAT:Fib ratio provided a better surface for attachment of ASCs than hydrogels with 1:1 – DAT:Fib ratio. They both provide lower viability when compared with tissue culture plate surface (TCPS).

It is understandable to have less viability on 1:1 - DAT:Fib hydrogels when compared to 1:3 - DAT:Fib hydrogels. This is because most cultivable cell types like stiffer materials to attach and proliferate (Wells, 2008; Mih et al., 2012). According to Wells (2008), cells cultured on very soft materials remain spherical, and growth arrested because of minimal attachment. They become highly prone to apoptosis by time. On the contrary, cells cultured on stiff materials spread on surface and become highly proliferative. In addition, surface of silk fibroin hydrogels was shown to be supportive for cell adhesion and proliferation (Sah and Pramanik, 2011), and silk fibroin coated surfaces increased cell proliferation by activating CD44 proteins on cell surface which induce proliferation

pathways (Yang et al., 2014). All of these studies are parallel to our results with higher viability on DAT:Fib - 1:3 hydrogels.

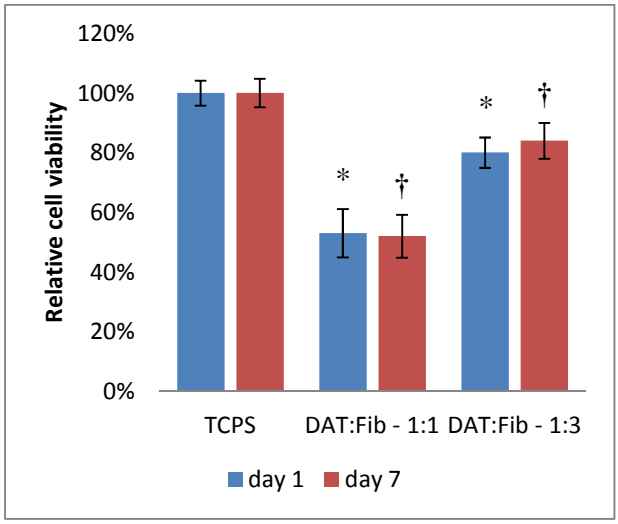

Figure 21. Relative viability of ASCs on hydrogels. Cell numbers were optimized by comparing with monolayer culture on TCPS. Viability on TCPS was accepted as 100%, cell viability on DAT:Fib hydrogels are presented as relative viability. DAT:Fib - 1:3 group has a better viability percentage on it (n=3). * and † show significant difference between groups ($p<0.05$). DAT: Fib groups were statistically lower than positive control (TCPS) as determined by one-way ANOVA with Tukey's comparison test ($p<0.05$).

3.5.6. Cell Encapsulation

ASCs were encapsulated inside hydrogels shortly after vortexing the DAT:Fib mixture. In many encapsulation methods, cells were included initially in gelation procedure which usually decreased cell survival (Cheung et al., 2014). In this study, gelation was triggered without cells, so without giving any harm to cells. The only important thing was to put cells into the mixture before its viscosity becomes too high as it will not allow homogenous distribution of cells.

In first encapsulation trials, cell viability was lower. This was probably because of the low pH of the hydrogel caused by high fibroin ratio with low pH. After adjusting the pH of the gel to the physiological pH by $NaHCO_3$, cell viability was increased. ASCs remained spherical in hydrogels (Figure 22). This is commonly seen in encapsulation studies, and it is probably because of the stiffness of the hydrogels (Nicodemus and Bryant, 2008; Rocha et al., 2011; Hassan et at., 2013). According to Hassan et al. (2013) cells remain in rounded morphology because of the highly cross-linked network. Lee et al. (2007) showed that cells could spread inside the hydrogel only after sufficient degradation. When we look at the viability results (Figure 23), we can see that hydrogels with 1:3 - DAT:Fib ratio provides a better 3D environment than hydrogels with 1:1 - DAT:Fib ratio. It is also compatible with results of the viability tests on the gel.

Viability stainings with Calcein-AM & Propidium Iodide (PI) were also performed. Calcein-AM is normally a non-fluorescent molecule. However, if it enters inside a viable cell, acetomethoxy (AM) group is cleaved by intracellular esterases, and cell is seen green under fluorescent light because of the fluorescence of rest Calcein part. On the other hand, PI is a fluorescent molecule which gives a red color under fluorescent light. It cannot enter into cell normally, but if the cell membrane is disturbed like in dead cells, it can enter into the cell. Therefore, after Calcein-AM & PI staining, alive cells are seen as green and dead cells as red. After we performed this staining, it was observed that there were more viable cells in 1:3 DAT:Fib hydrogels, so this group was chosen for further in vitro and in vivo studies (Figure 22).

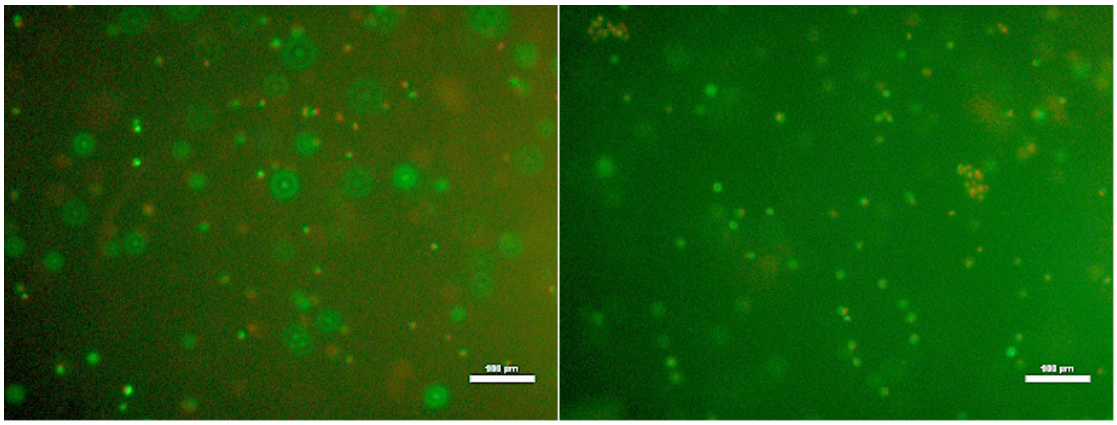

Figure 22. Viability staining with Calcein AM and Propidium iodide (PI) after 24h of ASC encapsulation into hydrogels. **a)** Viability in DAT:Fib 1-1 hydrogels **b)** Viability in DAT:Fib 1:3 hydrogels. Calcein AM stains alive cells to green, while PI stains dead cells to red. There were more dead (red) cells in DAT:Fib 1:1 hydrogels. Scale bar is 100 µm.

There is no consensus on whether survival and proliferation of encapsulated ASCs are higher in stiffer or softer matrices. However, if matrix is too loose, it is difficult for cells to attach matrix components and proliferate. Also, soft matrices are very difficult to manipulate and analyze. On the other hand, if matrix is too stiff, cells may not move and perform cellular activities for survival. Therefore, there should be an optimum range of stiffness for both proliferation and differentiation. For instance, Wang et al. (2008) found that hydrogels prepared from 4% fibroin solution by sonication was very supportive for MSC viability and proliferation after encapsulation. On the contrary, they showed that hydrogels prepared from 12% fibroin did not allow cell survival for a long time. Moreover, they could not analyze hydrogels with less fibroin ratio because of difficulty in manipulation. In our study, hydrogels with 1:3 - DAT:Fib ratio had a 6% final fibroin concentration. By thinking softening effect of DAT in hydrogel, it can be said that our results were similar to the results of Wang et al. (2008). In addition, Mousavi and Hamdy (2015) offered that stiffer matrices may accelerate proliferation and

differentiation activities by decreasing the cell maturation time. Also, hydrogels with 1:3 - DAT:Fib ratio had a similar mechanical property to the natural adipose tissue.

According to all these findings and analyses, we decided to choose hydrogel group with 1:3 - DAT:Fib ratio for the *in vivo* experiments.

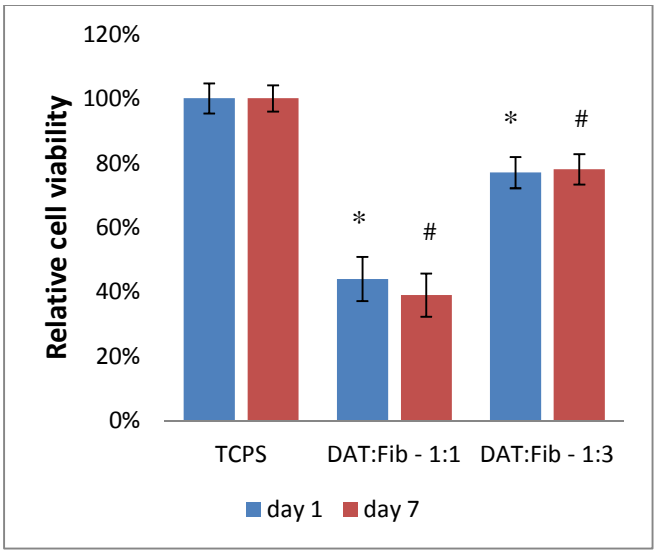

Figure 23. Relative viability of ASCs encapsulated inside hydrogels. Cell numbers were optimized by comparing with monolayer culture on TCPS. Viability on TCPS was accepted as 100%, cell viability on DAT:Fib hydrogels are presented as relative viability. These results showed that DAT:Fib - 1:3 group is better for viability (n=3). * and # show significant difference between these groups. Cell viability in DAT:Fib groups was statistically lower than in positive control (TCPS) group as determined by one-way ANOVA with Tukey's comparison test ($p<0.05$).

3.5.7. Differentiation in Hydrogels

Hydrogels with 1:1 and 1:3 DAT:Fib ratios were analyzed in terms of their effects on ASCs differentiation by encapsulation of 1 week pre-differentiated ASCs into adipogenic and endothelial lineage.

In both types of hydrogels, adipogenic cells with lipid vesicles were observed in 3rd day cryosections (Figures 24 and 25). However, in 1:3 - DAT:Fib hydrogels, there were more lipid vesicles in some cells which showed that cellsweare in a later stage of adipogenesis. Normally, ASCs prefer softer matrices for adipogenic differentiation (Park et al., 2011; Lee et al., 2013). Therefore, it might be expected that adipogenesis level should be higher in 1:1 - DAT:Fib hydrogels. However, cell viability in 1:1 - DAT:Fib hydrogels was lower. Zhao et al. (2014) showed that MSCs were inclined to differentiate into the mature cells in matrices having similar mechanical properties with their own natural microenvironment. It was observed that 1:3 - DAT:Fib hydrogel had similar mechanical properties with natural adipose tissue and so, it is proper for the adipogenesis of ASCs. Additionally, it was relatively difficult to handle 1:1 - DAT:Fib hydrogels during sectioning for histological analysis. Therefore, 1:3 - DAT:Fib composition was ideal for encapsulating cells and obtaining desired endothelial and adipogenic differentiation.

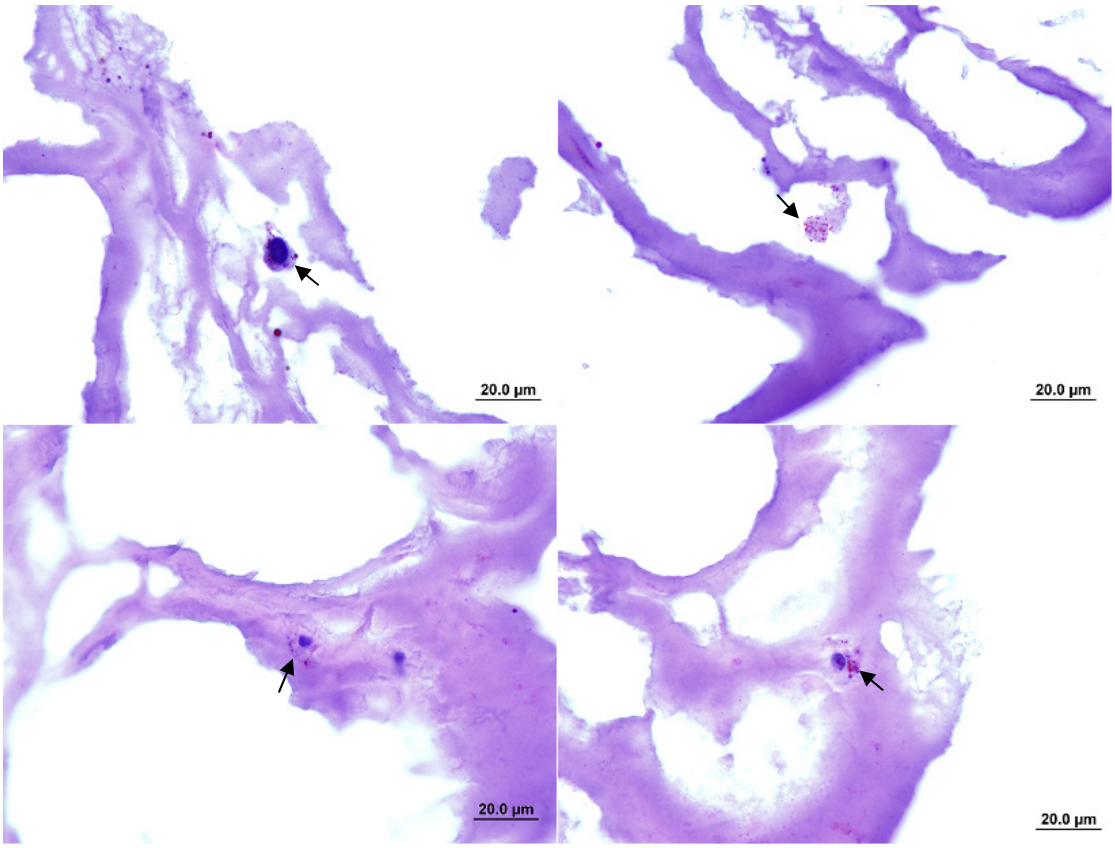

Figure 24. Oil Red O and H&E stainings of DAT:Fib - 1:1 hydrogel cryosections after 3 days of encapsulation of ASCs pre-differentiated into adipogenic lineage. Arrows show lipid vesicles inside cells. Thickness of cryosections was 5 µm. Scale bar is 20 µm.

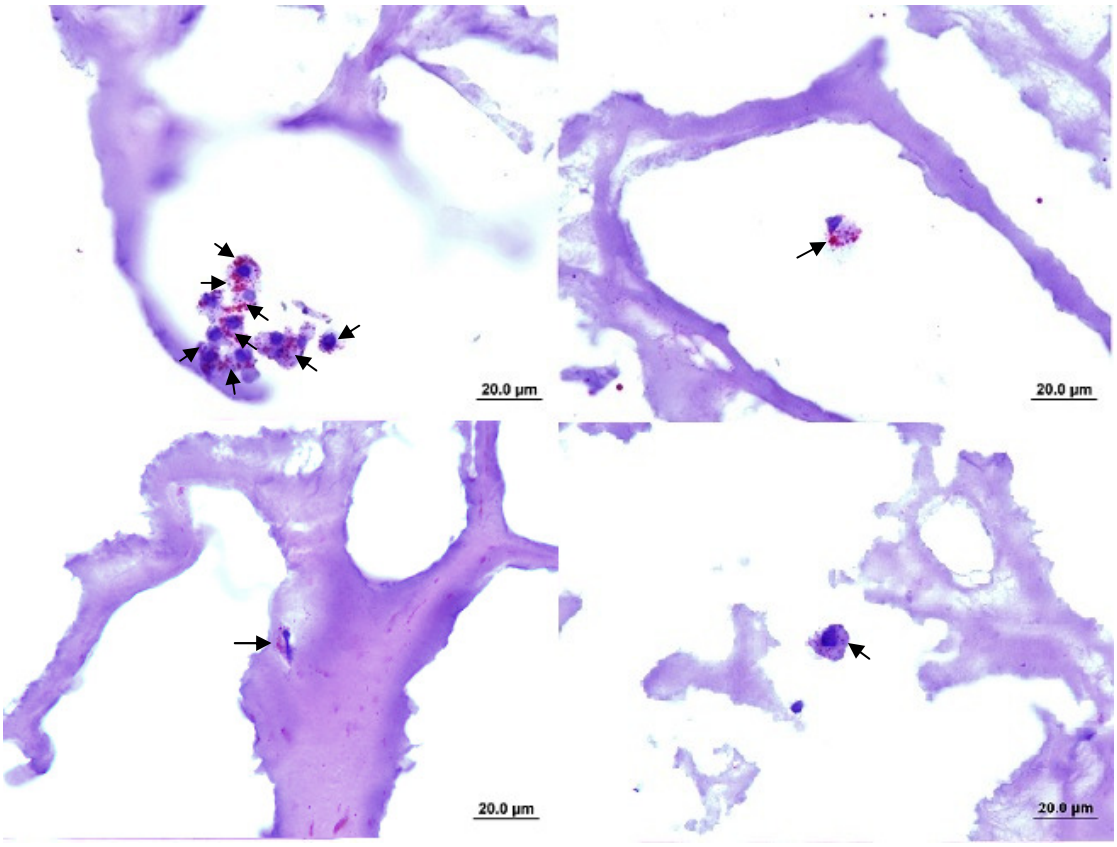

Figure 25. Oil Red O and H&E staining of DAT:Fib - 1:3 hydrogel cryosections after 3 days of encapsulation of ASCs pre-differentiated into adipogenic lineage. Arrows show lipid vesicles inside cells. Thickness of cryosections was 5 µm. Scale bar is 20 µm.

In terms of endothelial differentiation 1:3 - DAT:Fib hydrogels had also better results compared to 1:1- DAT:Fib hydrogel. It can be seen in Figure 26 that most of pre-differentiated ASCs remain in spherical shape in 1:1 - DAT:Fib hydrogels. Only few cells were elongated through matrix, however no end-to-end linking of cells or capillary-like structures were observed (Figure 26). On the other hand, in 1:3 - DAT:Fib hydrogels pre-differentiated ASCs elongated through the matrix direction, linked end-to-end with each other, and formed capillary-like structures by surrounding a space inside matrix (Figure 27).

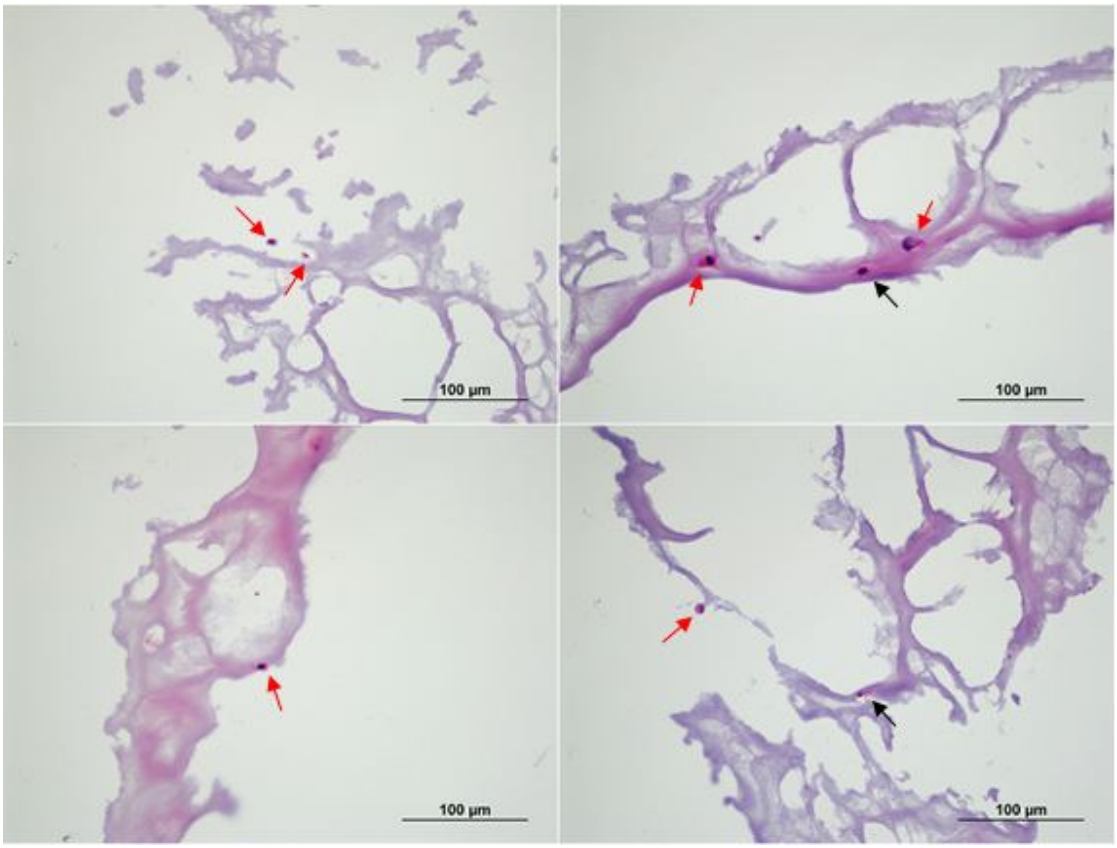

Figure 26. H&E staining of 1:1 - DAT:Fib hydrogel cryosections on 3rd day after encapsulation of ASCs pre-differentiated into endothelial lineage. Black arrows show endothelial-like cells which were elongated in the matrix direction, and red arrows show cells of spherical shape. There were no capillary-like structures in the sections. Thickness of cryosections was 5 µm. Scale bar is 100 µm.

This is an expected result, because endothelial cells prefer stiffer matrices for making angiogenic sprouts (Hanjaya-Putra et al., 2010; Lee et al., 2013). According to Hanjaya-Putra et al., VEGF concentration and mechanical properties of matrix determine endothelial progenitor cell (EPC) behaviour together. High VEGF concentrations activates matrix metalloproteinases (MMPs) which are required for angiogenic

sprouting. Together with this induction, stiffer materials upregulates tube formation activities in EPCs.

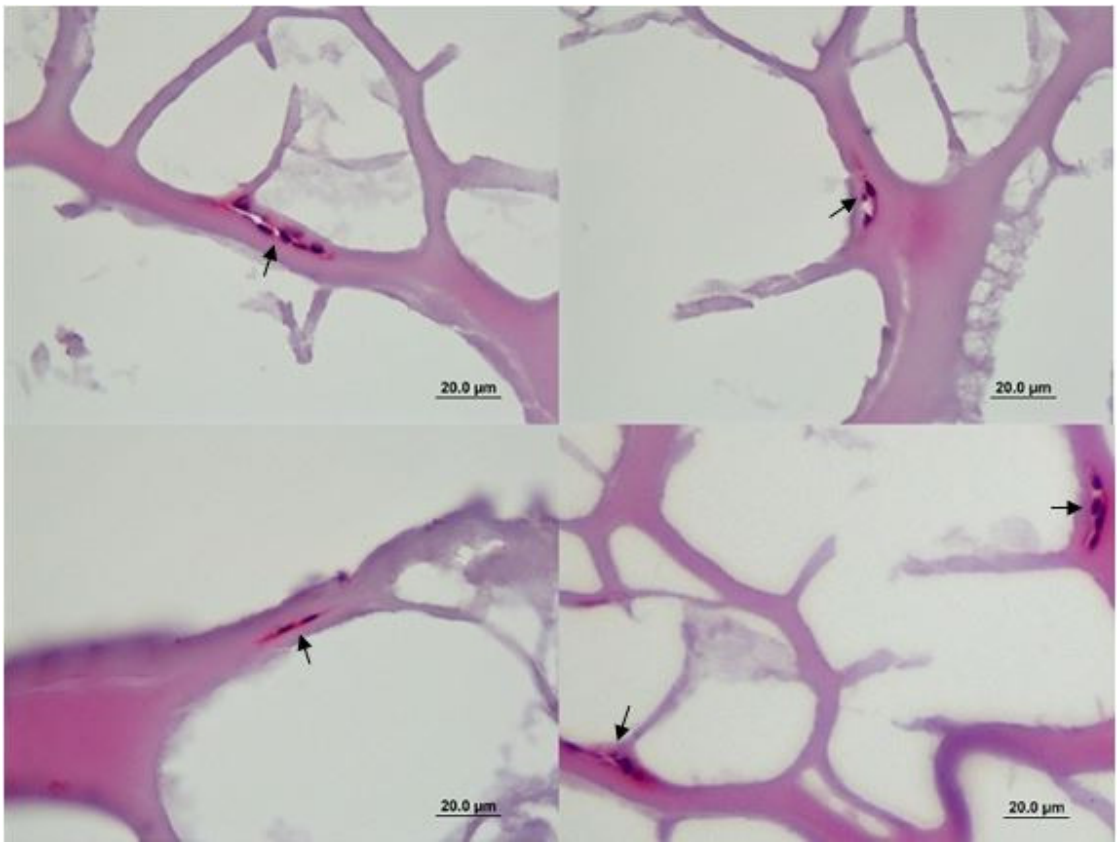

Figure 27. H&E staining of 1:3 - DAT:Fib hydrogel cryosections after 3 days of encapsulation of ASCs pre-differentiated into endothelial lineage. Arrows show endothelial-like cells elongated in matrix direction and form capillary-like structures by linking end-to-end. Thickness of cryosections was 5 µm. Scale bar is 20 µm.

In our study, ASCs were initially induced with EGM-2 and extra VEGF for 1 week. Therefore, 1:3 - DAT:Fib hydrogels behaved as a proper matrix for sprouting and tube formations due to its stiffness.

Endothelial and adipogenic pre-differentiated cells were also encapsulated together into 1:3 – DAT:Fib hydrogels. After 7 days of encapsulation sections were taken from hydrogels. To show adipogenic differentiation, Oil Red O staining was performed (Figure 28). On the other hand, endothelial differentiation was analyzed by immunufluorescent staining using FITC conjugated anti-vWF antibody (Figure 29). By Oil Red O staining, it is possible to see both pre-adipogenic cells which have lipid vesicles and thin, elongated cells which are probably pre-endothelial cells (Figure 28). Anti-vWF staining showed that these elongated cells expressed vWF, which showed that cells continued to differentiate into endothelial lineage after encapsulation (Figure 29).

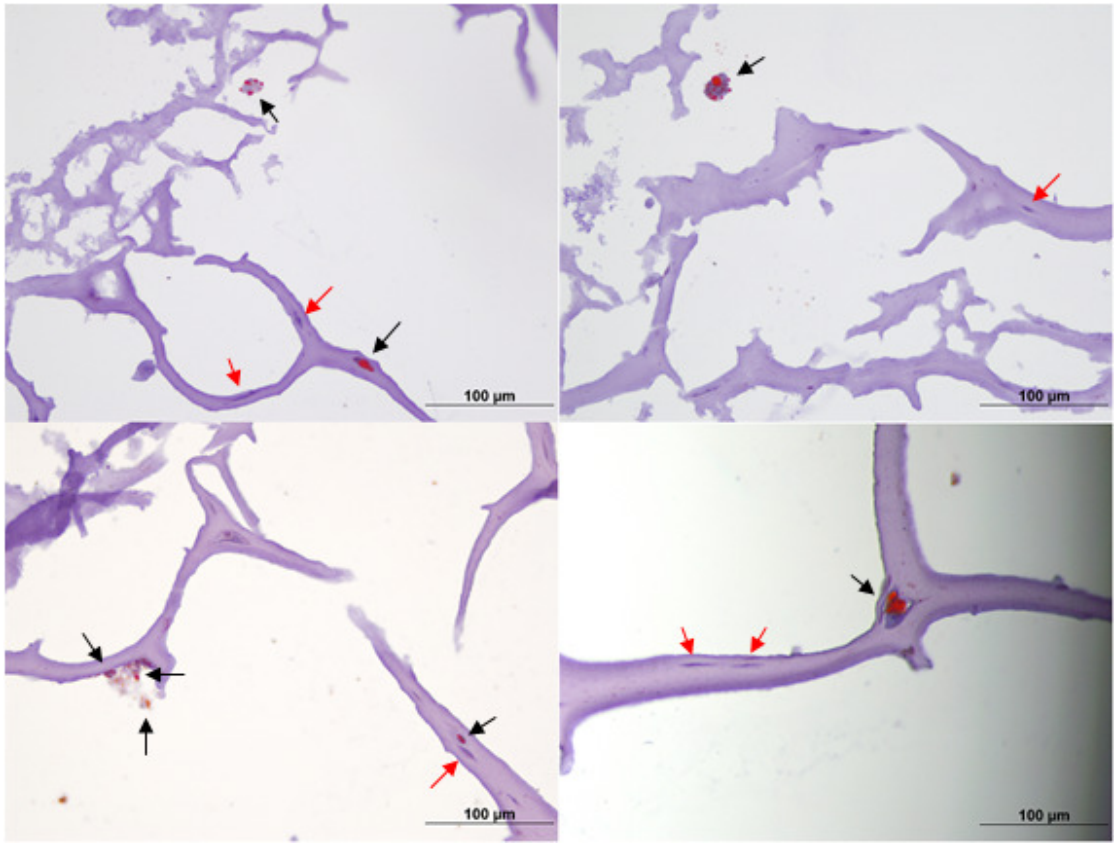

Figure 28. Oil Red O staining of DAT:Fib - 1:3 hydrogel cryosections after 7 days of encapsulation of ASCs pre-differentiated into adipogenic endothelial lineages. Black arrows show stained lipid vesicles inside pre-adipogenic cells. Red arrows show lipid-

free elongated cells which are possibly endothelial differentiated cells. Both types of cells continued to differentiate into committed cell lineage even if they were encapsulated into same scaffold. Thickness of cryosections was 5 µm. Scale bar is 100 µm.

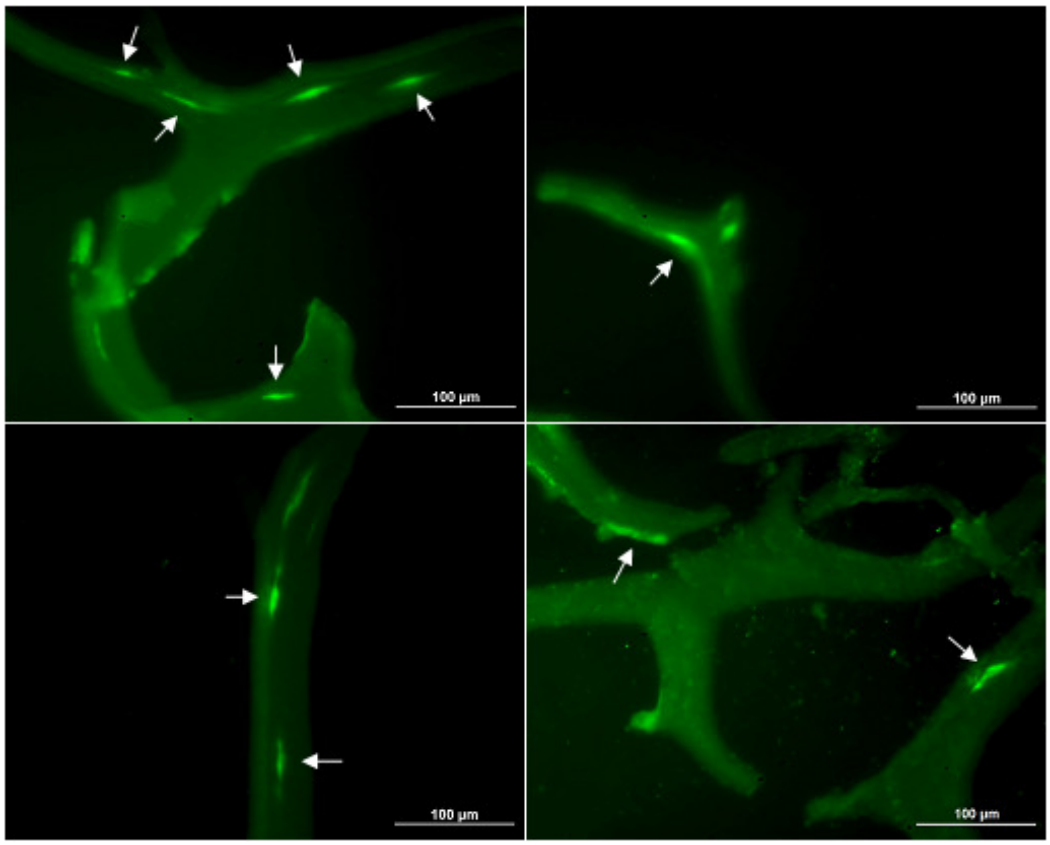

Figure 29. Immunofluorescent staining of 1:3 - DAT:Fib hydrogel sections by FITC conjugated Anti-vWF antibody. Sections were taken after 7 days of encapsulation of endothelial pre-differentiated cells. Arrows show elongated and thinned cells expressing vWF which is a characteristics of endothelial cells. Thickness of cryosections was 5 µm. Scale bar is 100 µm.

3.6. *In Vivo* Studies

According to the results of mechanical tests and cell culture studies with viability and differentiation analyses, 1:3 - DAT:Fib hydrogels were chosen for the *in vivo* studies.

Firstly, empty hydrogels were implanted subcutaneously to see body response to the hydrogel (Figure 30). On 7^{th} day of implantation, hydrogels were explanted to analyze early body response. 7^{th} day was chosen to minimize the effect of normal scar response to the suture. It was observed that hydrogel was covered by a thin fibrous tissue as a normal foreign material response (Figure 31a). There was no significant immune reaction around the implant. However, some multinucleated giant cells were observed on hydrogels probably for degradation starting outside of the disc (Figure 31b). Cracks seen in the middle of the implant and space between tissue and implant were probably caused by tissue sectioning process.

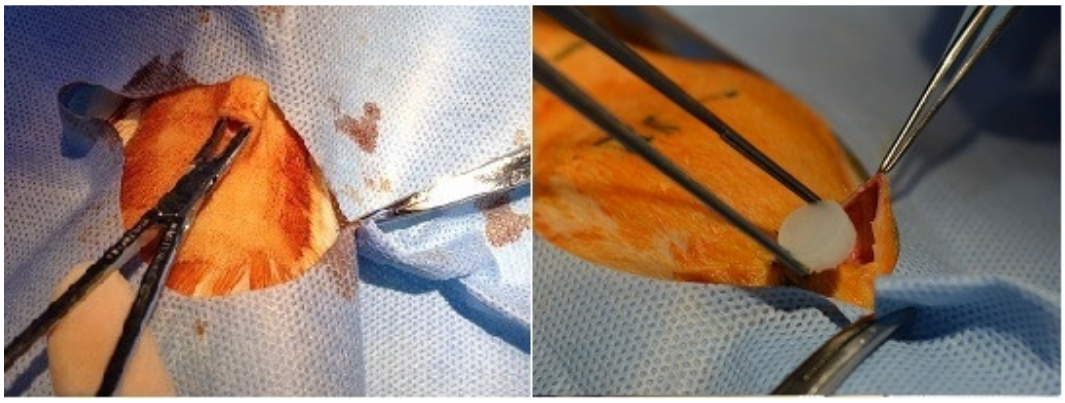

Figure 30. Subcutaneous implantation of hydrogel disc. A chamber was created under the skin, and disc formed hydrogel was placed in this chamber.

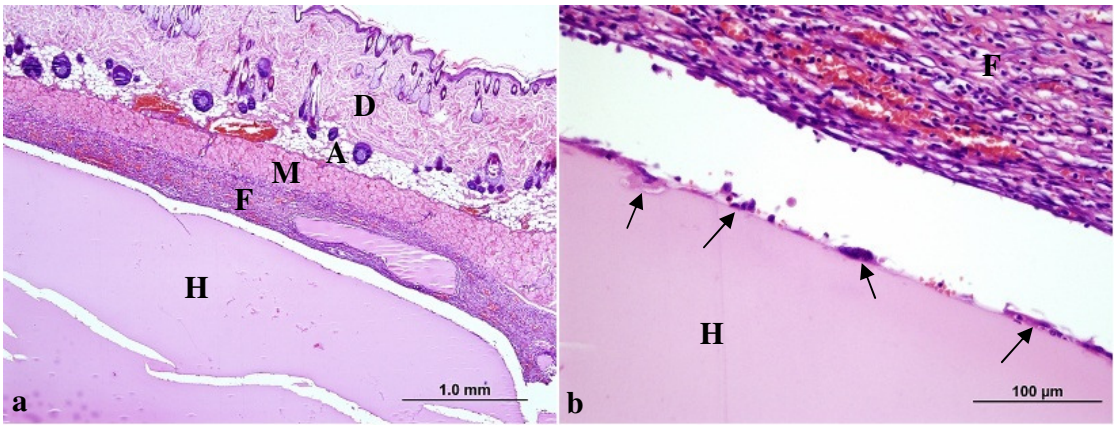

Figure 31. Histological analysis by H&E staining of subcutaneously implanted empty hydrogels after 7 days of implantation. **a)** Layers around hydrogel: H; hydrogel, F; fibrous tissue, M; muscle tissue, A; adipose tissue, D; Dermis. It can be seen that hydrogel remained undegraded, and a thin fibrous tissue was formed around it. Scale bar is 1 mm. **b)** Interface between hydrogel and host tissues. Arrows show multinucleated giant cells starting to degrade hydrogel particles by phagocytosis. Scale bar is 100 µm.

Analysis of hydrogels extracted after 21 days showed that fibrous tissue covering the hydrogel was thinner and it entered into hydrogel (Figure 32a). Hydrogel was degraded by the immune cells in fibrous tissue starting from outside (Figure 32b and Figure 32d). Normal degradation by hydrolysis should have also been in this period. However, most of the implant remained intact. It was also observed that many capillaries reached into the central parts of hydrogel (Figure 32c). This is a very important result since it shows vascularization of implant by host capillaries even without presence of cells inside it. In many studies, a functional vascularization was achieved in several weeks (Gafni et al., 2006; Cheng et al, 2009; Young et al., 2014). Therefore, vascularization in 3 weeks without any cells may be evaluated as a successful result. By encapsulation of ASCs pre-differentiated into endothelial lineage inside these hydrogels, vascularization process is expected to be accelerated. In 7^{th} day samples of this group, it was observed that neovascularization had started around hydrogel (Figure 34a and 34b). However,

therefore no vascular network in the central parts which were formed by pre-endothelial cells or from surrounding tissue. However, in 14th day samples, hydrogel was highly vascularized (Figure 34c). Capillaries reached to the central parts (Figure 34d). Therefore, it can be said that most of vascularization process of implant took place between 1st and 2nd week after implantation. It was faster than empty hydrogel. Encaspulation of pre-endothelial cells might have effects on this situation. They might break scaffold because of their angiogenic potential, and might help host fibrous tissue with capillaries to reach the central part. Also, it is expected that encapsulation of ASCs pre-differentiated into adipogenic lineage will provide new adipose tissue formation while hydrogel is being degraded by host response, and rapid vascularization will bring nutrients and oxygen to these regenerative cells. Figure 33 shows that pre-differentiated cells had begun to accumulate lipid vesicles in 1st week. It was also observed that some adipose-tissue like structures formed in some places inside hydrogel (Figure 35c and 35d). These kind of structures might be formed by pre-adipogenic cells encapsulated inside hydrogel in case of they remained alive. Figure 34a and 34b show that small capillaries or blood itself reached to central parts of scaffold where they are close enough for O_2 and nutrient diffusion, so they could feed cells. Probably, there will be more adipose tissue formation by time. Young et al. (2014) observed new adipose tissue formation in hydrogel after 4 weeks of implantation. Therefore, our results, according to observation of 1st and 2nd week-samples, are promising since we saw a newly formed adipose-like tissue in some regions.

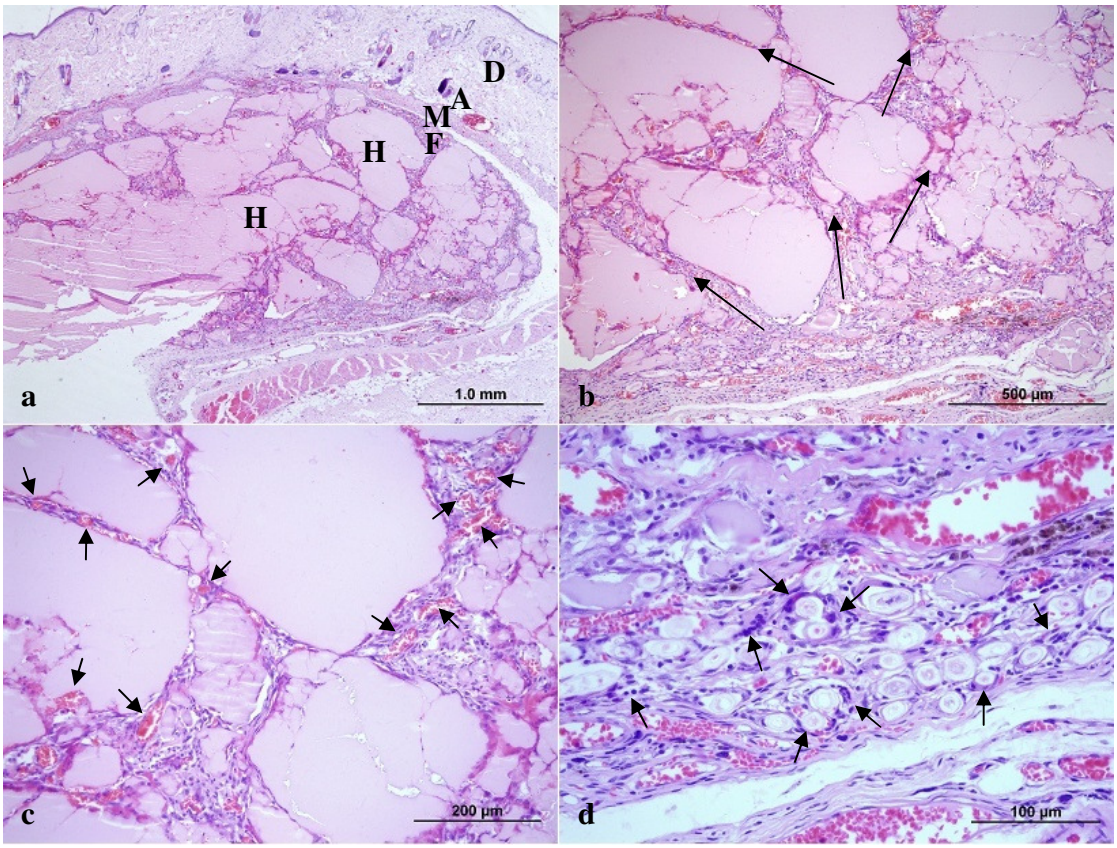

Figure 32. Histological analysis by H&E staining of subcutaneously implanted empty hydrogels after 21 days of implantation. **a)** Layers around hydrogel: H; hydrogel, F; fibrous tissue, M; muscle tissue, A; adipose tissue, D; Dermis. Scale bar is 1 mm. **b)** Vascularized fibrous tissue penetrating into the hydrogel by degrading through arrow directions. Scale bar is 500 µm. **c)** Capillary formations inside hydrogel. Arrows show capillary forming endothelial cells. Scale bar is 200 µm. **d)** Degradation of hydrogel starting from outside. Arrows show multinucleated giant cells engulfing hydrogel particles. Scale bar is 100 µm.

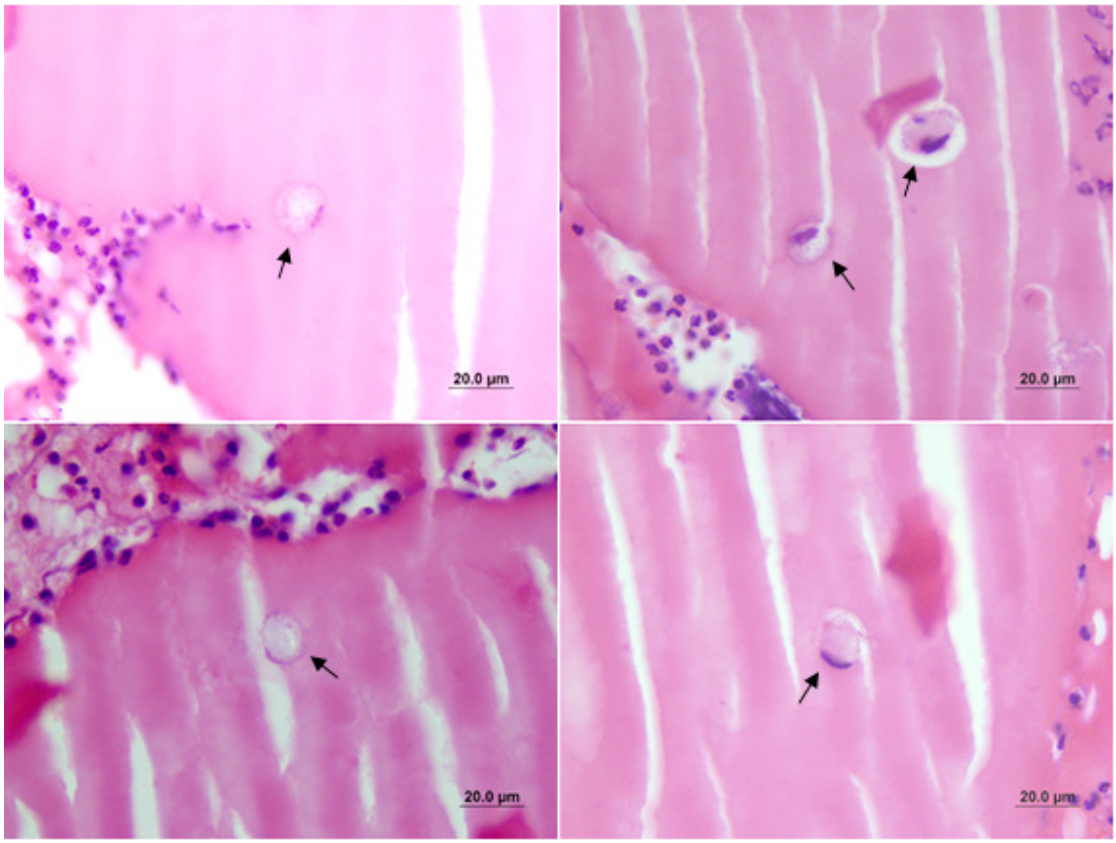

Figure 33. Histological analysis by H&E staining of subcutaneously implanted hydrogels with pre-adipogenic and pre-endothelial cells after 7 days of implantation. Arrows show lipid vesicle accumulated cells, their nuclei were pushed to sides of cells. This is characteristic of adipogenic differentiated cells.

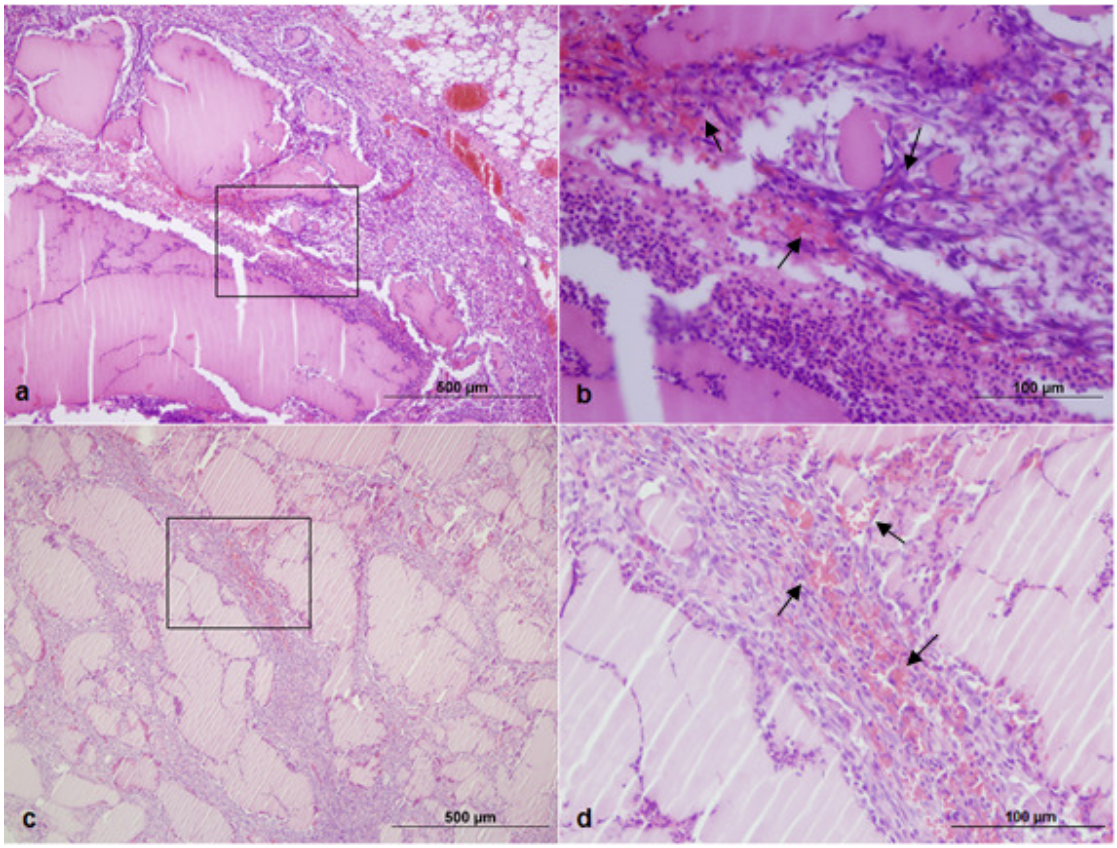

Figure 34. Histological analysis by H&E staining of subcutaneously implanted hydrogels with pre-adipogenic and pre-endothelial cells after 7 days (a and b) and 14 days (c and d) of implantation. Arrows in b, show neovascularization site around hydrogel, and in a, show capillaries inside hydrogel.

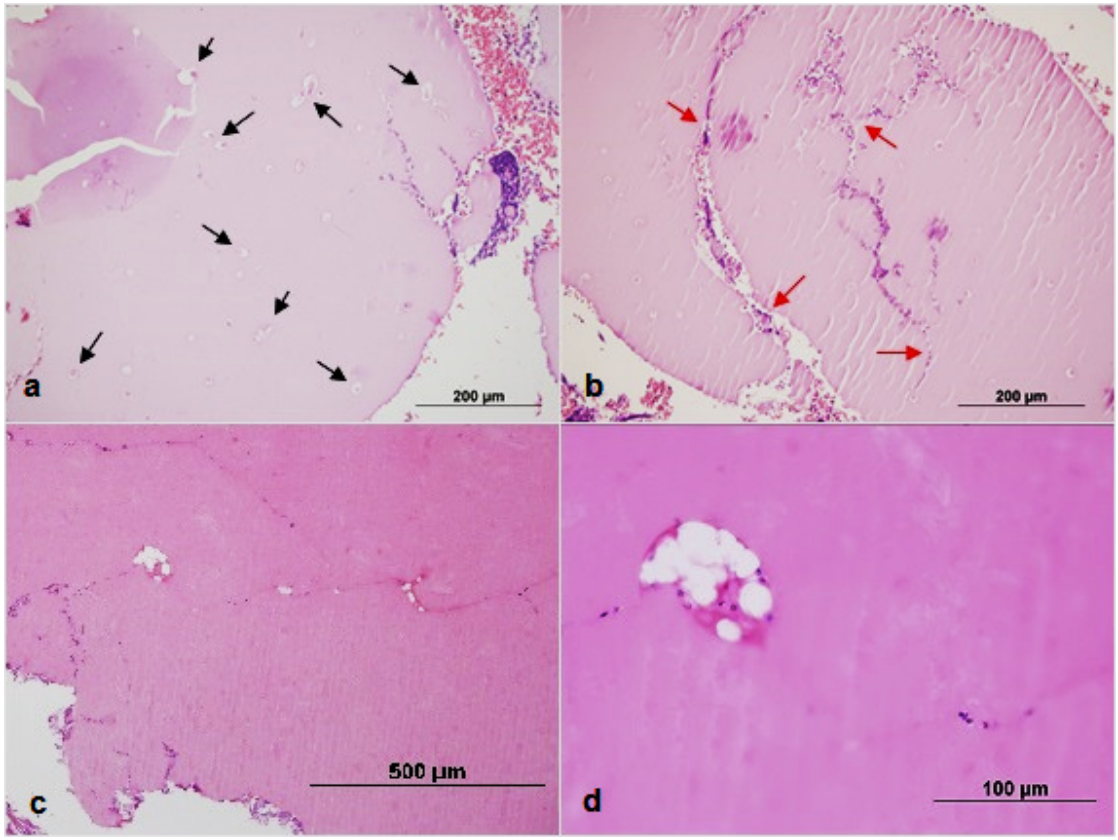

Figure 35. Histological analysis by H&E staining of subcutaneously implanted hydrogels with pre-adipogenic and pre-endothelial cells after 14 days of implantation. Black arrows in a, show cells probably remained alive and had potential to form adipose tissue by time, thanks to the small capillaries or blood which are close enough to nutrient and O_2 diffusion. Red arrows in b, show small capillaries and sometimes blood coming with fibrous tissue. These small capillaries might fuse with endothelial-differentiated cells encapsulated in hydrogel. In c and d, an adipose tissue-like structure was formed probably by these alive cells.

To investigate the potential of cell encapsulated hydrogel system to obtain a vascularized filler material around a blood vessel hydrogel system was implanted around a blood vessel. For this purpose, vortexed mixtures of DAT and fibroin were poured in a silicone mold to allow gelation around blood vessel (Figure 36a). After 10-15 minutes

gelation was observed, and mold was removed (Figure 36b). However, this method was not proper to obtain identical implants in terms of shape and mechanical properties and to compare results with each other. Therefore, it was decided to prepare hydrogels out of body in same sizes and shapes with a rift for blood vessel (Figure 36c).

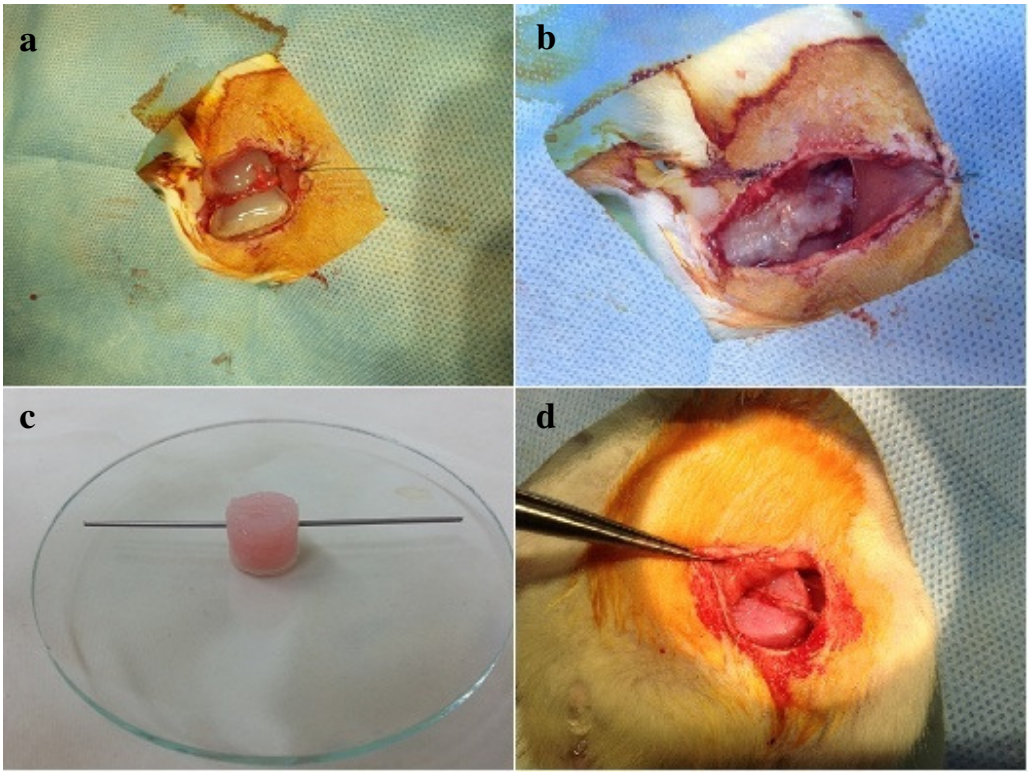

Figure 36. *In vivo* gelation and implantation of hydrogel. **a)** Just after vortex **b)** After 15 minutes **c)** Prepared hydrogels with vessel rift. 1 mm-diameter steel rod is used to mimic blood vessel. **d)** Implantation of hydrogels underneath the host vessel by replacing the vessel inside rift.

In vivo analyses of cell encapsulated hydrogels are under study for now. Implantations of 2nd and 3rd experimental groups, which were hydrogels implanted around host vessel with pre-differentiated ASCs into adipogenic lineage, and hydrogels implanted subcutaneously with pre-differentiated cells into adipogenic and endothelial lineages,

were performed (Figure 36d). Analyses of these groups at different time intervals, and implantations and analyses of other groups will be performed as future studies.

These results showed us that decellularized human lipoaspirates, as a component of hydrogel scaffold, did not create any significant immune response in rat body. Therefore, xenogenic materials can be used as scaffold materials after an effective decellularization process. That means a wide range of animals may be used as scaffold source in tissue engineering studies. In fact, for adipose tissue engineering, human lipoaspirates are proper too, because they are normally waste materials and can be obtained in high amounts.

Another important result of this study is its clinical applicability. For animal studies, no immune-suppressive agents were used. Instead, autologous ASCs were isolated from each rat, encapsulated into hydrogels after pre-differentiations, and implanted into the same rat. This procedure can easily be applied for the patients without using any immune-suppresive agents.

CHAPTER 4

CONCLUSION

In this study, it is tried to offer solutions for two main problems in adipose tissue engineering: vascularization and proper scaffold selection. DAT/Fibroin hydrogel has many natural ECM components which provides biocompatibility and bioactivity. Because of its fibroin content, its mechanical strength could be adjusted by changing the fibroin ratio. These conditions allowed DAT/Fibroin hydrogels to mimic natural tissue.

1:3 DAT:Fib ratio hydrogels had similar mechanical properties to natural adipose tissue and were found to resistant to *in vitro* degradation. *In vitro* cell culture analysis also showed that it was ideal for cell survival and proliferation. Moreover, it was observed that hydrogels with 1:3 - DAT:Fib ratio supported both adipogenic and endothelial differentiation of encapsulated cells. Therefore, hydrogels with 1:3 DAT:Fib ratio was chosen for *in vivo* studies. The hydrogels were shown to be biocompatible by subcutaneous implantation. High amount of vascularization by host capillary invasion through hydrogel observed suggest that implantation of hydrogels with pre-differentiated endothelial-like cells would highly accelerate the vascularization process. Also, encapsulation of pre-differentiated adipogenic cells may provide adipose tissue regeneration while hydrogel is degrading by host immune cells.

Results showed that that it is possible to develop a patient-specific vascularized adipose tissue by using autologous stem cells. This procedure can be applied directly in clinical treatments.

As a conclusion, 1:3 - DAT:Fib injectable hydrogels with encapsulated ASCs pre-differentiated into endothelial and adipogenic lineage, hold promise for adipose tissue

engineering and have potential for clinical applications such as filling defects in esthetical reconstructive surgery.

REFERENCES

Ailhaud, G. Development of White Adipose Tissue and Adipocyte Differentiation. Adipose Tissues. Georgetown, Texas: Landes Bioscience 2001; 27-35.

Atala, A., Bauer, S.B., Soker, S., Yoo, J.J., Retik, A.B. Tissue-engineered autologous bladders for patients needing cystoplasty. Lancet. 2006 Apr 15;367(9518):1241-6.

Badylak, S.F., Freytes, D.O., Gilbert, T.W. Extracellular matrix as a biological scaffold material: Structure and function. Acta Biomater. 2009; 5(1):1–13.

Badylak, S.F., Gilbert, T.W. Immune Response to Biologic Scaffold Materials. Semin Immunol. 2008 Apr; 20(2): 109–116.

Barry, F.P., Murphy, J.M. Mesenchymal stem cells: clinical applications and biological characterization. Int J Biochem Cell Biol 2004; 36:568-84.

Bettinger, C.J., Weinberg, E.J., Kulig, K.M., Vacanti, J.P., Wang, Y., Borenstein, J.T., Langer, R. Three-dimensional microfluidic tissue-engineering scaffolds using aflexible biodegradable polymer. Adv Mater. 2005 Dec 8;18(2):165-169.

Brown, B.N., Freund, J.M., Han, L., Rubin, J.P., Reing, J.E., Jeffries, E.M., Wolf, M.T., Tottey, S., Barnes, C.A., Ratner, B.D., Badylak, S.F. Comparison of three methods for the derivation of a biologic scaffold composed of adipose tissue extracellular matrix. Tissue Eng Part C Methods. 2011 Apr; 17(4):411-21.

Carmeliet, P. Mechanisms of angiogenesis and arteriogenesis. Nat Med. 2000 Apr;6(4):389-95.

Caspi, O., Lesman, A., Basevitch, Y., Gepstein, A., Arbel, G., Habib, I.H., Gepstein, L., Levenberg, S. Tissue engineering of vascularized cardiac muscle from human embryonic stem cells. Circ Res. 2007 Feb 2;100(2):263-72.

Celedón, J.C., Palmer, L.J., Xu, X., Wang, B., Fang, Z., Weiss, S.T. Sensitization to silk and childhood asthma in rural China.Pediatrics. 2001 May;107(5):E80.

Chen, R.R., Silva, E.A., Yuen, W.W., Mooney, D.J. Spatio-temporal VEGF and PDGF delivery patterns blood vessel formation and maturation. Pharm Res. 2007 Feb;24(2):258-64.

Cheng, M.H., Uriel, S., Brey, E.M. Tissue derived materials for adipose regeneration. Bioengineering research in chronic wounds. In: Gefen A, editor. Springer; 2009 Volume 1, pp. 281–299.

Cheung, H.K., Han, T.T., Marecak, D.M., Watkins, J.F., Amsden, B.G., Flynn, L.E. Composite hydrogel scaffolds incorporating decellularized adipose tissue for soft tissue engineering with adipose-derived stem cells. Biomaterials. 2014 Feb;35(6):1914-23.

Cho, S.W., Kim, S.S., Rhie, J.W., Cho, H.M., Choi, C.Y., Kim, B.S. Engineering of volume-stable adipose tissues. Biomaterials. 2005;26:3577.

Choi, J.H., Gimble, J.M., Lee, K., Marra, K.G., Rubin, J.P., Yoo, J.J., Vunjak-Novakovic, G., Kaplan, D.L. Adipose tissue engineering for soft tissue regeneration. Tissue Eng Part B Rev. 2010 Aug;16(4):413-26.

Clark, E.R., Clark, E.L. Microscopic observations on the growth of blood capillaries in the living mammal. Am J Anat. 1939;64:251–299.

Conconi, M.T., Ghezzo, F., Dettin, M., Urbani, L., Grandi, C., Guidolin, D., Nico, B., Di Bello, C., Ribatti, D., Parnigotto, P.P. Effects on in vitro and in vivo angiogenesis

induced by small peptides carrying adhesion sequences. J Pept Sci. 2010 Jul;16(7):349-57.

Cox, B., Emili, A. Tissue subcellular fractionation and protein extraction for use in massspectrometry-based proteomics. Nat Protoc. 2006; 1(4):1872–1878.

Crapo, P.M., Gilbert, T.W., Badylak, S.F. An overview of tissue and whole organ decellularization processes. Biomaterials. 2011 Apr;32(12):3233-43.

Dahl, S.L., Koh, J., Prabhakar, V., Niklason, L.E. Decellularized native and engineered arterial scaffolds for transplantation. Cell Transplant 2003;12:659–66.

Dardik, A., Chen, L., Frattini, J., Asada, H., Aziz, F., Kudo, F.A., Sumpio, B.E. Differential effects of orbital and laminar shear stress on endothelial cells. J Vasc Surg. 2005 May;41(5):869-80.

De Filippo, R.E., Yoo, J.J., Atala, A. Urethral replacement using cell seeded tubularized collagen matrices. J Urol. 2002 Oct;168(4 Pt 2):1789-92; discussion 1792-3.

De Ugarte, D.A., Ashjian, P.H., Elbarbary, A., Hedrick, M.H. Future of fat as raw material for tissue regeneration. Ann Plast Surg. 2003;50:215-9.

De Ugarte, D.A., Morizono, K., Elbarbary, A., Alfonso, Z., Zuk, P.A., Zhu, M., Dragoo, J.L., Ashjian, P., Thomas, B., Benhaim, P., Chen, I., Fraser, J., Hedrick, M.H. Comparison of multi-lineage cells from human adipose tissue and bone marrow. Cells Tissues Organs. 2003;174:101-9.

Deckers, M.M., van Bezooijen, R.L., van der Horst, G., Hoogendam, J., van Der Bent, C., Papapoulos, S.E., Löwik, C.W. Bone morphogenetic proteins stimulate angiogenesis through osteoblast-derived vascular endothelial growth factor A. Endocrinology. 2002 Apr;143(4):1545-53.

Druecke, D., Langer, S., Lamme, E., Pieper, J., Ugarkovic, M., Steinau, H.U., Homann, H.H. Neovascularization of poly(ether ester) blockcopolymer scaffolds in vivo: long-term investigations using intravital fluorescent microscopy. J Biomed Mater Res A. 2004 Jan 1;68(1):10-8.

Ehrbar, M., Djonov, V.G., Schnell, C., Tschanz, S.A., Martiny-Baron, G., Schenk, U., Wood, J., Burri, P.H., Hubbell, J.A., Zisch, A.H. Cell-demanded liberation of VEGF121 from fibrin implants induces local and controlled blood vessel growth. Circ Res. 2004 Apr 30;94(8):1124-32.

Enerbäck, S. The origins of brown adipose tissue. N Engl J Med. 2009 May 7;360(19):2021-3.

Farndale, R.W., Buttle, D.J., Barrett, A.J. Improved quantitation and discrimination of sulphated glycosaminoglycans by use of dimethylmethylene blue. Biochim Biophys Acta. 1986 Sep 4;883(2):173-7.

Fischer, L.J., McIlhenny, S., Tulenko, T., Golesorkhi, N., Zhang, P., Larson, R., Lombardi, J., Shapiro, I., DiMuzio, P.J. Endothelial differentiation of adipose-derived stem cells: effects of endothelial cell growth supplement and shear force. J Surg Res. 2009 Mar;152(1):157-66.

Flynn, L.E. The use of decellularized adipose tissue to provide an inductive microenvironment for the adipogenic differentiation of human adipose-derived stem cells. Biomaterials. 2010 Jun; 31(17):4715-24.

Freytes, D.O., Badylak, S.F., Webster, T.J., Geddes, L.A., Rundell, A.E. Biaxial strength of multilaminated extracellular matrix scaffolds. Biomaterials. 2004 May;25(12):2353-61.

Freytes, D.O., Martin, J., Velankar, S.S., Lee, A.S., Badylak, S.F. Preparation and rheological characterization of a gel form of the porcine urinary bladder matrix. Biomaterials. 2008 Apr;29(11):1630-7.

Falke, G., Yoo, J.J., Kwon, T.G., Moreland, R.R., Atala, A. Formation of corporal tissue architecture in vivo using human cavernosal muscle and endothelial cells seeded on collagen matrices. Tissue Eng. 2003 Oct;9(5):871-9.

Gafni, Y., Zilberman, Y., Ophir, Z., Abramovitch, R., Jaffe, M., Gazit, Z., Domb, A., Gazit, D. Design of a filamentous polymeric scaffold for in vivo guided angiogenesis. Tissue Eng. 2006 Nov;12(11):3021-34.

Gesta, S.,Tseng, Y.H., Kahn, C.R. Developmental origin of fat: tracking obesity to its source. Cell. 2007 Oct 19;131(2):242-56.

Gilbert, T.W., Freund, J.M., Badylak, S.F. Quantification of DNA in biologic scaffold materials. J Surg Res. 2009;152:135–9.

Gilbert, T.W., Sellaro, T.L., Badylak, S.F. Decellularization of tissues and organs. Biomaterials. 2006 Jul;27(19):3675-83.

Gimble, J.M. Adipose tissue-derived therapeutics. Expert Opin Biol Ther. 2003 Aug;3(5):705-13.

Gonzalez-Rey, E., Gonzalez, M. A., Varela, N., O'Valle, F., Hernandez-Cortes, P., Rico, L., Büscher, D., Delgado, M. Human adipose-derived mesenchymal stem cells reduce inflammatory and T cell responses and induce regulatory T cells in vitro in rheumatoid arthritis. Annals of the Rheumatic Diseases. 2010;69:241–248.

Gorschewsky, O., Puetz, A., Riechert, K., Klakow, A., Becker, R. Quantitative analysis of biochemical characteristics of bone-patellar tendon-bone allografts. Biomed Mater Eng. 2005; 15(6):403–411.

Green, H., Meuth, M. An established pre-adipose cell line and its differentiation in culture. Cell. 1974; 3:127-33.

Gui, L., Chan, S.A., Breuer, C.K., Niklason, L.E. Novel utilization of serum in tissue decellularization. Tissue Eng Part C Methods. 2010; 16(2):173–184.

Hanjaya-Putra, D., Yee, J., Ceci, D., Truitt, R., Yee, D., Gerecht, S. Vascular endothelial growth factor and substrate mechanics regulate in vitro tubulogenesis of endothelial progenitor cells. J Cell Mol Med. 2010 Oct;14(10):2436-47.

Hassan, W., Dong, Y., Wang, W. Encapsulation and 3D culture of human adipose-derived stem cells in an in-situ crosslinked hybrid hydrogel composed of PEG-based hyperbranched copolymer and hyaluronic acid. Stem Cell Res Ther. 2013 Mar 21;4(2):32.

Helisch, A. and Schaper, W. Arteriogenesis: the development and growth of collateral arteries. Microcirculation. 2003 Jan;10(1):83-97.

Hirschi, K.K. et al. Endothelial cells modulate the proliferation of mural cell precursors via platelet-derived growth factor-BB and heterotypic cell contact. Circ Res. 1999 Feb 19;84(3):298-305.

Hirschi, K.K., Skalak, T.C., Peirce, S.M., Little, C.D. Vascular assembly in natural and engineered tissues. Ann N Y Acad Sci. 2002 Jun;961:223-42.

Hopkinson A, Shanmuganathan VA, Gray T, Yeung AM, Lowe J, James DK, et al. Optimization of amniotic membrane (AM) denuding for tissue engineering. Tissue Eng Part C Methods. 2008; 14(4):371–381.

Horan, R.L., Antle, K., Collette, A.L., Wang, Y., Huang, J., Moreau, J.E., Volloch, V., Kaplan, D.L., Altman, G.H. In vitro degradation of silk fibroin. Biomaterials. 2005 Jun;26(17):3385-93.

Hutmacher, D.W., Sittinger, M,. Risbud, M.V. Scaffold-based tissue engineering: rationale for computer-aided design and solid free-form fabrication systems. Trends Biotechnol. 2004 Jul;22(7):354-62.

Jain, R.K., Patrick, A., Josh, T., Dan, G.D., Dai, F. Engineering vascularized tissue. Nat Biotechnol. 2005 Jul;23(7):821-3.

Jeong, J.H. Adipose Stem Cells as a Clinically Available and Effective Source of Adult Stem Cell Therapy. Int J Stem Cells. 2008 Nov; 1(1): 43–48.

Johnson, P.C., Mikos, A.G., Fisher, J.P., Jansen, J.A. Strategic directions in tissue engineering. Tissue Eng. 2007 Dec;13(12):2827-37.

Kang, J.H., Gimble, J.M., and Kaplan, D.L. In vitro 3D model for human vascularized adipose tissue. Tissue Eng Part A. 2009 Aug;15(8):2227-36.

Karal-Yılmaz, O., Serhatlı, M., Baysal, K., Baysal, B.M. Preparation and in vitro characterization of vascular endothelial growth factor (VEGF)-loaded poly(D, Llactic-co-glycolic acid) microspheres using a double emulsion/solvent evaporation technique.J Microencapsul. 2011;28(1):46-54.

Kässmeyer, S., Plendl, J., Custodis, P., Bahramsoltani, M. New insights in vascular development: vasculogenesis and endothelial progenitor cells. Anat Histol Embryol. 2009;38:1-11.

Kershaw, E.E.,Flier, J.S. Adipose tissue as an endocrine organ. J Clin Endocrinol Metab. 2004 Jun;89(6):2548-56.

Klebe, R.J. Isolation of a collagen-dependent cell attachment factor. Nature. 1974;250:248–51.

Kluger, P.J., Wyrwa, R., Weisser, J., Maierle, J., Votteler, M., Rode, C., Schnabelrauch, M., Walles, H., Schenke-Layland, K. Electrospun poly(D/L-lactideco- L-lactide) hybrid

matrix: a novel scaffold material for soft tissue engineering.J Mater Sci Mater Med. 2010 Sep;21(9):2665-71.

Kneser, U., Polykandriotis, E., Ohnolz, J., Heidner, K., Grabinger, L., Euler, S., Amann, K.U., Hess, A., Brune, K., Greil, P., Stürzl, M., Horch, R.E.Engineering of vascularized transplantable bone tissues: induction of axial vascularization in an osteoconductive matrix using an arteriovenous loop. Tissue Eng. 2006 Jul;12(7):1721-31.

Ko, C., Dixit, V., Shaw, W., Gitnick, G. In vitro slow release profile of endothelial cell growth factor immobilized within calcium alginate microbeads.Artif Cells Blood Substit Immobil Biotechnol. 1995;23(2):143-51.

Kubo, Y., Kaidzu, S., Nakajima, I., Takenouchi, K. & Nakamura, F. Organization of extracellular matrix components during differentiation of adipocytes in long-term culture. In Vitro Cell Dev Biol Anim. 2000 Jan;36(1):38-44.

Lanza, R., Langer, R., Vacanti, J. Principles of tissue engineering. 3rd ed. Burlington, MA: Elsevier Academic Press, 2007.

Lee, J., Abdeen, A.A., Zhang, D., Kilian, K.A. Directing stem cell fate on hydrogel substrates by controlling cell geometry, matrix mechanics and adhesion ligand composition. Biomaterials. 2013 Nov;34(33):8140-8.

Lee, K., Villena J.A., Moon, Y.S., Kim, K.H., Lee, S., Kang, C., Sul, H.S. Inhibition of adipogenesis and development of glucose intolerance by soluble preadipocyte factor-1 (Pref-1). J Clin Invest. 2003 Feb;111(4):453-61.

Lee, P.F., Bai, Y., Smith, R.L., Bayless, K.J., Yeh, A.T. Angiogenic responses are enhanced in mechanically and microscopically characterized, microbial transglutaminase crosslinked collagen matrices with increased stiffness. Acta Biomater. 2013 Jul;9(7):7178-90.

Lee, S.H., Moon, J.J., Miller, J.S., West, J.L. Poly(ethylene glycol) hydrogels conjugated with a collagenase-sensitive fluorogenic substrate to visualize collagenase activity during three-dimensional cell migration. Biomaterials. 2007 Jul;28(20):3163-70.

Liu, H., Slamovich, E.B., Webster, T.J. Less harmful acidic degradation of poly(lactic-co-glycolic acid) bone tissue engineering scaffolds through titania nanoparticle addition. Int J Nanomedicine. 2006; 1(4): 541-545.

Lowe, C.E., O'Rahilly, S., Rochford, J.J. Adipogenesis at a glance. J Cell Sci. 2011 Aug 15;124(Pt 16):2681-6.

Malda, J., Rouwkema, J., Martens, D.E., Le Comte, E.P., Kooy, F.K., Tramper, J., van Blitterswijk, C.A., Riesle, J. Oxygen gradients in tissue-engineered PEGT/ PBT cartilaginous constructs: measurement and modeling. Biotechnol Bioeng. 2004 Apr 5;86(1):9-18.

Mandrup, S., Lane, M.D. Regulating adipogenesis. J Biol Chem. 1997 Feb 28;272(9):5367-70.

Mauney, J.R., Nguyen, T., Gillen, K., Kirker-Head, C., Gimble, J.M., Kaplan, D.L. Engineering adipose-like tissue in vitro and in vivo utilizing human bone marrow and adipose-derived mesenchymal stem cells with silk fibroin 3D scaffolds. Biomaterials. 2007;28:5280.

Meissburger, Bettina. Molecular mechanisms of adipogenesis in obesity and the metabolic syndrome. Unpublished Dr. Sc. thesis. 2010. ETH Zurich.

Mih, J.D., Marinkovic, A., Liu, F., Sharif, A.S., Tschumperlin, D.J. Matrix stiffness reverses the effect of actomyosin tension on cell proliferation. J Cell Sci. 2012 Dec 15;125(Pt 24):5974-83.

Mousavi, S.J., Hamdy Doweidar, M. Role of Mechanical Cues in Cell Differentiation and Proliferation: A 3D Numerical Model. PLoS One. 2015 May 1;10(5):e0124529.

Nicodemus, G.D., Bryant, S.J. Cell Encapsulation in Biodegradable Hydrogels for Tissue Engineering Applications. Tissue Eng Part B Rev. 2008 Jun; 14(2): 149–165.

Niemela, S., Miettinen, S., Sarkanen, J.R., Ashammakhi, N. Adipose Tissue and Adipocyte Differentiation: Molecular and Cellular Aspects and Tissue Engineering Applications. Topics in Tissue Engineering. 2008; Vol 4, 1-26.

Novosel, E.C., Kleinhans, C., Kluger, P.J. Vascularization is the key challenge in tissue engineering. Adv Drug Deliv Rev. 2011 Apr 30;63(4-5):300-11.

Panilaitis, B., Altman, G.H., Chen, J., Jin, H.J., Karageorgiou, V., Kaplan, D.L. Macrophage responses to silk. Biomaterials. 2003 Aug;24(18):3079-85.

Park, J.S., Chu, J.S., Tsou, A.D., Diop, R., Tang, Z., Wang, A., Li, S. The effect of matrix stiffness on the differentiation of mesenchymal stem cells in response to TGF-β. Biomaterials. 2011 Jun;32(16):3921-30.

Petersen, T.H., Calle, E.A., Zhao, L., Lee, E.J., Gui, L., Raredon, M.B., et al. Tissue-engineered lungs for in vivo implantation. Science. 2010; 329(5991):538–541.

Pola, R., Ling, L.E., Silver, M., Corbley, M.J., Kearney, M., Blake Pepinsky, R., Shapiro, R., Taylor, F.R., Baker, D.P., Asahara, T., Isner, J.M. The morphogen Sonic hedgehog is an indirect angiogenic agent upregulating two families of angiogenic growth factors. Nat Med. 2001 Jun;7(6):706-11.

Prasertsung, I., Kanokpanont, S., Bunaprasert, T., Thanakit, V., Damrongsakkul, S. Development of acellular dermis from porcine skin using periodic pressurized technique. J Biomed Mater Res B Appl Biomater. 2008; 85(1):210–219.

Prins, J.B., O'Rahilly, S. Regulation of adipose cell number in man. Clin Sci (Lond). 1997; 92:3-11.

Prior, B.M., Yang, H.T., Terjung, R.L. What makes vessels grow with exercise training? J Appl Physiol (1985). 2004 Sep;97(3):1119-28.

Probst, M., Dahiya, R., Carrier, S., Tanagho, E.A. Reproduction of functional smooth muscle tissue and partial bladder replacement. Br J Urol. 1997 Apr;79(4):505-15.

Reing, J.E., Brown, B.N., Daly, K.A., Freund, J.M., Gilbert, T.W., Hsiong, S.X., et al. The effects of processing methods upon mechanical and biologic properties of porcine dermal extracellular matrix scaffolds. Biomaterials. 2010; 31(33):8626–8633.

Richardson, T.P., Peters, M.C., Ennett, A.B., Mooney, D.J. Polymeric system for dual growth factor delivery. Nat Biotechnol. 2001 Nov;19(11):1029-34.

Risau, W., Flamme, I. Vasculogenesis. Annu. Rev. Cell Dev. Biol. 1995; 11:73–91.

Rocha, P.M., Santo, V.E., Gomes, M.E., Reis, R.L., Mano, J.F. Encapsulation of adipose derived stem cells and transforming growth factor-b1 in carrageenan-based hydrogels for cartilage tissue engineering. J Bioact Compat Polym. 2013 May;26(5): 493–507.

Rockwood, D.N., Preda, R.C., Yücel, T., Wang, X., Lovett, M.L., Kaplan, D.L. Materials fabrication from Bombyx mori silk fibroin. Nat Protoc. 2011 Sep 22;6(10):1612-31.

Rodriguez, A., Cao, Y.L., Ibarra, C., Pap, S., Vacanti, M., Eavey, R.D., Vacanti, C.A.Characteristics of cartilage engineered from human pediatric auricular cartilage.Plast Reconstr Surg. 1999 Apr;103(4):1111-9.

Rosen, E.D., MacDougald, O.A. Adipocyte differentiation from the inside out. Nat Rev Mol Cell Biol. 2006 Dec;7(12):885-96.

Rosen, E.D.,Spiegelman, B.M. Molecular regulation of adipogenesis. AnnuRev Cell Dev Biol. 2000;16:145-71.

Rouwkema, J., de Boer, J., Van Blitterswijk, C.A. Endothelial cells assemble into a 3-dimensional prevascular network in a bone tissue engineering construct. Tissue Eng. 2006 Sep;12(9):2685-93.

Rouwkema, J., Rivron, N.C., van Blitterswijk, C.A. Vascularization in tissue engineering Trends Biotechnol. 2008 Aug;26(8):434-41.

Sah, M.K., Pramanik, K. Preparation, characterization and in vitro study of biocompatible fibroin hydrogel. African J Biotechnol. 2011 Aug;10(40):7878-7892.

Schultheiss, D., Gaboue, A.I., Cebotari, S., Tudorache, I., Walles, T., Schlote, N., Wefer, J., Kaufmann, P.M., Haverich, A., Jonas, U., Stief, C.G., Mertsching, H. Biological vascularized matrix for bladder tissue engineering: matrix preparation, reseeding technique and shortterm implantation in a porcine model. J Urol. 2005 Jan;173(1):276-80.

Seddon, A.M., Curnow, P., Booth, P.J. Membrane proteins, lipids and detergents: not just a soap opera. Biochim Biophys Acta. 2004;1666:105–17.

Selvarajan, S., Lund, L.R., Takeuchi, T., Craik, C.S., Werb, Z. A plasma kallikrein-dependent plasminogen cascade required for adipocyte differentiation. Nat Cell Biol. 2001 Mar;3(3):267-75.

Sensebé, L., Krampera, M., Schrezenmeier, H., Bourin, P., Giordano, R. Mesenchymal stem cells for clinical application. Vox Sanguinis. 2010; 98, 93–107.

Shepherd, B.R., Enis, D.R., Wang, F., Suarez, Y., Pober, J.S., Schechner, J.S. Vascularization and engraftment of a human skin substitute using circulating progenitor cell-derived endothelial cells. FASEB J. 2006 Aug;20(10):1739-41.

Soong, H.K., Kenyon, K.R. Adverse reactions to virgin silk sutures in cataract surgery. Ophthalmology. 1984 May;91(5):479-83.

Spiegelman, B.M., Farmer, S.R. Decreases in tubulin and actin gene expression prior to morphological differentiation of 3T3 adipocytes. Cell. 1982 May;29(1):53-60.

Symonds, M.E. Adipose Tissue Biology. New York, Springer, 2012.

Takahashi, T., Kalka, C., Masuda, H., Chen, D., Silver, M., Kearney, M., Magner, M., Isner, J.M., Asahara, T. Ischemia- and cytokine-induced mobilization of bone marrow-derived endothelial progenitor cells for neovascularization. Nat. Med. 1999; 5:434–438.

Teh, T.K., Toh, S.L., Goh, J.C. Optimization of the silk scaffold sericin removal process for retention of silk fibroin protein structure and mechanical properties.Biomed Mater. 2010 May 11;5(3):035008.

Thevenot, P.T., Nair, A.M., Shen, J., Lotfi, P., Ko, C.Y., Tang, L. The effect of incorporation of SDF-1alpha into PLGA scaffolds on stem cell recruitment and the inflammatory response. Biomaterials. 2010 May;31(14):3997-4008.

Tong, Q., Dalgin, G., Xu, H., Ting, C.N., Leiden, J.M., Hotamisligil, G.S. Function of GATA transcription factors in preadipocyte-adipocyte transition. Science. 2000 Oct 6;290(5489):134-8.

Tong, Q., Hotamisligil, G.S. Molecular Mechanisms of Adipocyte Differentiation. Rev Endocr Metab Disord. 2001 Oct;2(4):349-55.

Tontonoz, P., Hu, E.D., Spiegelman, B.M. Stimulation of Adipogenesis in Fibroblasts by Ppar-Gamma-2, a Lipid-Activated Transcription Factor. Cell. 1994 Dec 30;79(7):1147-56.

Tullberg-Reinert, H., Jundt, G. In situ measurement of collagen synthesis by human bone cells with a sirius red-based colorimetric microassay: effects of transforming

growth factor beta 2 and ascorbic acid 2-phosphate. Histochem Cell Biol. 1999 Oct;112(4):271-6.

Turner, A.E., Yu, C., Bianco, J., Watkins, J.F., Flynn, L.E.The performance of decellularized adipose tissue microcarriers as an inductive substrate for human adipose-derived stem cells.Biomaterials. 2012 Jun;33(18):4490-9.

Uriel, S., Huang, J.J., Moya, M.L., Francis, M.E., Wang, R., Chang, S.Y., Cheng, M.H., Brey, E.M. The role of adipose protein derived hydrogels in adipogenesis. Biomaterials. 2008 Sep;29(27):3712-9.

Uriel, S., Labay, E., Francis-Sedlak, M., Moya, M.L., Weichselbaum, R.R., Ervin, N., Cankova, Z., Brey, E.M. Extraction and assembly of tissue-derived gels for cell culture and tissue engineering. Tissue Eng Part C Methods. 2009 Sep;15(3):309-21.

Uygun, B.E., Soto-Gutierrez, A., Yagi, H., Izamis, M.L., Guzzardi, M.A., Shulman, C., et al. Organ reengineering through development of a transplantable recellularized liver graft using decellularized liver matrix. Nat Med. 2010; 16(7):814–820.

Wang, X., Kluge, J.A., Leisk, G.G., Kaplan, D.L. Sonication-induced gelation of silk fibroin for cell encapsulation. Biomaterials. 2008 Mar;29(8):1054-64.

Wells, R.G. The role of matrix stiffness in regulating cell behavior. Hepatology. 2008 Apr;47(4):1394-400.

Wisser, D., Steffes, J. Skin replacement with a collagen based dermal substitute, autologous keratinocytes and fibroblasts in burn trauma.Burns. 2003 Jun;29(4):375-80.

Yamahara, K., Itoh, H. Potential use of endothelial progenitor cells for regeneration of the vasculature, Ther Adv Cardiovasc Dis. 2009 Feb;3(1):17-27.

Yanez, R., Lamana, M.L., Garcia-Castro, J., Colmenero, I., Ramírez, M., Bueren, J.A. Adipose tissue-derived mesenchymal stem cells have in vivo immunosuppressive

properties applicable for the control of the graft-versus-host disease. Stem Cells. 2006; 24:2582-2591.

Yang B, Zhang Y, Zhou L, Sun Z, Zheng J, Chen Y, et al. Development of a porcine bladder acellular matrix with well-preserved extracellular bioactive factors for tissue engineering. Tissue Eng Part C Methods. 2010; 16(5):1201–1211.

Yang, J., Zhou, W., Zheng, W., Ma, Y., Lin, L., Tang, T., Liu, J., Yu, J., Zhou, X., Hu, J. Effects of myocardial transplantation of marrow mesenchymal stem cells transfected with vascular endothelial growth factor for the improvement of heart function and angiogenesis after myocardial infarction. Cardiology. 2007;107(1):17-29.

Yang, M.H., Yuan, S.S., Chung, T.W., Jong, S.B., Lu, C.Y., Tsai, W.C., Chen, W.C., Lin, P.C., Chiang, P.W., Tyan, Y.C. Characterization of silk fibroin modified surface: a proteomic view of cellular response proteins induced by biomaterials. Biomed Res Int. 2014;2014:209469.

Young, D.A., Bajaj, V., Christman, K.L. Award winner for outstanding research in the PhD category, 2014 Society for Biomaterials annual meeting and exposition, Denver, Colorado, April 16-19, 2014: Decellularized adipose matrix hydrogels stimulate in vivo neovascularization and adipose formation. J Biomed Mater Res A. 2014 Jun;102(6):1641-51.

Young, D.A., Ibrahim, D.O., Hu, D., Christman, K.L. Injectable Hydrogel Scaffold from Decellularized Human Lipoaspirate. ActaBiomater. 2011 Mar;7(3):1040-9.

Yucel, T., Cebe, P., Kaplan, D.L. Vortex-induced injectable silk fibroin hydrogels.Biophys J. 2009 Oct 7;97(7):2044-50.

Zaoming, W., Codina, R., Fernández-Caldas, E., Lockey, R.F. Partial characterization of the silk allergens in mulberry silk extract.J InvestigAllergolClinImmunol. 1996 Jul-Aug;6(4):237-41.

Zhang, H.H., Kumar, S., Barnett, A.H., Eggo, M.C. Ceiling culture of mature human adipocytes: use in study of adipocyte functions. J Endocrinol. 2000 Feb;164(2):119-28.

Zhang, P., Baxter, J., Vinod, K., Tulenko, T.N., Di Muzio, P.J. Endothelial differentiation of amniotic fluid-derived stem cells: synergism of biochemical and shear force stimuli. Stem Cells Dev. 2009 Nov;18(9):1299-308.

Zhao, W., Li, X., Liu, X., Zhang, N, Wen, X. Effects of substrate stiffness on adipogenic and osteogenic differentiation of human mesenchymal stem cells. Mater Sci Eng C Mater Biol Appl. 2014 Jul 1;40:316-23.

Zheng, M.H., Chen, J., Kirilak, Y., Willers, C., Xu, J., Wood, D. Porcine small intestine submucosa (SIS) is not an acellular collagenous matrix and contains porcine DNA: possible implications in human implantation. J Biomed Mater Res B Appl Biomater. 2005 Apr;73(1):61-7.

Zhong, W., Tian, K., Zheng, X., Li, L., Zhang, W., Wang, S., Qin, J. Mesenchymal stem cell and chondrocyte fates in a multishear microdevice are regulated by Yes-associated protein. Stem Cells Dev. 2013 Jul 15;22(14):2083-93.

Zhu, W., Nelson, C.M. Adipose and mammary epithelial tissue engineering. Biomatter. 2013 Jul-Sep;3(3).

Zisch, A.H., Lutolf, M.P., Hubbell, J.A. Biopolymeric delivery matrices for angiogenic growth factors. Cardiovasc Pathol. 2003 Nov-Dec;12(6):295-310.

Zuk, P.A., Zhu, M., Ashjian, P., De Ugarte, D.A., Huang, J.I., Mizuno, H., Alfonso, Z.C., Fraser, J.K., Benhaim, P., Hedrick, M.H. Human adipose tissue is a source of multipotent stem cells. Mol Biol Cell. 2002;13(12):4279-95.

Zuk, P.A., Zhu, M., Mizuno, H., Huang, J., Futrell, J.W., Katz, A.J., Benhaim, P., Lorenz, H.P., Hedrick, M.H. Multilineage cells from human adipose tissue: Implications for cell-based therapies. Tissue Eng. 2001;7:211–228.

APPENDIX A

CALIBRATION CURVES

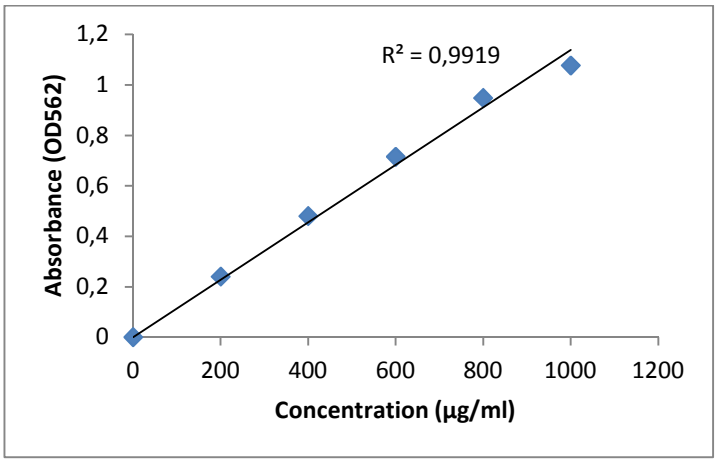

Figure A1. Calibration curve constructed with BSA standards (0-1000 µg/mL) for BCA total protein assay.

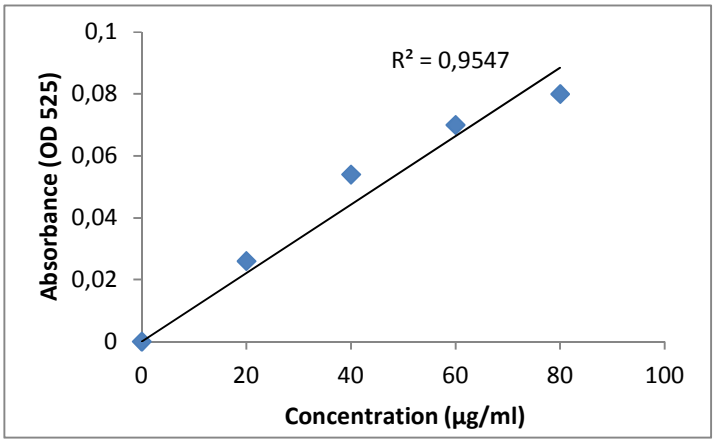

Figure A2. Calibration curve for total sGAG assay constructed with ChS standards (0-80 µg/mL) for DMMB assay.

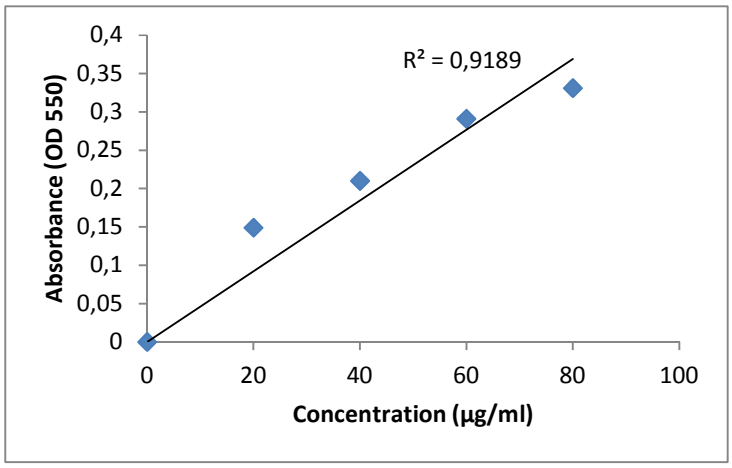

Figure A3. Calibration curve for total collagen assay using bovine collagen standards (0-800 µg/mL).

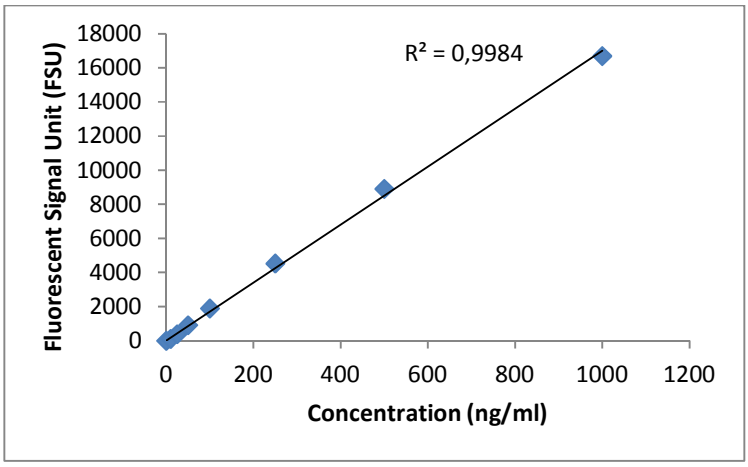

Figure A4. Calibration curve for DNA Quantitation constructed with calf thymus DNA standards (0-1000 ng/mL).